NETHERLANDS INSTITUTE FOR SEA RESEARCH

Sediments, fauna and the dispersal of radionuclides at the N.E. Atlantic dumpsite for low-level radioactive waste

Report of the Dutch DORA program

M.M. Rutgers van der Loeff & M.S.S. Lavaleye

Front cover: Physiographic Diagram of the North Atlantic by B. C. Heezen and M. Tharp, Copyrighted © 1984 by Marie Tharp, published by permission of Marie Tharp. The position of the dumpsite is indicated. The deep water in the eastern basin is ventilated from the south.
Back cover: Rat-tail fish *Coryphaenoides armatus* caught at the dumpsite.

Sediments, fauna, and the dispersal of radionuclides at the N.E. Atlantic dumpsite for low-level radioactive waste

Report of the Dutch DORA program

M.M. Rutgers van der Loeff & M.S.S. Lavaleye

Netherlands Institute for Sea Research, P.O. Box 59,NL 1790 AB DEN BURG, TEXEL

1986

SEDIMENTS, FAUNA, AND THE DISPERSAL OF RADIONUCLIDES AT THE NE ATLANTIC DUMPSITE FOR LOW-LEVEL RADIOACTIVE WASTE

Final report of the Dutch DORA program

M.M. RUTGERS VAN DER LOEFF AND M.S.S. LAVALEYE
NIOZ, P.O. Box 59, 1790 AB Den Burg, Texel, The Netherlands.

CONTENTS

1. INTRODUCTION

1.1. RESEARCH AT THE DUMPSITE

Since 1967, the dumping of low level radioactive waste in the deep sea has normally taken place under the auspices of NEA, the Nuclear Energy Agency of the Organization for Economic Co-operation and Development (OECD). To further the objectives of the Convention on the Prevention of Marine Pollution by Dumping of Wastes and other Matter (the London Dumping Convention), the OECD Council established in 1977 a Multilateral Consultation and Surveillance Mechanism for Sea Dumping of Radioactive Waste. According to the terms of this Mechanism, NEA (1980) prepared a review of the suitability of the dumpsite that had been in use since 1974. The Steering Committee for Nuclear Energy of the NEA considered in 1980 that, on the basis of the review, the existing site was suitable for continued dumping for the next five years. At the same time, the Steering Committee agreed on the need for developing a coordinated site-specific program to increase current knowledge of the processes controlling the transfer of radionuclides in the marine environment, so that future assessments could be based on more accurate and comprehensive scientific data.

An international Coordinated Research Project (CRESP) was then set up to yield the required information and build more site-specific models. Within CRESP, scientific experts from NEA member countries have discussed research priorities and divided research tasks. The Netherlands agreed to perform a biological and geochemical investigation of the dumping area. On behalf of the Dutch government, the Netherlands Energy Research Foundation (ECN) asked the Netherlands Institute for Sea Research (NIOZ) to carry out this research.

The aim of the Dutch contribution, which has been called the DORA project, is to supply additional information on those geochemical and biological characteristics of the dumpsite that can affect the transport of radionuclides once they have been released from the waste packages. Moreover, it is envisioned to give a description of the local fauna, which is needed for the evaluation of the possible radiation risk for marine organisms. This is the final report of the project, which started in May 1982 and lasted four years. It is based on the analyses of samples that have been collected during two expeditions, in 1982 and in 1984. Part of the results of the 1982 expedition has been presented earlier in an interim report (RUTGERS VAN DER LOEFF & LAVALEYE, 1984) and as various contributions to the interim oceanographic description of the dumpsite (DICKSON *et al.*, 1985), which formed the scientific basis for the 1985 review of the suitability of the dumpsite (NEA, 1985).

1.2. ACKNOWLEDGMENTS

We thank captain L.J. Blok and the crew of M.S. Tyro and commander J. van Aalst and the crew of H.Ms. Tydeman for their support during the expeditions. The assistance from NIOZ technicians during preparations and during the actual expeditions has been of great value. Echosounder profiles during the 1982 cruise were recorded by J. van Weereld. Much of the laboratory work was performed by D.A. Waijers, C.M. Oomens-Meeuwsen (Geochemistry) and G.J. Zigterman (Biology). Additional assistance was ob-

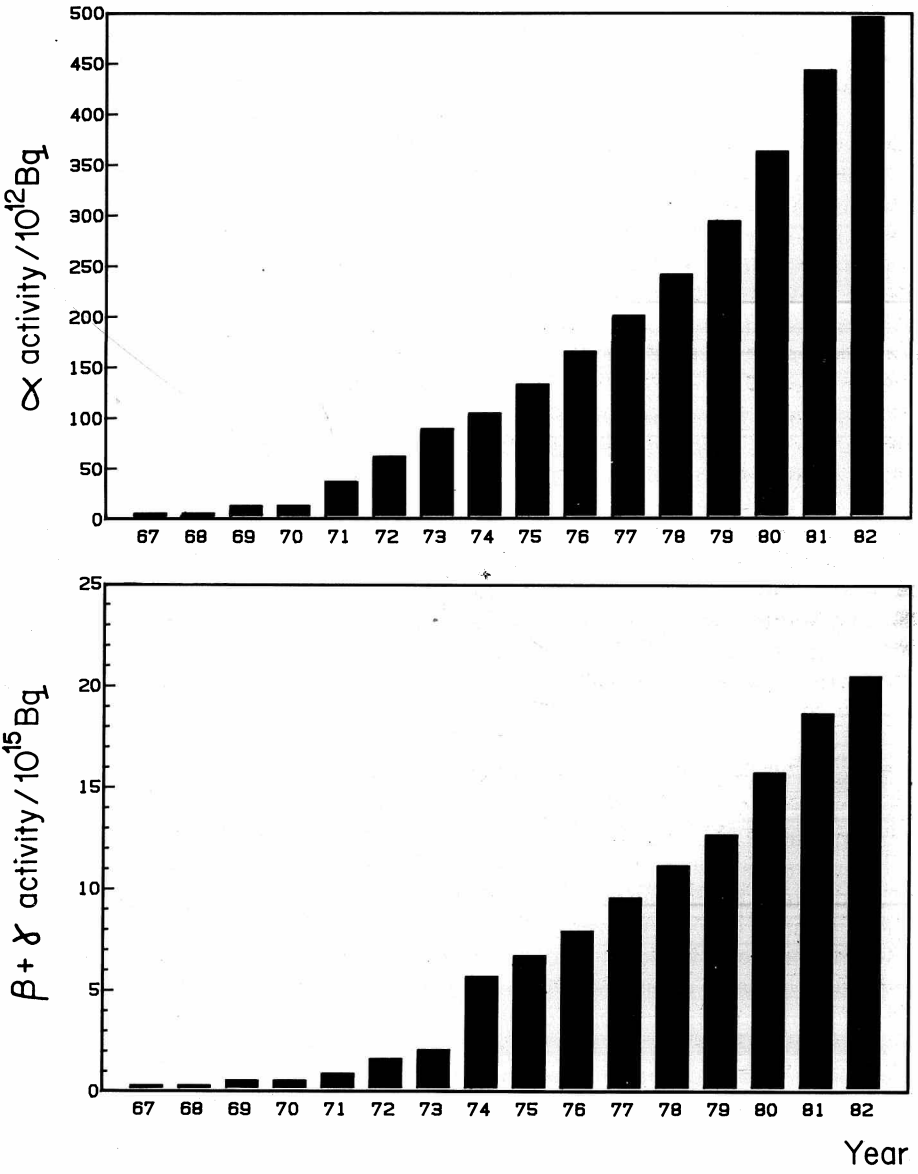

Fig.1.1. Cumulative amounts of radioactivity dumped under NEA auspices in the NE Atlantic ocean. Above: α activity; below: β + γ activity (from 1975 onwards exluding tritium).

tained during the cruises from J. Hegeman (organic carbon), R.T.P. de Vries (nutrients), G. Berger (^{222}Rn and ^{210}Pb), B. van Megen, M. Leopold, E. Okkels and J. van Elk. W. Frankema, H. Stil and R van Kempen contributed to the work in the laboratory. X-ray diffraction analyses were performed by Sj. v.d. Gaast and J. Reijmer; J. Kalf did the X-ray fluorescence analyses. The micro-paleontological data of the gravity cores are derived from a study by Y. Coenegracht. The data on diversity and feeding types of Nematoda were taken from a study by P.R. Speijer (Laboratory of Nematology, University of Wageningen). The fishes caught with the trawl were identified with help of J.IJ. Witte. We thank J.H.F.Jansen, W. Salomons, H. Elderfield, E.K. Duursma, P.J. Kershaw and J.J. Zijlstra for helpful discussions. H. Hobbelink, B. Verschuur, R. Nichols and B. Aggenbach, and B. Bak, J. Mulder and I. Pool took care of illustrations and printing. Neutron activation analyses were performed by H. v.d. Sloot, J. Woittiez and J. Zonderhuis (ECN) and ^{14}C analyses by W.G. Mook (isotope physics laboratory, Groningen) and by G. Possnert (Tandemacceleratorlaboratoriet, University of Uppsala). ETS measurements during the 1982 cruise would not have been possible without the help of Miriam Sibuet, CNEXO. M. Wedborg gave us her computer code for the evaluation of alkalinity. The cooperation of B. Verkerk and A.W. van Weers (ECN) was very much appreciated. We further acknowledge the support obtained from Kristinebergs Marine Biological Station, Sweden, the Netherlands National Geologic Survey, the State Museum of Natural History (Leiden) and the Netherlands Council for Sea Research.

The project was financed by the Netherlands Energy Research Foundation, the Dutch government (ministry of environment and ministry of economic affairs), contributions from the Swiss and Belgian governments and through contracts with the Commission of the European Communities (No. BIO-B-509-NL (N) and BI6-54-NL)

1.3. SOURCE TERM: the radionuclides of interest.

The dumping of radioactive waste in the N.E. Atlantic started in 1949, but remained small until the early sixties. The amounts increased gradually until 1982 when the last dumping operation was carried out. In total, 666 TBq of α activity and 41600 TBq of β and γ activity (including 24300 TBq of ^{3}H) were dumped. Various sites have been in use, but the major part has been dumped at about the same location: from 1971-1976 a circular area was used, and from 1977-1982 an overlapping rectangular area, which is what we now call the "NEA dumpsite" (Fig. 2.1). The amounts dumped under NEA auspices in the period 1967-1982 are shown in Fig. 1.1 (adapted from NEA, 1985).

The waste contains a mixture of fission and activation products from many sources. The approximate composition of all cumulative dumpings in the N.E. Atlantic at the time of discharge is given in Fig. 1.2.a for the α activity and in Fig. 1.2.b for the β and γ emitting radionuclides. The figures also show how the activities change with time as a result of radioactive decay. The α emitting isotopes are generally much more long-lived than the β and γ emitters: at the time of dumping $\beta + \gamma$ activity exceeds α activity by nearly two orders of magnitude. After 85 years, $\beta + \gamma$ activity falls below α activity and the only remaining significant member of the former group is then ^{14}C.

Among the α emitters, Pu isotopes and ^{241}Am are clearly the most important (Fig. 1.2.a). During the first 100 years, ^{241}Am activity increases by ingrowth from ^{241}Pu, and ^{210}Po increases by ingrowth from ^{226}Ra. Ingrowth of other nuclides like ^{237}Np is insignificant on the activity scales presented.

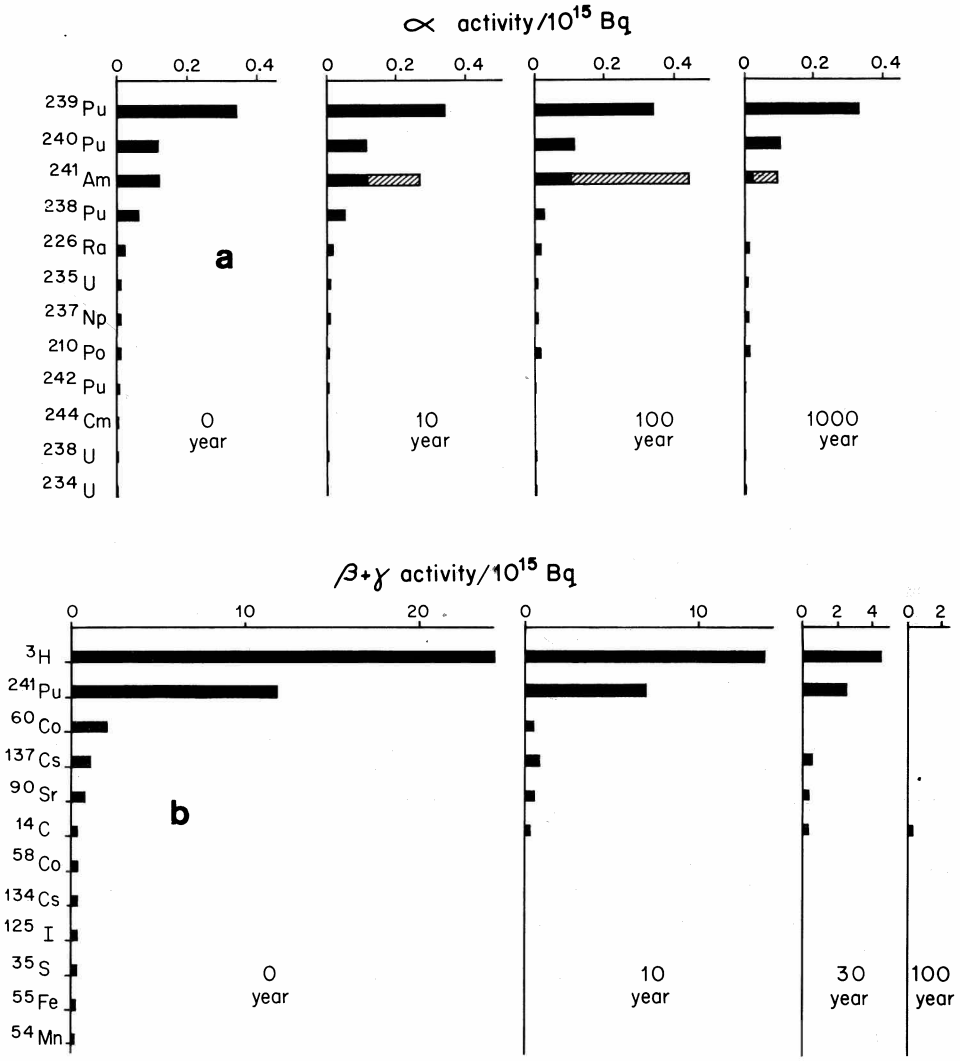

Fig.1.2. above: Composition of α activity at the time of dumping and after 10, 100, and 1000 years. Ingrowth of ^{241}Am from ^{241}Pu, and of ^{210}Po from dumped ^{226}Ra is indicated by hatching. below: Composition of $\beta + \gamma$ activity at the time of dumping, and after 10, 30, and 100 years.

The most important radionuclides:
For a preliminary evaluation which nuclides are most important for the present study, it is useful to compare the activity of each nuclide in the waste with the activity of that nuclide that is present from other sources in the surface sediment at the dumpsite. Such a comparison is presented in Table 1.I for the most abundant radioisotopes.

Table 1.I. Radionuclide activities (TBq/4000 km^2) from natural and man-made sources in the mixed layer[a] (6 cm) of the dumpsite.

isotope	half-life (years)	mixed-layer inventory: natural	mixed-layer inventory: fall-out	dumping[b]: t=0	dumping[b]: t=100 y
α emitters:					
$^{239+240}$Pu	24065(^{239}Pu) 6537(^{240}Pu)	-.-	0.023[c]	452	450
^{241}Am	432.2	-.-	0.011[d]	118	408
^{226}Ra	1600	8.1[e]		17	16
^{210}Po	.379	14.6[f]		3.8	16[g]
^{235}U	$7.04\ 10^8$	0.20[h]		7.7	7.7
^{238}U	$4.47\ 10^8$	4.4		0.7	0.7
β and γ emitters:					
^{14}C	5730	2.7[i]	0.0[k]	340	340
^{137}Cs	30.2	-.-	0.6[l]	1040	105
^{3}H	12.3	-.-[m]		24000	87
^{90}Sr	28.1	-.-		760	64
^{241}Pu	13.2	-.-		11800	62
^{60}Co	5.26	-.-		2010	0.0

a 6 cm upper layer mixed by bioturbation (Kershaw 1985)
b All past dumpings. t=0: Cumulative values not corrected for decay
c This is 78% of the total inventory. Based on Noshkin (1985)
d from ^{241}Am/$^{239+240}$Pu = 0.5 (Noshkin, 1983)
e based on Kershaw (1985). ^{226}Ra activity is approximately constant over first 1m depth.
f ^{210}Pb activity is similar. Includes nearly 100% of unsupported ^{210}Pb inventory (6.5 TBq). Based on Kershaw (1985)
g close to secular equilibrium with dumped ^{226}Ra
h Activity is constant with depth.
i 85% $CaCO_3$ (this study) with apparent ^{14}C age of 3150 y (Kershaw, 1985). Mixed layer contains 26% of total inventory.
k negligible compared to natural abundance.
l based on one core (Noshkin, 1983).
m ^{3}H produced by cosmic rays is negligible

The estimated inventories of the waste radionuclides should not be taken as a measure of their radiological significance. The radiological hazard of a radionuclide does not only depend on its activity, but also on the nature of its radiation and on its behaviour in the environment, including its uptake by organisms. The radiotoxicity of radionuclides inhaled or ingested by man or marine organisms depends on the type and energy of the radiation emitted by the nuclide as well as on the metabolic characteristics of the element involved. α emitting radionuclides are for example generally more radiotoxic than β or γ emitting nuclides. A radiological assessment of the dumpsite covering these aspects has been made by NEA (1985).

In conclusion, we will have to focus our attention on the α emitters $^{239+240}$Pu and ^{241}Am, which are the radionuclides of most concern, especially on longer timescales. The discharged activity of other α emitters is much lower and comparable to the levels present at the dumpsite from the natural U decay series. β and γ emitters are of interest on a shorter timescale: their decay is essentially complete after about 100 years, except for ^{14}C (Fig. 1.2). Since the waste canisters are expected to withstand corrosion for some 20 years (NEA, 1985), the short-lived isotopes ($t_{0.5} <$ 1yr) are relatively unimportant, and the β and γ emitters of main concern are therefore ^{3}H, ^{241}Pu, ^{60}Co, ^{137}Cs, ^{90}Sr, and ^{14}C.

2. MATERIAL AND METHODS

2.1. CRUISES TO THE DUMPSITE

The first expedition was a joint Swiss-Belgian-Dutch cruise, organized from 19 August to 13 September 1982 with MS TYRO. A second expedition was organized from 26 March to 20 April 1984 with H. Ms. Tydeman. The position of the dumpsite is shown in Fig. 2.1 and on the front cover. Figure 2.1 also shows the sampling locations. Stations 1-15 were visited in 1982; stations 21-29 in 1984. Because the local bathymetry is not known in great detail, a 3.5 kHz echosounder was operated continuously during the cruises (Fig. 2.2). The data were required for decisions on trawling and coring.

2.2. SAMPLING SCHEME

Tables 2.I and 2.II show the geographical position, the water depth and the sampling program at each of the sampling stations during the first and second cruise, respectively. The same sampling techniques were used during both cruises:

CTD-Rosette sampler:11 Niskin bottles of 30 liter water content were mounted on a Rosette sampler. The CTD was equipped with a nephelometer and with an altitude sonar to measure height above the sea floor. Samples were used for nutrient and oxygen analyses, ^{222}Rn, suspended matter and organic carbon analyses (second cruise), and for $^{239+240}$Pu analysis by V. Noshkin (Livermore, US) (filtered samples from the first cruise; unfiltered samples from the second). During the first cuise, the Swiss team took samples for their study of the particulate material in the Benthic Nepheloid Layer (BNL) by Coulter counter methods and by EDAX analysis after filtration.

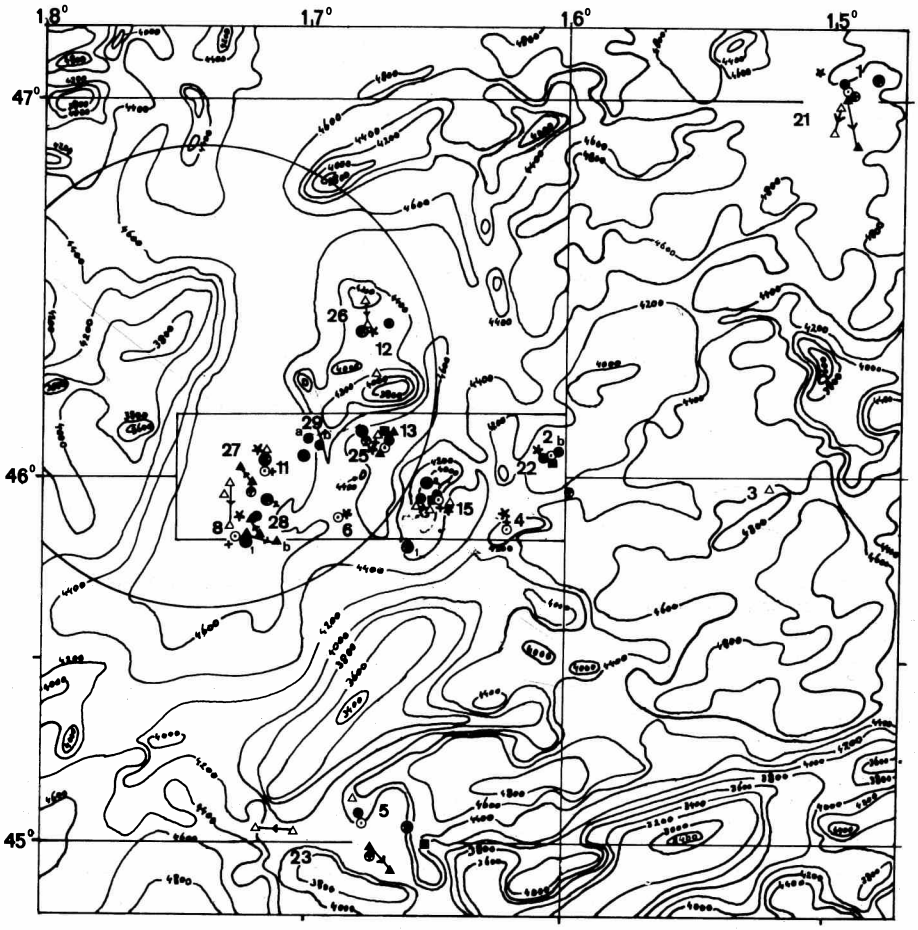

1982 expedition (station 1 - 15):
⊙ = Boxcore
✚ = Gravity core
✱ = CTD
△ = Trawl

1984 expedition (station 21 - 29):
● = Boxcore
■ = Horizontally sliced boxcore
⊕ = Gravity core
⊛ = CTD
▲→▲ = Trawl
△→△ = Bottom sledge

Fig.2.1. Map of the old (circle) and most recent (rectangle) dumpsite and its surroundings, with sampling stations. For the 1982 expedition only the position of the beginning of the fishing track of the trawls is indicated.

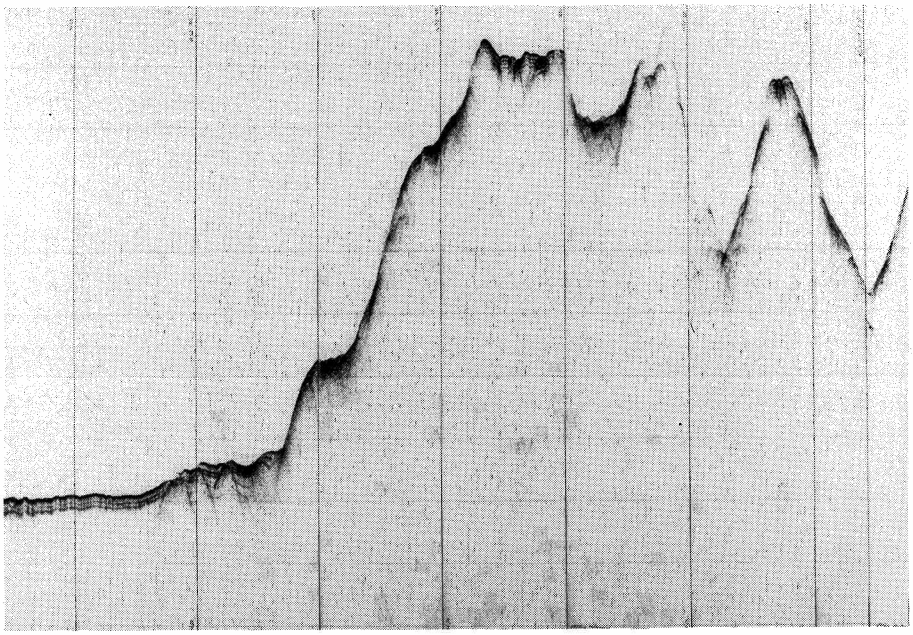

Fig.2.2. Echosounder reflection profile in eastern part of the dumpsite, showing steep hillsides. Vertical range 4125-4875 m. Vertical scale exaggerated 50x.

Boxcorer: Undisturbed bottom samples with a surface area of 0.25 m^2 and 20 to 30 cm deep were obtained with a Mark III boxcorer. Up to 20 subsamples for chemical and (micro)biological analyses were taken and the remaining sediment was sieved for the study of macrofauna. Special boxcores were collected in 1984 for the study of the vertical distribution of macrofauna.

Gravity corer: Cores up to 4m in length were obtained with a 125 mm diameter gravity corer. Boxcorer and gravity corer were operated with a 16 mm synthetic (Kevlar) wire. As this material has negligible underwater weight, the bottom contact of the corers could be observed very easily from the wire tension, and the use of a pinger was not necessary.

Trawl: Macrofauna from the deep-sea bottom was sampled with a 3.5 and a 5m Agassiz trawl. The sampled trajectory was approximately 10 km long and real fishing time was 2 to 3 hours. The use of a light weight synthetic wire during the first cruise may have resulted in a poor bottom contact. During the second cruise a steel wire was used.

Primary production: Primary production was measured three times from dawn to noon with the ^{14}C incubation technique.

Table 2.I. List of samples taken during the 1982 expedition. Station numbers with sample type, date, ship position during sampling, water depth and length of trawls. Sledge and trawl positions refer to the position of the ship at the beginning of the fishing track.

Station + sampling device	Date	Position N	Position W	Depth in m	Fishing time in min.
1C	25-8-82	47 04.43	15 02.96	4880	
1B	25-8-82	47 01.8	14 56.6	4800	
2B	26-8-82	46 03.3	16 03.2	4200	
2C	27-8-82	46 03.75	16 05.39	4413	
3T	31-8-82	45 58.5	15 13.0	4600	80
4C	1-9-82	45 53.7	16 13.66	4360	
4B	1-9-82	45 51.8	16 13.4	4300	
4G	1-9-82	45 52.1	16 13.4	4000	
5T	2-9-82	45 07.0	16 48.0	4300	217
5B	3-9-82	45 03.3	16 45.3	4325	
6C	3-9-82	45 53.14	16 50.54	4611	
6B	4-9-82	45 53.6	16 52.0	4570	
8C	4-9-82	45 53.09	17 14.78	4770	
8B	4-9-82	45 50.5	17 16.1	4725	
8G	4-9-82	45 48.8	17 17.3	4725	
8T	5-9-82	45 56.7	17 18.0	4725	195
11C	6-9-82	46 03.67	17 10.27	4765	
11B	6-9-82	46 01.1	17 08.9	4725	
11G	6-9-82	46 00.9	17 07.9	4725	
11T	6-9-82	46 04.1	17 08.9	4725	205
12C	7-9-82	46 22.91	16 44.89	4315	
12B	7-9-82	46 22.1	16 42.8	4200	
12T	7-9-82	46 17.0	16 44.2	4200-4700	255
13C	8-9-82	46 03.88	16 42.54	4766	
13B	8-9-82	46 04.7	16 42.3	4700	
13G	8-9-82	46 05.3	16 43.0	4725	
13T	8-9-82	46 07.0	16 43.4	4700-4200	200
15B	9-9-82	45 56.1	16 30.1	4000	
15C	9-9-82	45 54.61	16 33.38	200	
15G	9-9-82	45 54.9	16 31.5	4000	
15T	9-9-82	45 55.1	16 26.8	4500	240

B,BA: boxcore for study of geochemistry and meiofauna
BB: additional boxcore for biological study
BC: boxcore sliced horizontally
*: boxcore of 600 (instead of 2500) cm^2
C: CTD cast
S: bottom sledge
S+: sledge with coarse net
T,TB: trawl

Table 2.II. List of samples taken during the 1984 expedition. For explanations see Table 2.I.

Station + sampling device	Date	Position N	Position W	Depth in m	Fishing track in m	Fishing time in min.
21S	30-3-84	46 59.5	14 58.3	4776	8748	180
21B	30-3-84	47 03.2	14 57.8	4787		
21C	30-3-84	47 03.7	14 49.8	4788		
21T	30-3-84	47 01.1	14 56.4	4757	15792	317
21G	31-3-84	47 01.7	14 56.0	4786		
22BA	1-4-84	46 03.5	16 04.7	4310		
22BB	1-4-84	46 03.9	16 02.2	4236		
22BC	2-4-84	46 02.6	16 02.7	4266		
22G	2-4-84	45 57.4	15 59.3	4076		
23G	3-4-84	45 02.8	16 43.3	4257		
23S+	4-4-84	45 02.0	17 01.8	4086	3148	60
23BA	4-4-84	45 04.8	16 46.4	4333		
23T	5-4-84	44 59.6	16 43.3	4001	8890	174
23C	5-4-84	44 57.7	16 34.8	4246		
23BC	5-4-84	45 00.1	16 31.4	4580		
24C 1	5-4-84	45 48.1	16 36.4	4318		
24T	6-4-84	45 55.6	16 34.2	3999	5180	140
24BC	6-4-84	45 56.6	16 31.0	4085		
24C 2	6-4-84	45 58.4	16 32.0	4348		
24BA	6-4-84	45 56.9	16 30.1	3958		
24G	7-4-84	45 54.6	16 33.6	3890		
25BA	10-4-84	46 05.6	16 42.0	4723		
25BC	10-4-84	46 07.1	16 42.4	4721		
25G	10-4-84	46 05.1	16 44.3	4675		
25T	11-4-84	46 04.1	16 43.1	4720	8004	170
25C	11-4-84	46 05.7	16 47.3	4697		
26BA	11-4-84	46 24.5	16 41.3	4540		
26C	12-4-84	46 23.0	16 46.3	4291		
26S+	12-4-84	46 24.8	16 46.4	4085	6401	106
27C	13-4-84	46 02.6	17 09.5	4727		
27T	14-4-84	45 59.4	17 12.6	4723	5060	185
27S+	14-4-84	45 58.9	17 16.9	4717		
27G	15-4-84	45 57.3	17 11.8	4720		
28B*	15-4-84	45 53.9	17 11.4	4609		
28T	15-4-84	45 51.1	17 10.6	4602	5390	180
28C 1	15-4-84	45 49.4	17 12.9	4730		
28TB	16-4-84	45 51.3	17 13.3	4765	5885	185
28C 2	16-4-84	45 56.4	17 08.5	4655		
29C	16-4-84	46 03.2	17 00.0	4666		
29Ga	17-4-84	46 05.7	16 58.9	4620		
29Gb	17-4-84	46 04.8	16 56.2	4430		

3. GEOCHEMISTRY

3.1. INTRODUCTION

Radionuclides can be released from the waste canisters in dissolved or particulate form. Particulate corrosion products or debris will rapidly fall on the bottom, except for very small particles. The first transport pathways of these small particles and of dissolved components occur in the Benthic Nepheloid Layer (BNL): dispersion in the BNL and, depending on the adsorption equilibria with particles in the BNL, either transport with the residual current (about 2 $cm.s^{-1}$ northward, GURBUTT & DICKSON, 1983) or incorporation in the sediment toplayer. Once in the sediment, they will be mixed down by bioturbation and affected by early diagenetic processes. The ultimate fate of waste radionuclides is thus the net result of complicated pathways in the bottom water and in the sediment.

Research tasks have been divided among the various teams participating in CRESP: The structure of the BNL and the chemistry of particles within the BNL were studied by the Swiss group PROSPER (NYFFELER *et al.* 1984, 1985), and physical oceanographical research was done by investigators from UK (GURBUTT & DICKSON, 1983; DICKSON & GOULD, 1983). In the Dutch DORA project some work was also done on processes in the BNL (see section 3.8): the distribution of ^{222}Rn, dissolved and particulate organic carbon, and the usual hydrographic parameters temperature, salinity, nutrients and oxygen were measured and water samples were collected for Pu analyses by Noshkin (in part reported in NOSHKIN, 1985).

The emphasis of the Dutch geochemical work was put on transport processes within the sediment. In view of the discussion in the paragraph describing the source term, this means that the task of the geochemical project was to establish how early diagenetic processes in the sediment at the dumpsite would influence the transport of primarily $^{239+240}Pu$, ^{241}Am, ^{241}Pu, ^{3}H, ^{60}Co, ^{137}Cs, ^{90}Sr, and ^{14}C. Three approaches are possible:

a. Study of adsorption equilibria in laboratory experiments.

The transport of radionuclides in the environment is very much dependent on the partitioning between the dissolved and the particulate phase. This partitioning is influenced by solution and (co-) precipitation, by adsorption and by biological uptake. Goldberg (1954) postulated that trace element concentrations in the open ocean are controlled by adsorption-desorption equilibria. If that is true, the behaviour of a trace element can be described by the distribution coefficient K_d, preferably defined as the dimensionless ratio of adsorbed or total sediment-bound element to dissolved element. The sorption characteristics of marine sediments and diffusion within sediments of a variety of radionuclides has been studied extensively in laboratory experiments by Duursma (DUURSMA & BOSCH, 1970; DUURSMA & GROSS, 1971; DUURSMA, 1973; DUURSMA & EISMA, 1973). It turned out that the values obtained for the distribution coefficient of an element between sediment and water (K_d) were, apart from a clear grain-size effect, remarkably constant over a variety of natural sediments. This constant distribution may be related to adsorption equilibria with oxyhydroxides, an abundant phase in all oxidized sediments (EDGINGTON, 1981; LI, 1981). BACON & ANDERSON (1982) demonstrated that the distribution of Th isotopes in dissolved and particulate phase in the oceanic water column was in agreement with the model of equilibrium adsorption. It therefore appears that the con-

cept of distribution coefficients (K_d) is very useful in predicting the scavenging of radionuclides from the water column by sediment particles (DUURSMA & GROSS, 1971). It has to be borne in mind, however, that K_d values are not physical constants, but are related to sorption equilibria which can be highly dependent on chemical speciation of the radionuclides, the availablity of organic complexing agents, the surface condition of the sediment particle, and the pH and redox chemical state of the medium. When the strongest adsorption sites are not present in large excess, K_d decreases with increasing load of the adsorbed element, in accordance with the Langmuir equation (BALISTIERI & MURRAY, 1983). It is also possible that the distribution is not determined by adsorption equilibria, but rather by kinetic factors (SANTSCHI *et al.*, 1984) or by the solubility of a mineral phase. Within the sediment, all these conditions are subject to changes as a result of diagenetic reactions. The complex of reactions involved in $CaCO_3$ dissolution and early diagenesis of organic material, accompanied with many remobilization and precipitation reactions (BONATTI *et al.*, 1971; MANHEIM & SAYLES, 1974; BERNER, 1980), thus reduces in marine sediments the applicability of the concept of constant distribution coefficients (DUURSMA & GROSS, 1971; NELSON & LOVETT, 1980; SHOLKOVITZ *et al.*, 1982, RUTGERS VAN DER LOEFF & WAIJERS, 1986b).

We conclude that laboratory-derived K_d values are not of general applicability. If it were possible to determine the exact *in situ* speciation of an element, and the concentrations of and binding constants with all relevant ligands, it ought to be possible to calculate *in situ* distribution coefficients and corresponding mobilities. NELSON *et al.* (1985), for example, showed that a constant K_d could be used to describe the distribution of Pu in a lake, after correction had been made for the amount of Pu associated with dissolved organic matter. Since our understanding of the sediment-pore water system has generally not reached that point, we are forced to determine K_d values *in situ*. This means a selection of one of the following two approaches:

b. Use of natural, fall-out- or waste-derived activity as a tracer

The present concentrations in the sediment of the isotopes of interest are very low. Fall-out $^{239+240}Pu$, ^{241}Am and ^{137}Cs has reached the sea floor (Table 1.I), and their distribution does tell us something about their transport behaviour. Detailed analyses of oxidation states, adsorption equilibria and corresponding mobilities of these isotopes have been performed in Irish Sea sediments (KERSHAW *et al.*, 1986). Activities in this area are far above fall-out levels as a result of discharges from the Sellafield reprocessing plant. Similar studies are not possible at the activity levels that are now present at the dumpsite.

No radioactive contamination of the site from waste has yet been demonstrated, and since the lifetime of the waste canisters is estimated at about 20 years it would be unwise to base this research project on the use of waste-derived activity as a tracer.

c. Study of early diagenesis of stable analogs

Our understanding of diagenesis has improved substantially from studies of marine sedimentary pore waters (HARTMANN *et al.*, 1976 MANHEIM, 1976; SUESS, 1976; FROELICH *et al.*, 1979; BERNER, 1980 SAYLES , 1979, 1981). Likewise, a detailed analysis of sediment and pore water samples from the dumpsite will enable us to describe the diagenetic behaviour of selected elements. Descriptions of the behaviour of the radioisotopes of H, C, Co, Sr, and Cs can then be based on a study of their stable couterparts.

In the study of the behaviour of Pu and Am we are faced with the problem that stable isotopes of these elements do not exist. In this case much can be learned from a geochemical study of the behaviour of other elements (trace metals and rare earth elements) in the dumpsite sediment. Conclusions on the behaviour of Am and Pu can then be based on literature data, comparison with other areas, observations regarding the adsorption sites in the sediment, and analogies with other elements.

The present study deals with those characteristics of the sediment at the NEA dumpsite that affect sorption of radionuclides and their subsequent redistribution within the sediment. These characteristics include elemental and mineralogical composition of the sediment, composition of the pore water, distribution equilibria of elements between sediment and pore water, physical-chemical state of the sediment (pH, Eh) and all parameters that can elucidate the role of bioturbation.

In particular, four major diagenetic processes have been distinguished because they can be expected to affect the mobility of the above mentioned elements:

- mineralization of organic matter, influencing C, H, trace metals and probably rare earth elements and Pu
- redox changes, influencing Co and other trace metals, rare earth elements, Pu, and Am
- ion exchange, affecting Cs mobility
- dissolution of $CaCO_3$, influencing C and Sr

3.2. METHODS

Coring

Boxcores: 50 x 50 cm boxcores were subsampled on deck with PVC tubes. A rectangular subcore, 4 x 7 cm in cross-section, was cut in two 2-cm thick slices for immediate X-ray and colour photography.

A 6 cm diameter subcore was sectioned and used for measurement of Electron Transport System (ETS) activity according to OLANCZUK-NEYMAN & VOSJAN (1977).

Two 7 cm diameter subcores were immediately frozen for later sectioning and analysis for ^{210}Pb and $^{239+240}Pu$ profiles. (1982 cruise).

One subcore (3 cm diameter) was stored frozen, sectioned upon thawing in the laboratory and analyzed for organic carbon by wet oxidation (MENZEL AND VACCARO, 1964). (1982 cruise)

Three subcores were transported to a refrigerated laboratory-container for temperature equilibration at seafloor temperature (2°C).

One 6 cm diameter subcore with polyethylene liner was opened in a nitrogen-filled glove bag for measurements of pH and Eh by directly introducing electrodes into the sediment, and of dissolved oxygen by flushing the electrode of a Radiometer blood gas analyser with wet sediment from a plastic syringe.

A second subcore was used for the determination of the formation factor according to ANDREWS & BENNETT (1981), and of porosity from the weight loss after drying a measured volume of sediment.

The third subcore, 12 cm in diameter, was extruded, sectioned and squeezed through 0.2 μm cellulose nitrate filters in squeezers with all-teflon inner parts. Nitrogen pressure up to 5 atm was applied on a rubber diaphragm covered with parafilm. No precautions were taken to exclude contact with atmospheric oxygen since oxygen had been shown to be present throughout all boxcores. The teflon inner parts, teflon filter supports, filters and polyethylene or teflon sample bottles used for trace metal analyses had all been thoroughly rinsed in 6M hydrochloric acid and double distilled water before use.

Gravity cores were cut in 1m lengths. These were cut in half and transferred to the refrigerated container. One half was photographed, sealed in plastic and stored at 4°C for reference. The other half was analysed for pH and O_2 as described above. Within a nitrogen-filled glove bag, sediment from selected depth horizons was transferred to squeezers. Care was taken to discard the surface layer and to avoid sampling the outermost 1-cm of the core to prevent contamination and artefacts from smearing. Squeezing was done as described above, but in some occasions the pressure was increased to 35 atm. Further treatment and analyses were identical to the ones described for boxcore samples.

Pore water analyses

The first 2 ml was discarded. A subsequent 10 ml aliquot was used for nutrient and dissolved organic carbon analyses. The method of HELDER & DE VRIES (1979) was followed for ammonia and standard autoanalyzer techniques for the other nutrients. Silicate was determined within 24 hours on board ship. During the 1982 cruise, the samples for nitrate, nitrite, phosphate, and ammonia analyses were stored frozen and analysed within one month; during the 1984 cruise they were processed on board ship within 24 hours. Blank measurements showed that the filters were contaminated with ammonia, probably as a result of uptake from the atmosphere during drying of the acid-cleaned filters in a clean-air bench. Ammonia values will therefore not be reported. Dissolved organic carbon (DOC) was determined in two duplicate 2-ml aliquots following the method of MENZEL & VACCARO (1964) after removal of all inorganic carbonates with 250 μl of 1.8 n H_3PO_4 and purging with CO_2-free oxygen gas. Results were corrected for blanks (1.9 μgC per ampoule, corresponding to 0.9 mgC.l^{-1}).

Samples for trace metal analyses (minimum: 20 ml) were acidified with 1 ml.l^{-1} of 6M HCl suprapur and stored at 4°C. Trace metal contents were determined by flameless AAS using direct injection for Mn and a preconcentration technique for Fe, Cu, Cd, Ni and Co (DANIELSSON *et al.*, 1979). Analytical blanks for these metals were less than 0.1, 1.0, 0.05, 0.005, 0.02, and 0.003 μg.l^{-1}, respectively. Blanks run through all procedures, including filtration in the teflon squeezers on board, were 0.1, 1.3, 0.3, 0.016, 0.02, and 0.003 μg.l^{-1}, respectively.

Alkalinity was determined on board ship by potentiometric titration of a 10 ml aliquot filling a narrow mouth polytethylene bottle covered with parafilm. 0.1M hydrochloric acid was added from a microburette and alkalinity was evaluated according to JOHANSSON & WEDBORG (1982). Since a minimum of 32 ml of pore water had been drawn through the filters previous to the alkalinity sample, the risk of contamination from the acid cleaning procedure (FROELICH *et al.*, 1979) was small.

Sediment analyses
Squeezed sediment cakes were divided in two parts and sealed in polyethylene bags. One half was stored at 4°C and used for analysis of

Mineralogy. Carbonate was dissolved in an acetate buffer at pH > 4.8. The bulk of the remaining fraction as well as an oriented sample of the size fraction < 2 μm of it, were analysed with X-ray diffraction after saturation with Ca from calcium acetate.
^{14}C-age of carbonate-carbon by mass spectrometry for bulk-carbonate (isotope physics laboratory, Groningen), and by accelerator mass spectrometry for hand-picked Foraminifera shells (tandemacceleratorlaboratoriet, University of Uppsala).

The other half of the sediment cake was stored frozen, lyophillized, homogenized and analysed for:
The elements Na, K, Sc, Cr, Fe, Co, As, Br, Rb, Cs, La, Ce, Nd, Sm, Eu, Yb, Lu, Hf, and Th by neutron activation analysis at the Energy Research Foundation, Petten (VAN DER SLOOT & ZONDERHUIS, 1979).

The major elements Ca, Mg, Si, Al, Fe, Mn, Ti, K, and Na by X-ray fluorescence.
Cation Exchange Capacity (CEC) by saturating 500 mg on a membrane filter with 1M sodium acetate, rinsing with ethanol (96%), eluating with 1M ammonium acetate and measuring Na in the eluate with Atomic Absorption Spectrometry.
Organic carbon (VAN IPEREN & HELDER, 1985).
Ca by dissolution of carbonates in 1M HCl and titration with EGTA.
Ca, Mg, Sr, Al, Si, Fe, Mn, Cu, Zn, Ni, Co, Cd, Cr with Atomic Absorption Spectrometry after a selective extraction procedure.

Table 3.I. Sequential extraction procedure

	name	extractant	repeat	extracted fraction	ref.
1	HAC	NaOAc (1M) + HAc, pH 5.0	*3	carbonate, sorbed,salt	Lyle et al., (1984)
2	HAM	$NH_2OH.HCl$(1M) + Na citrate (0.175M), pH 5.0	*3	Mn-oxyhydroxide	Lyle et al., (1984)
3	CH	$NH_2OH.HCl$(1M) + HAc (25% v/v)	1	Fe-oxyhydroxide	Chester & Hughes (1967)
4	HCl	HCl (1M)	1	residual leachable	
5	RES	$HCl/HNO_3/HF$	1	residual	Rantala & Loring (1975)

The selective extraction procedure

0.5 g aliquots of freeze-dried and homogenized sediment were sequentially extracted using the procedure outlined in Table 3.I, modified from LYLE *et al.* (1984) and ROBBINS *et al.* (1984), and the extracts were analysed with atomic absorption spectrometry (AAS). Matrix interferences occurring in the analysis of Cd, Co and Ni in HAC extracts with flameless AAS were eliminated by the freon-dithiocarbamate extraction method (DANIELSSON *et al.*, 1979). A leach of organically bound material with sodium dodecyl sulfate-$NaHCO_3$, used by LYLE *et al.* between steps 1 and 2, yielded only negligible amounts of all investigated trace metals, and was therefore omitted in our procedure in order to prevent interference from the required heating to 80°C with the following extraction steps. An independent check on the extraction procedure from a destruction of the bulk sediment was unsuccessful. Due to the high carbonate content of the samples, calciumfluoride precipitates formed after destruction with HF (RANTALA & LORING, 1975). These precipitates could not be removed by reheating (suggested by ROBBINS *et al.*, 1984), and removed appreciable amounts of trace metals.

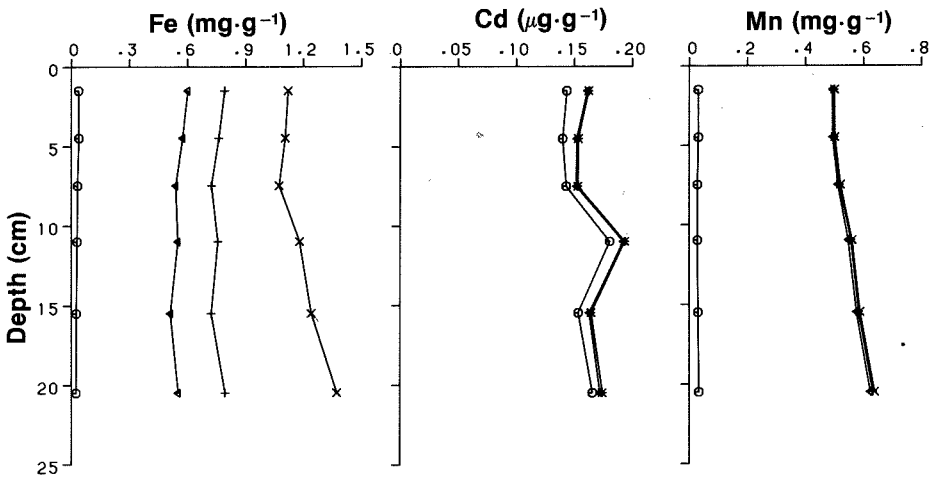

Fig.3.1. Cumulative amounts of Fe (mg/g), Cd (μg/g), and Mn (mg/g) extracted by HAC (o), HAM (◁), CH (+), and HCl (x) from core 6B.

Evaluation of the selective extraction method

The ability of the selective attack to distinguish between various operationally defined phases in the sediment is demonstrated in Fig. 3.1 for an oxidized boxcore. The HAC attack dissolves completely the calcite which makes up 85% (top) to 79% (bottom) of the sediment in this core. Beside Ca and Sr, this extract contains the major part of HCl-extractable Cd (Fig.3.1.b).

The HAM leach releases all Mn and the Co and Ni associated with it (Fig. 3.1.c). This leach is thus specific for the Mn-oxyhydroxides.

The CH leach (extractant from CHESTER & HUGHES, 1967) releases additional amounts of Fe (Fig. 3.1.a), without attacking clay minerals too heavily, and is therefore meant to distinguish which metals are associated with Fe-oxyhydroxides (*e.g.* Zn and Cu) rather than with Mn. As the discrimination between this leach and the next one (HCl-leach) is not well-defined, and as the vertical distribution of the metals was very similar in both leaches, the CH leach was omitted in the later analyses.

The HCl leach is included for reference, since it has often been used in the literature. At this pH all metals bound to exchangeable sites should be released, and the cumulative amount of metals released including this leach can be considered as the maximum amount available for adsorption equilibria.

One might argue that the treatment of the sediment before the extraction procedure would favour oxidation of reduced species, and thus lead to an increase in the reducible fraction. In the present study of deep-sea sediments, the reducible fraction of samples derived from depths where oxygen was depleted was negligible (Fig. 3.26), indicating that no serious oxidation had occurred.

The same sequential extraction scheme was applied to the study of the behaviour of REE in the sediment. In the study of trace metals, each sequential extract was analysed, but this procedure was not suitable for the study of REE, since the expected REE concentrations in the extracts were too low for an accurate determination with INAA. (Recently, however, PETERSON *et al.*, 1986, presented analytical methods to concentrate the extracts and measure REE in the concentrates). We therefore decided to analyse the material left after each extraction step rather than the extract itself. From each sample we prepared a 1.5-g aliquot of washed but otherwise untreated sediment, and three 1.5-aliquots of the residues remaining after one, two or all three of the sequential extractions denoted by HAC, HAM, and HCl (Table 3.I). The resulting samples were oven dried (70°C), homogenized, and analysed by INAA at the Netherlands Energy Research Foundation.

Bottom water analyses

Nutrients were measured as described above. Oxygen was determined by Winkler titration. For particulate organic carbon (POC), 1-liter samples were filtered over glass-fiber filters, and the filters were analysed for organic carbon by the method of MENZEL & VACCARO (1964). Results were corrected for blanks (4.5 μgC per sample, corresponding to 4.5 μgPOC.l^{-1}). Total organic carbon (TOC) was determined with the same method in three replicate 5-ml aliquots. Suspended sediment load was determined by weighing, using 10 to 20-liter samples and nuclepore filters. Blanks were between 0 and 3 μg.l^{-1}.

^{222}Rn was measured in 20-liter samples by α counting using equipment developed by Guy Matthieu (Lamont-Doherty Geological Observatory). Supported ^{222}Rn was measured by adsorption of Radium on MnO_2 fibers, and counting ^{222}Rn as above after ingrowth from its parent ^{226}Ra.

3.3 RECENT SEDIMENTOLOGICAL HISTORY

The surface sediment in the whole area consists of carbonate ooze, and accumulates at present at a rate of approximately 2 $cm.kyr^{-1}$ (KERSHAW, 1985). Biogenic inputs predominate, and calcite from Foraminifera and coccoliths makes up about 85% of the recent sediment.

The sedimentary record shows that terrigenous inputs have been much larger in the past. Most important is the input of terrigenous material by the ice. During glaciations, this caused an increase in the sediment accumulation rate, although biogenic inputs were lower than at present (RUDDIMAN & MCINTYRE, 1976). Sand and pebble-sized debris are common in glacial deposits, although they consitute only one quarter of the ice-rafted material (MOLNIA, 1983). The occurrence of large debris in sediments of much younger than glacial ages (surface sediment in boxcores; trawl catches) indicates that icebergs have continued to reach these latitudes far into Holocene times.

The site is located at a transition zone between two sources of turbidity currents. The central valley is connected to the Maury Channel (see map on front cover) through which turbidity currents flow from Iceland southward to these latitudes (RUDDIMAN & MCINTYRE, 1976). We have not found an indication of such deposits in our cores. Just east of the site is the Porcupine Abyssal Plain, where many turbidites are present from continental sources. Echosounding profiles (Fig. 3.2) reveal many layers that represent most probably turbidites. Core 21G, our only long core from the abyssal plain, contained a 180 cm turbiditic interval at 50 cm below the surface, with an estimated age between 30 and 50 kyr (Fig. 3.3).

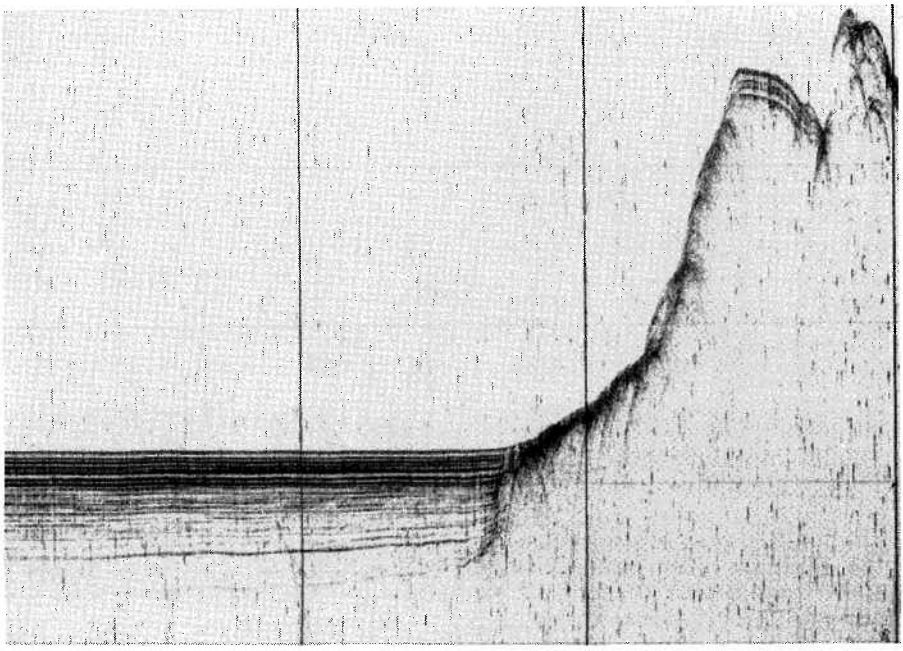

Fig.3.2. West (left) to east (right) echosounder reflection profile from the Porcupine Abyssal plain, showing numerous turbidites. At right the beginning of the Armorican seamount. Vertical range 4575-4875 m. Vertical scale exaggerated 50x.

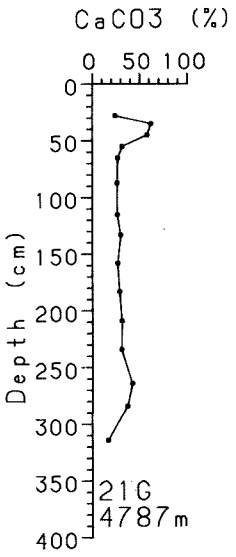

Fig.3.3. $CaCO_3$ profile of core 21G. The top of this core was lost.

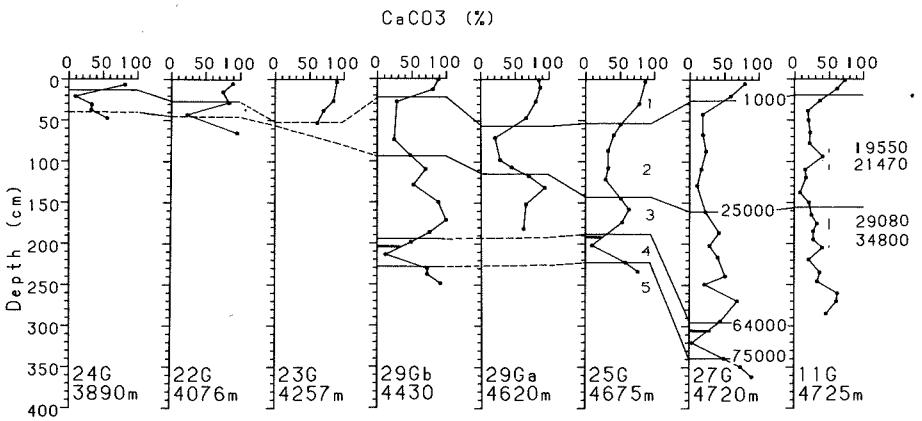

Fig.3.4. $CaCO_3$ concentration profiles in order of increasing water depth of all cores with undisturbed sedimentary record. Carbonate stages and the ages (in yr BP) of the climatic transitions are indicated. Bars represent dark layer with volcanogenic particles. Numbers beside profile 11G are ^{14}C ages (yr BP) of Foraminifera shells.

The sedimentological history of the site is well revealed by the carbonate stratigraphy (Fig. 3.4). Since carbonate dissolution after burial below the bioturbated layer is negligible (section 3.5.3), the carbonate profiles are a good representation of the composition of the surface sediment at the time of deposition. Carbonate profiles of 8 gravity cores are presented in Fig. 3.4 in order of increasing water depth. Except for core 21G with an apparent turbiditic interval, visual and X-ray inspection of these cores gave no indication of disturbed sedimentary records. Carbonate stages 1 (Holocene: 11000 BP to present) and 2 (last glaciation: 25000 BP-11000 BP with glacial maximum around 18000 BP) are easily distinguished. The higher $CaCO_3$ contents below belong to stage 3 (interstadial: 64000 BP-25000 BP). Stage 4 (glacial period from 75000 BP-64000 BP) could be identified by extremely low carbonate values and by a conspicuous dark band, about 1 cm wide, containing glass and pumice. Although the content of these volcanogenic particles was not high, this band corresponds most probably to the volcanic ash layer that was dated by RUDDIMAN (RUDDIMAN & GLOVER, 1972; RUDDIMAN, 1977) at 65000 BP. The layer was reached in 4 cores (21G, 25G, 27G and 29Gb).

It is apparent from Fig.3.4 that the sediment accumulation rate increases with water depth. Estimates of recent accumulation rates from the thickness of the Holocene deposit are biased by the possible loss of surface meterial during coring with a gravity corer. Below, rates of sediment accumulation calculated from the carbonate profiles are subject to errors as a result of core shortening. It is well documented (LEBEL *et al.*, 1982; BLOMQVIST, 1985) that spacing between layers in gravity cores is reduced through a sideward loss of material during the penetration of the corer. The effect increases with increasing core length and decreasing core diameter. Although this may cause the calculated values of sediment accumulation rates to be too low by a factor of up to 2, the differences observed between stations are real. In the deep stations in the central valley, the calculated sediment accumulation rate during the last glaciation (25000 BP-11000 BP) was 7-10 $cm.kyr^{-1}$, whereas the corresponding value for the top of Finn Seamount (core 24G) and core 22 is only 2 $cm.kyr^{-1}$.

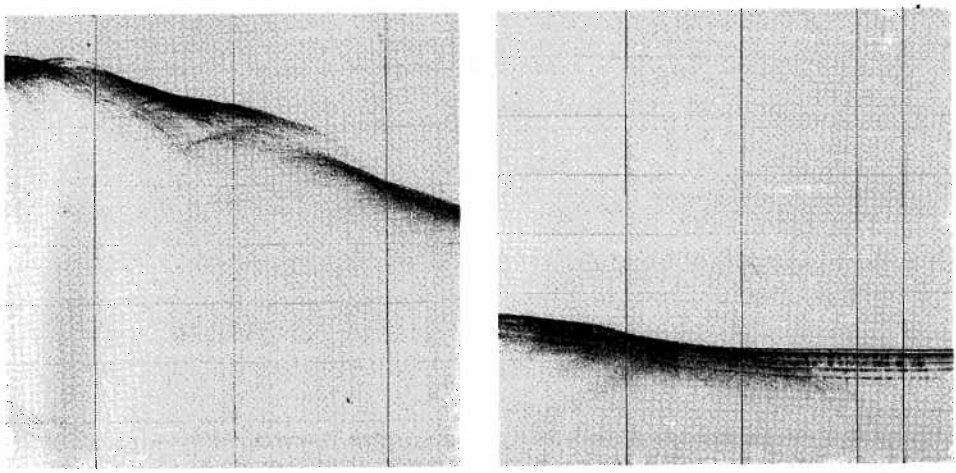

Fig.3.5. left. Echosounder reflection profile during coring at station 12, showing hard bottom, giving a second reflection. Vertical range 4125-4875 m. right. Echosounder reflection profile during coring at station 13, showing soft, layered sediment. Vertical range 4125-4875 m.

The reason for this difference is winnowing by bottom currents (Kidd, 1983). This winnowing results in a relatively coarse sediment on the hills with large Foraminifera tests and abundant ice-rafted debris (data of Jaquet in RUTGERS VAN DER LOEFF *et al.*, 1985). The seafloor is here much harder than in the valleys, which is apparent from the corer penetration (Fig. 3.4) and from echo reflection profiles (Fig. 3.5). Another consequence is that sediments at topographic highs have lower organic matter content and a higher permeability, two factors that together have a significant effect on the penetration of oxygen into the sediment (section 3.5.1.2; RUTGERS VAN DER LOEFF & WAIJERS, 1986a). A difference in the sedimentation regime is also evidenced by the observation that the Benthic Nepheloid Layer is much more developed in the valleys than over the hills (NYFFELER *et al.*, 1985).

Fig.3.6 shows $CaCO_3$ content and the abundance of planktonic Foraminifera in core 11G, taken in the valley in the western part of the site. Beds that appeared as dense layers on X-radiographs are also indicated. ^{14}C ages of bulk carbonate are higher above these beds than below (Table 3.II), suggesting that the beds are associated with a slump or other kind of reworking. However, since these coarse-grained beds contain much ice-rafted material, and since it is known that this material contains appreciable amounts of limestone (BRAMLETTE & BRADLEY, 1941), we feared that the ^{14}C ages might be influenced by fossil carbonate. We checked this in two ways:

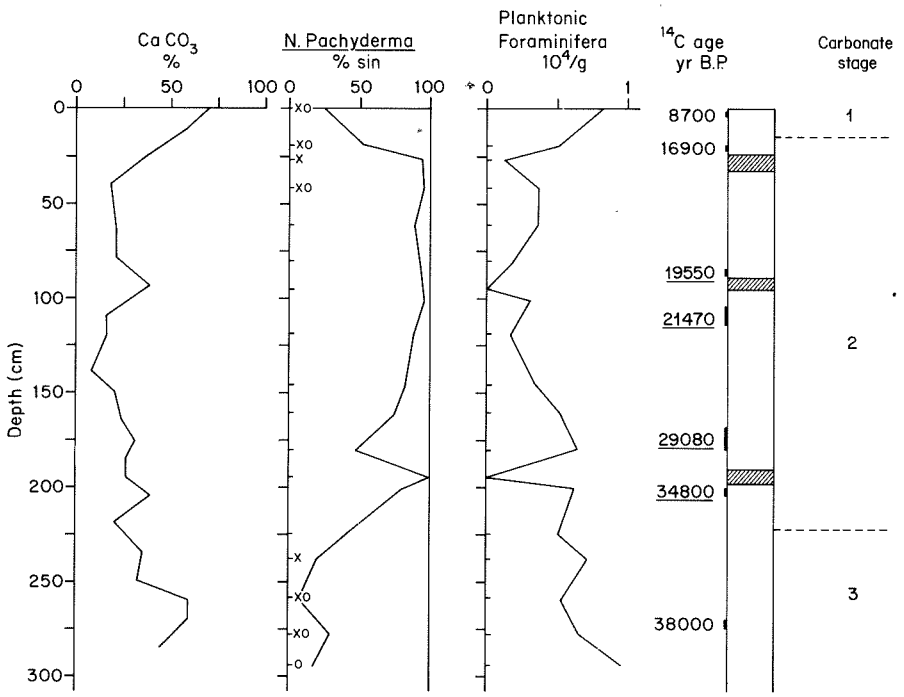

Fig.3.6. Sedimentological data of core 11G: Carbonate content, percentage of left-turned specimens among *Neogloboquadrina pachyderma* and the occurrence of *Globorotalia hirsuta* (x) and *G. truncatulinoides* (o), number of planktonic Foraminifera per gram of sediment, carbonate ^{14}C ages (if underlined: of planktonic Foraminifera; if not: of bulk carbonate), and inferred stratigraphy with carbonate stages.

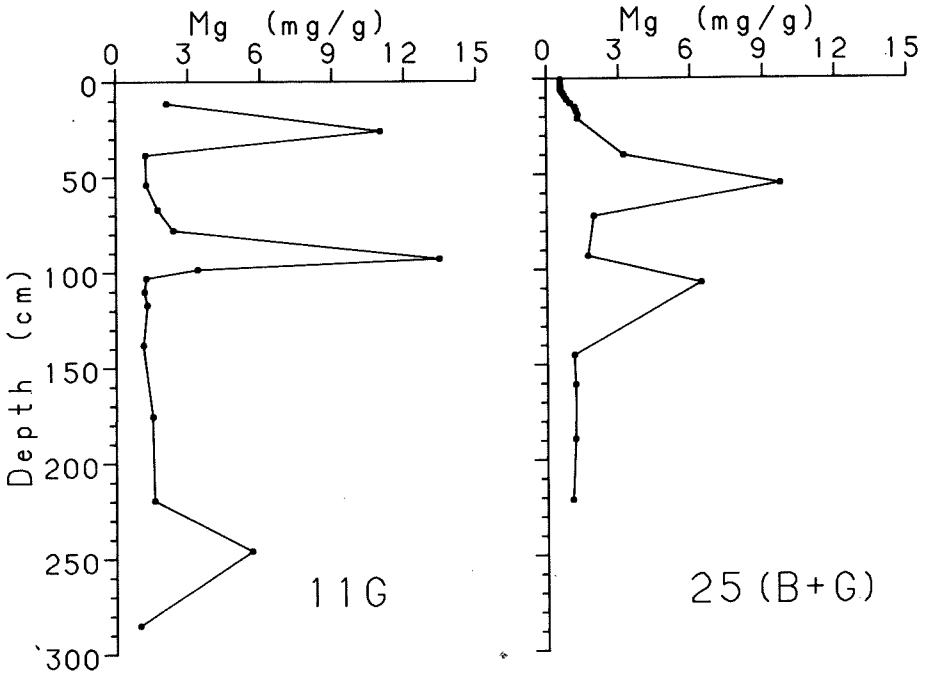

Fig.3.7. Cumulative amounts (in mg.g^{-1} of total sediment) of Mg extracted by HAM, CH, and HCl after previous dissolution of calcite with HAC in cores 11G (left) and 25G (right). Peaks indicate the presence of ice-rafted dolomite.

Table 3.II. Radiocarbon ages (yr BP) of bulk $CaCO_3$ and of hand-picked pelagic Foraminifera at four depths in core 11G, and estimates of fossil admixture.

depth (cm)	^{14}C age of bulk carbonate	^{14}C age planktonic Foraminifera	inferred fossil admixture (% of carbonate)	dolomite admixture (from Mg data)	
				content (as % of carbonate)	error in age estimate (years)
85- 89	28100 (+700)	19550 (+260)	65	12.6	-1113
104-110	24460 (±450)	21470 (±330)	30	3.6	-303
170-182	32800 (±800)	29080 (±530)	36	3.4	-286
203-204.5	29800 (±600)	34800 (±1100)	-.-	3.4	-286

First, the dolomite content in the sediment was estimated from the Mg content in a 1M HCl extract after all calcite had previously been dissolved with 1M acetate/acetic acid buffer (pH 5). (Fig. 3.7). The coarse-grained layers contain indeed relatively large amounts of dolomite, but if the ^{14}C ages are corrected for the dilution by this amount of fossil carbonate, the age reversals remain (Table 3.II).

Second, ^{14}C determinations were made on hand-picked samples of planktonic Foraminifera, using accelerator mass spectrometry. The resulting ages are in conformity with a continuous, undisturbed sedimentary record (Table 3.II and Fig. 3.6). Age determinations based on bulk carbonate were indeed up to 8500 yr in error, corresponding to a fossil component of up to 65% of the carbonate. From the data in Table 3.II, we find an average sediment accumulation rate of 7.6 cm.kyr^{-1} during the late Pleistocene (35-20 kyr BP), in accordance with estimates based on carbonate stratigraphy (Fig. 3.4).

The two most recent periods of intensive input from ice-rafting at station 11 can now be dated: The layer at 95 cm was deposited 20000 years ago, the layer at 25 cm at the wane of the Pleistocene, not long before 11000 BP. (The top of this core must have been lost). Similar beds at 105 and 55 cm, respectively, in core 25G (Fig. 3.7) represent most probably the same deposits. The carbonate stratigraphy of core 25G (Fig. 3.4) agrees with this explanation.

Local erosion

From the limited literature data available from sections in the hill areas, KIDD (1983) concluded that erosion or redeposition of sediment at these locations must be assumed to be minor, at least, not in the form of submarine slides or slumps. Any data about the occurrence of such processes in the trough area was however lacking. Two out of the ten cores we collected showed evidence of reworking and horizontal sediment transport: one from the trough (8G), and one from the Porcupine Abyssal Plain (21G, see above; Figs 3.2 and 3.3). For one core from the hill area (15G) reworking is likely.

Core 8215G (Fig. 3.8) contained one bed resembling the two beds discussed of core 8211G: a coarse layer with old bulk-carbonate on top of younger carbonate. ^{14}C-data on hand-picked Foraminifera are not available. As in core 11G, the age reversal might be explained by dilution by fossil carbonate. In this case, however, this explanation is contradicted by the abundance of planktonic Foraminifera in the samples, and by the high

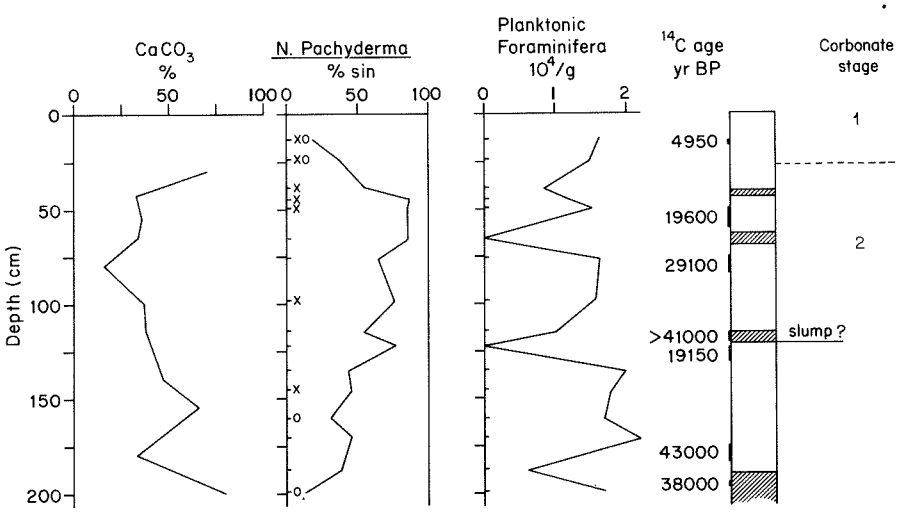

Fig.3.8. Sedimentological data of core 15G. For explanations see Fig.3.6.

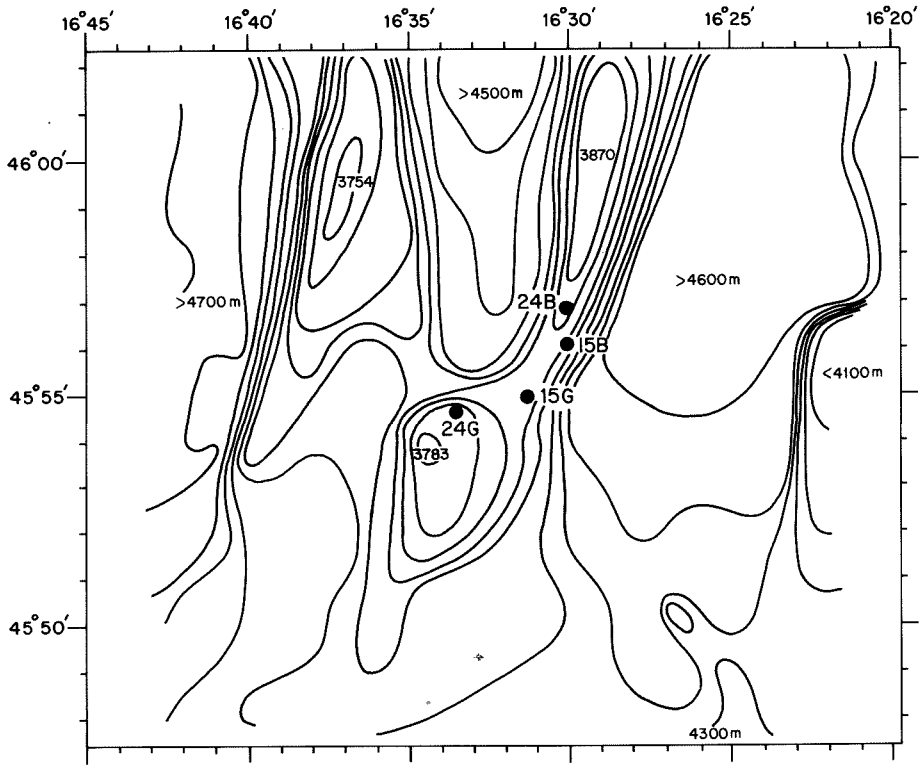

Fig.3.9. Map of the area around Finn seamount (from DICKSON, 1983, adjusted according to our own soundings) with locations of cores.

inferred sediment accumulation rate in comparison with other cores from similar depths (Fig. 3.4). Moreover, it could not explain the occurrence of *Globorotalia hirsuta* at 96 cm depth. We therefore consider the data as indications of a slide or slump. The core was taken at 4000 m in the valley between two seamounts. The position of cores 8215G and 8215B is indicated in Fig. 3.9 on a map of the Finn seamount area (after DICKSON, 1983, and adjusted using our own soundings). A 25% slope was preserved in boxcore 8215B. The supposed slide in core 8215G may have been derived from the steep hillsides of the neighbouring seamounts.

Core 8208G (of which the top was lost) contained several turbiditic deposits or slumped beds, as evidenced by data in Fig. 3.10. X-radiographs (Fig. 3.11) revealed the layered structure of these beds. The core was taken in the deep valley in the W part of the site, and the slides may have been derived from the hillsides nearby. The most evident slump or turbidite was found here at a depth of 173 cm in the core. At this depth, a recent sediment surface (^{14}C age 11-14 cm below the interface is 7500 yr) was covered by older sediment containing material with a ^{14}C age of 31 kyr and a bed of coarse grained sediment with anomalous elemental and mineralogical composition (see section 3.4). Benthic Foraminifera found in this turbiditic deposit were not different from the ones found in core tops in the area, suggesting a local origin of the material.

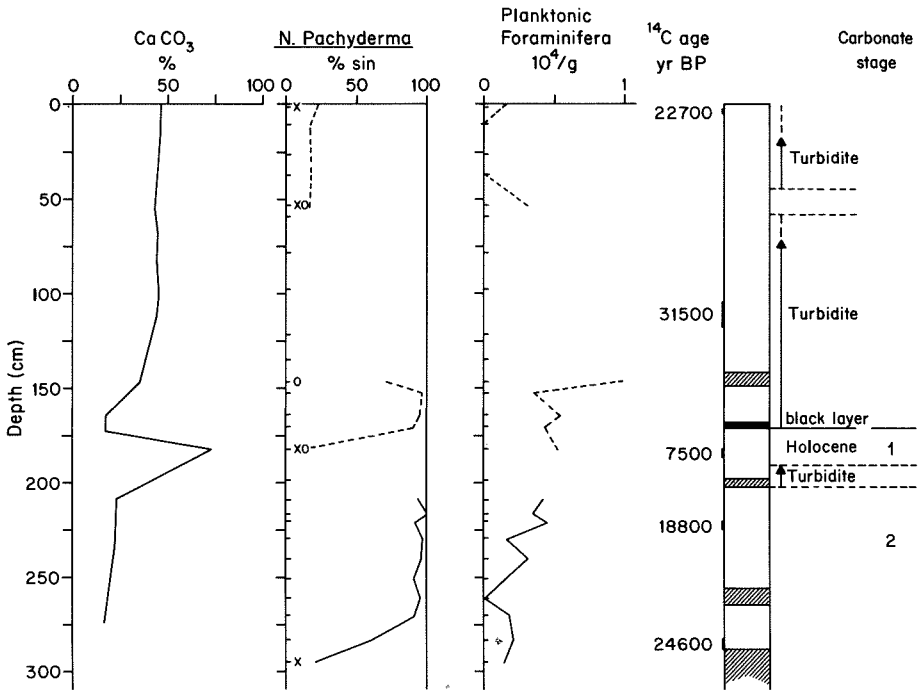

Fig.3.10. Sedimentological data of core 8G. For explanations see Fig.3.6.

WEAVER & SCHULTHEISS (1983b) showed that gravity cores may repenetrate the sediment and thus resample the sediment surface. This explanation for the occurrence of recent material below the slumped bed is unlikely because no sudden decrease in wire tension was observed after the extraction of the corer from the seabottom. Moreover, the black colour of the interface indicates reducing conditions, a usual phenomenon when fresh organic material is covered by a slump or turbidite. The coincidence that a repenetration would have occurred just below such an interface appears quite unlikely.

The high nitrate concentration in the pore water of the buried layer, relative to the layers above and below (Fig. 3.12) indicates that the turbidite occurred even more recently. Even though the actual NO_3 gradient in and around the layer is poorly known, the mere existence of the nitrate maximum allows some interesting conclusions to be made. Nitrate reduction has apparently caused a decrease in NO_3 above and below the buried top layer of about 25 cm. A minimum estimate of the upward and downward diffusive fluxes from this layer, obtained by assuming a linear gradient between sampling intervals, is 3.6 and 2.8 10^{-15}mol.cm^{-2}s^{-1}, respectively (porosity = 0.75; $D_s(NO_3)$ = 3.5 10^{-6} cm^{2}s^{-1}). The amount of nitrate initially present in the buried top 25 cm can be estimated as 1.0 10^{-6} mol.cm^{-2} from the nitrate profile in the top sediment of a boxcore taken nearby (Fig. 3.12.b, curve A), augmented by the nitrate resulting from oxidation of organic matter with buried oxygen (16/138 times the O_2 inventory in the same boxcore)(curve B). Diffusion along the gradients in Fig. 3.12.a transports away this nitrate at a rate that would cause the concentration to fall below the observed value within a few years.

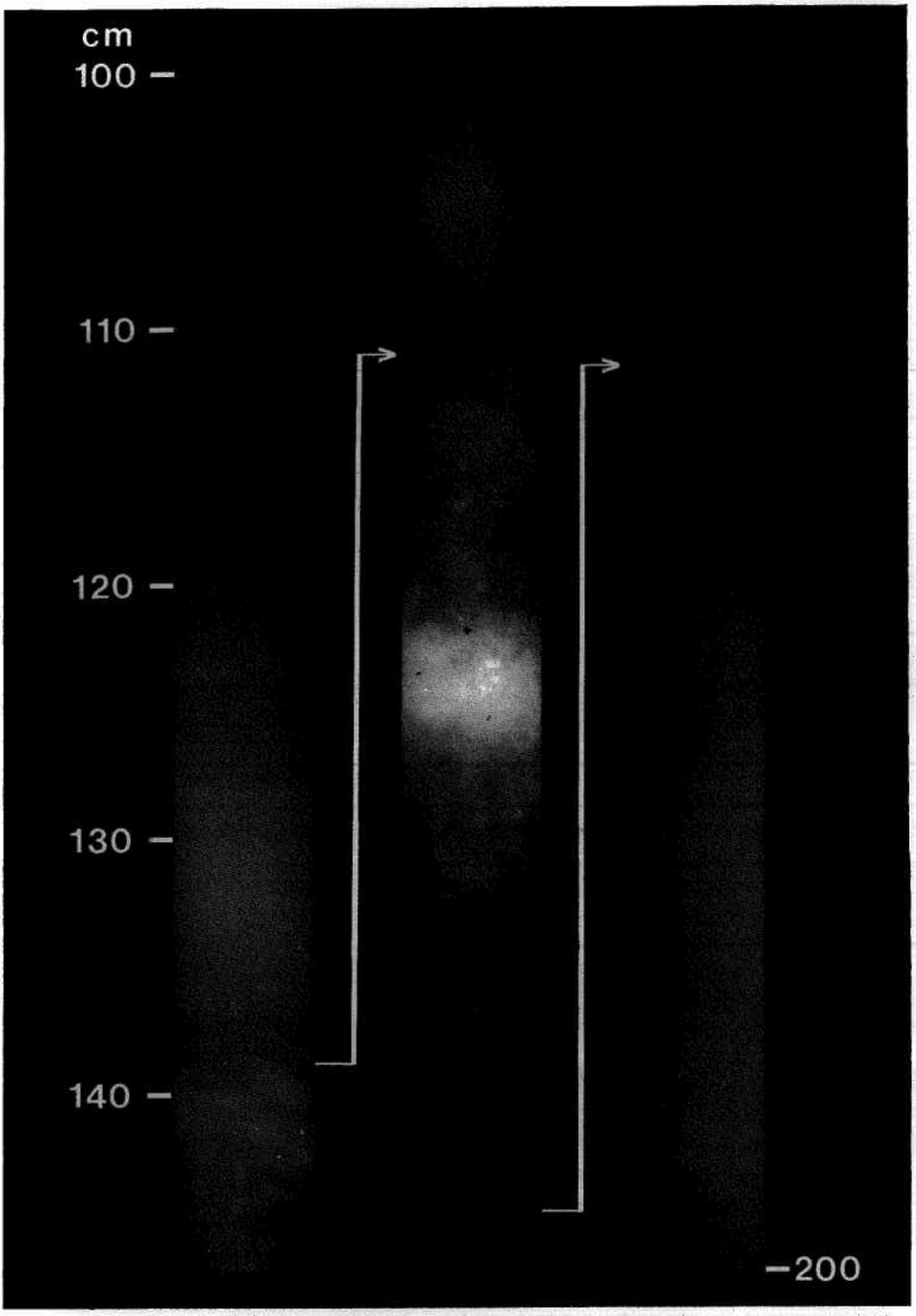

Fig.3.11. X-radiograph of the 100 to 200 cm section of core 8G, showing layered structure indicative of a turbiditic deposit.

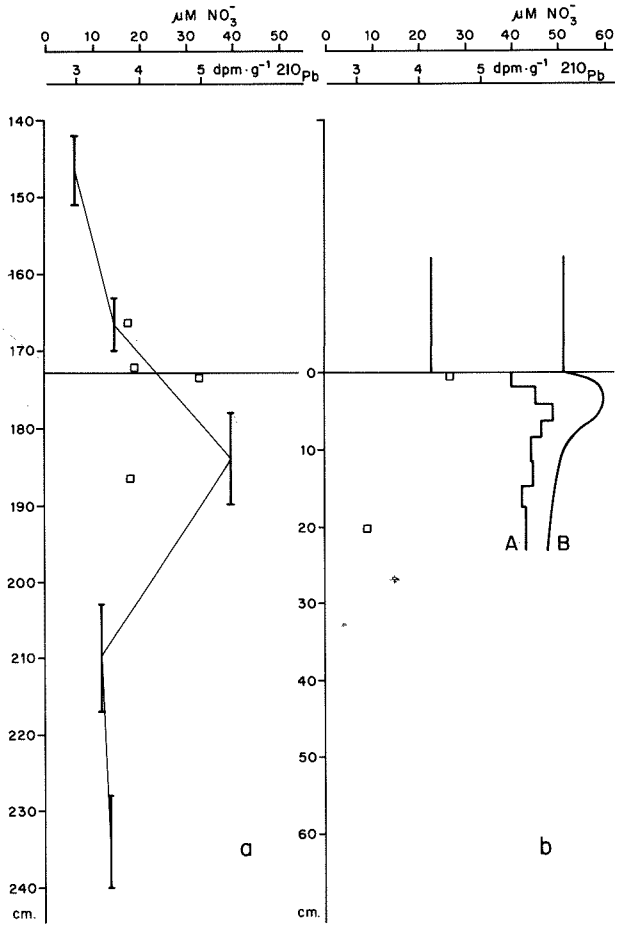

Fig.3.12. a. Interstitial nitrate (vertical bars) and ^{210}Pb activity (open squares) around the buried interface in core 8G, b. interstitial nitrate (curve A) and potential nitrate (curve B, including nitrate produced by oxic mineralization) and ^{210}Pb activity (open squares) in nearby boxcore 8B.

Additional evidence for the recent date of this slump comes from ^{210}Pb data , showing that some ^{210}Pb (halflife 22.3 yr) is left at the buried sediment surface. A calculation of excess ^{210}Pb is not possible for lack of data on the ^{226}Ra background of the samples.

The nitrate and ^{210}Pb data indicate that the slump must have occurred during the past few years and may have been triggered by a dumping operation.

3.4 ELEMENTAL AND MINERALOGICAL COMPOSITION OF THE SEDIMENT

3.4.1. MINERALOGICAL COMPOSITION

Remains of Foraminifera and coccoliths (mainly calcite) make up the bulk of the sediment. X-ray diffraction patterns of the fine fraction ($< 2\ \mu m$) of the non-carbonate phase of 32 samples taken from boxcores (1,4,8, and 15) as well as from several meters depth in gravity cores (8 and 11) , show a remarkably constant composition of the clay minerals smectite, illite, chlorite and kaolinite. This constant composition of the clay fraction was confirmed by RUCH *et al.*(1984). These authors found the following average composition of the clay fraction of the carbonate-free material in the 22-cm boxcore from station 8: 4% K-feldspar, 5% plagioclase, 14% kaolinite, 12% chlorite, 45% mica-phengite, 4% quartz, 2% amphibole and 14% smectite (note: all data expressed as relative peak intensities in the X-ray diffractograms). In the 2-16 μm fraction, RUCH *et al.* observed a distinct trend of downcore increasing amounts of K-feldspar, plagioclase, quartz and amphibole, and decreasing amounts of chlorite, kaolinite and especially mica-phengite in the boxcore below the bioturbated layer. They interpreted these trends as the result of the slowly changing regime in sedimentation since the last glaciation: a decreasing input of ice-rafted material and an increasing input of tropical/temperate origin.

We observed a similar signal of ice-rafting in the mineralogical composition of the bulk non-carbonate phase of samples of box- and gravity cores from the same station: A coarse-grained bed in the turbiditic deposit in core 8G (143-155 cm, Figs. 3.10 and 3.11), had a relatively low smectite content but high contents of quartz, feldspar, dolomite, vermiculite and amphibole. This material also had an anomalous trace element composition and cation exchange capacity (see below). Similar beds showed up on X-radiographs of other gravity cores (Figs. 3.6 and 3.8), and contain apparently ice-rafted material. .

3.4.2. MAJOR ELEMENTS

The elemental composition of the sediment has been determined by EGTA titration (Ca) and Atomic Absorption Spectroscopy (Sr) of the HCl extract and by neutron activation (NA) and X-ray fluorescence (XRF) of bulk samples. $CaCO_3$ content of the sediment varies between 82% and 88% at the sediment surface down to 3.5% in a deposit from the glacial maximum at 70000 BP (Fig. 3.4). HCl-extractable Sr covaries with Ca (Sr/Ca $= 2.10^{-3}$, atomic ratio). Most elements, however, are associated with the non-carbonate fraction. It is therefore appropriate to express the elemental composition on a carbonate-free basis. From the correlation of Ca content with the results of XRF analyses for other major elements in 28 samples (from various depths in boxcores 1B ,4B, 8B, and 15B, and in gravity cores 8G and 11G), the major element composition of the carbonate-free material has been calculated by extrapolation to 0% $CaCO_3$ (Table 3.III). The concentrations of the major element oxides add to 90%; loss on ignition accounts for the remaining 10%. The results compare well with the data obtained with other methods by our Swiss colleagues for surface samples from the same stations (Table 3.III).

Table 3.III. Major element composition of NEA dumpsite sediments expressed on dry $CaCO_3$-free basis

source:				
reference	1)		2)	3)
stations	1, 2, 4, 8 11, 13, 15		1, 2, 4, 6 11, 13, 15	6
sediment depth(cm)	0-220		0-1	0-8
method *	XRF	NA	EDAX	NA
composition (%):				
SiO_2	56.5		59.2	53.5
Al_2O_3	17.0		17.1	20.0
Fe_2O_3	7.4	7.8	4.9	7.5
K_2O	3.9	3.3	2.4	4.0
TiO_2	0.8		<5	0.9
MgO	3.5			
Na_2O	0.8			

1) This work
2) data of Jaquet in Rutgers van der Loeff et al. (1985)
3) Wyttenbach and Tobler (1984)

*: XRF=X-ray fluorescence; NA=neutron activation analysis; EDAX=Energy dispersive X-ray analysis.

3.4.3. TRACE ELEMENTS

Fig. 3.13 shows the relation with $CaCO_3$ of selected elements in 44 sediment samples, analysed with neutron activation analysis. These samples are taken from 9 cores distributed over the dumping area (Boxcores 1, 2, 4, 8, 13, and 15; gravity cores 8, 11, and 15) and vary in sediment depth from 0-1.5 cm (surface) to 215 cm. The samples were not washed in order to prevent any loss of trace elements by the rinsing procedure, but the results were corrected for salt errors from chloride measurements in acetic acid/acetate extracts (pH 5). A list of correlations of various elements with $CaCO_3$ content is given in Table 3.IV. The sample from the coarse-grained layer in the turbidite from core 8208G deviates from all linear correlations: the coarse admixture, consisting predominantly of quartz and feldspar, reduces not only the smectite content and cation exchange capacity, but also the trace element contents. The linear relations shown in Fig. 3.13 suggest a conservative mixing of carbonate and non-carbonate fractions. The estimates of the concentrations in the detrital phase, calculated from extrapolation to 0% $CaCO_3$, are compared in Table 3.IV with data of WYTTENBACH & TOBLER (1984) for surface sediments of the dumpsite. The concentration of the carbonate endmember could also be estimated from these correlations, but these estimates are very sensitive to the presence of a third phase, like hydroxides and adsorbed water, and to small errors in the Ca determination. Indeed, the sum of $CaCO_3$ content and the residual weight after dissolution of

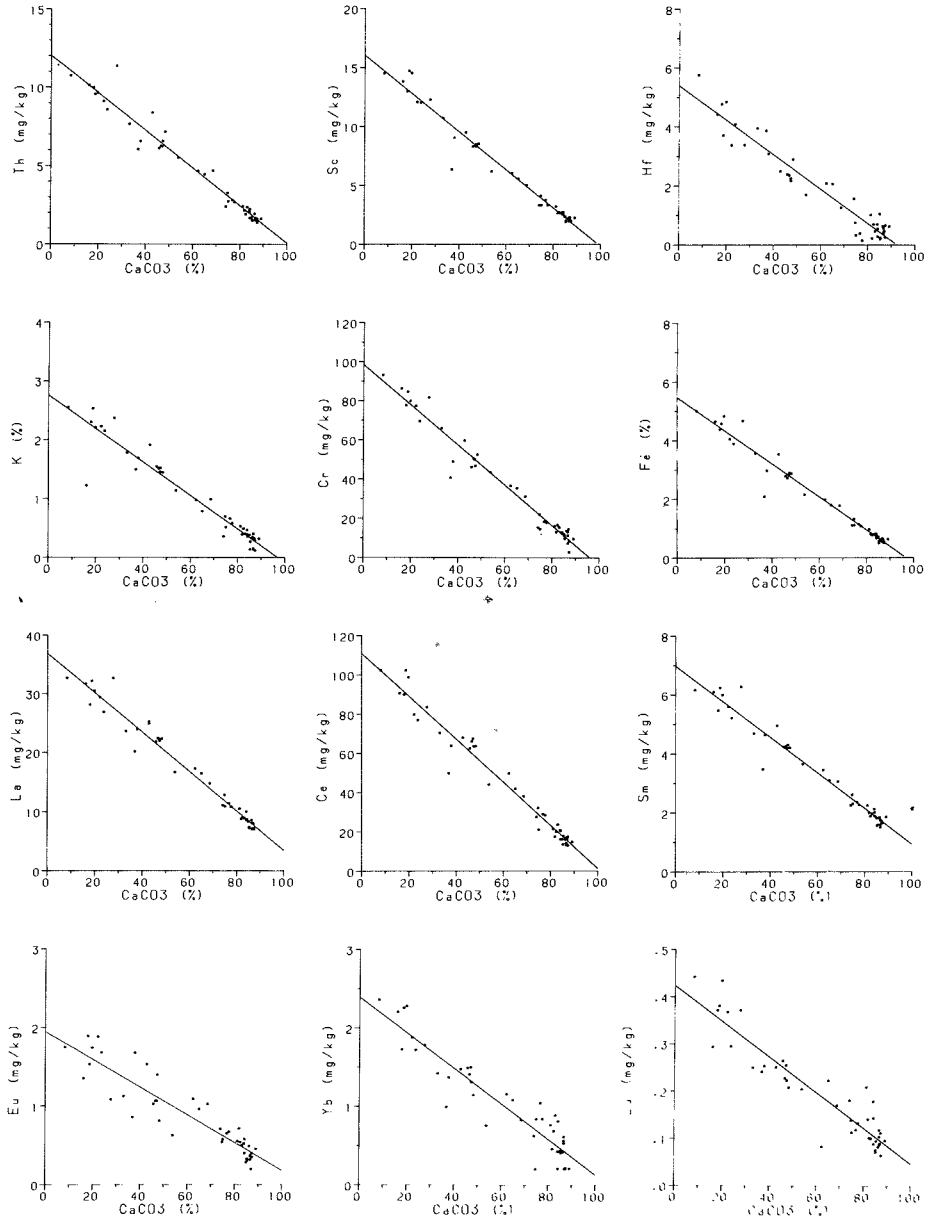

Fig.3.13. Contents of some major and trace elements as a function of $CaCO_3$ content in 44 sediment samples.

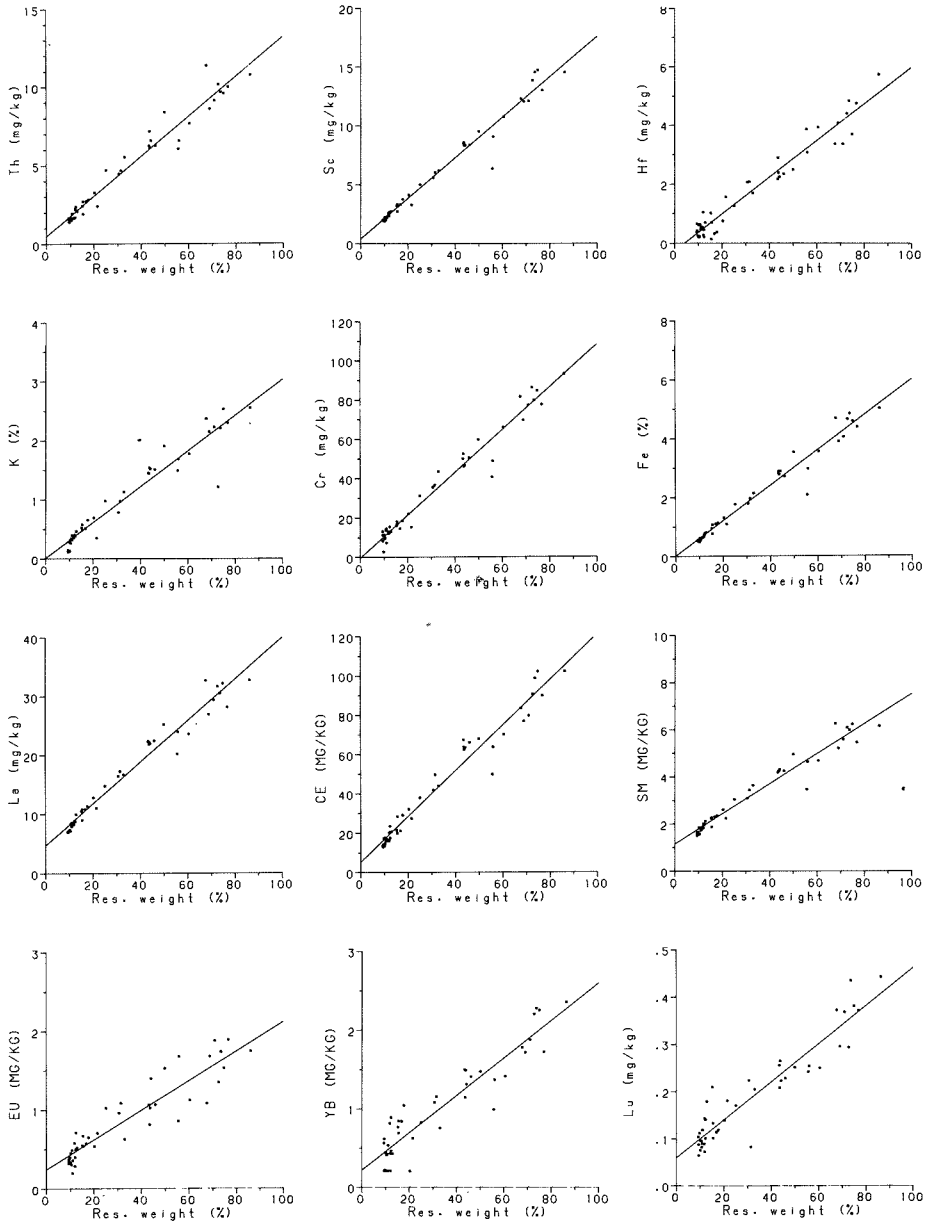

Fig.3.14. Contents of some major and trace elements as a function of weight remaining after dissolution of $CaCO_3$ in 44 sediment samples.

Table 3.IV. Linear correlation coefficients of concentrations of various elements and $CaCO_3$ in 44 sediment samples and estimates (± standard errors) of the contents in the residual phase, compared with literature data.

	conc. unit	correlation results r^2	correlation results extrapolated concentration at 0 % $CaCO_3$	literature data 1)	literature data 2)
Th	mg/kg	0.962	12.0 ± 0.3	17.4 ± 0.8	
Sc	mg/kg	0.969	16.0 ± 0.3	19.9 ± 0.5	
Hf	mg/kg	0.931	5.4 ± 0.2	4.9 ± 0.3	
K	%	0.922	2.76 ± 0.09	2.79 ± 0.07	
Cr	mg/kg	0.966	98.3 ± 1.9	101 ± 4	
Fe	%	0.966	5.46 ± 0.10	3.94 ± 0.16	
Co	mg/kg	0.825	23.4 ± 1.0	10.8 ± 0.2	
La	mg/kg	0.970	36.8 ± 0.7	26.5 ± 0.5	46.4
Ce	mg/kg	0.964	110.8 ± 2.2	48.8 ± 1.2	92.3
Sm	mg/kg	0.961	7.0 ± 0.1	3.4 ± 0.1	7.5
Eu	mg/kg	0.842	1.95 ± 0.08	0.71 ± 0.02	1.67
Yb	mg/kg	0.874	2.39 ± 0.09	1.76 ± 0.09	3.20
Lu	mg/kg	0.866	0.42 ± 0.02	0.28 ± 0.01	.50

1) Analysis of residual material after leaching surface sediments with 1 n HCl, Wyttenbach and Tobler (1984)
2) REE contents in lithogenic phase of surface sediments according to partitioning model of Peterson et al., 1986 (see section 3.6.4).

Table 3.V. Linear correlation coefficients of concentrations of various elements with residual weight in 44 sediment samples and estimates (± standard errors) of the contents in the carbonate phase, compared with literature data.

	conc. unit	correlation results r^2	correlation results extrapolated concentration at 0 % residual weight	literature data 1)	2)	3)	4)	5)
Th	mg/kg	0.959	0.5 ± 0.2	-0.11 ± 0.04				
Sc	mg/kg	0.971	0.4 ± 0.2	-0.029 ± 0.052				
Hf	mg/kg	0.947	-0.2 ± 0.1	-0.030 ± 0.023				
K	%	0.929	0.01 ± 0.06					
Cr	mg/kg	0.966	-0.3 ± 1.4	-0.67 ± 0.75				
Fe	%	0.966	0.02 ± 0.08	0.09 ± 0.05			0.22	0.0006
La	mg/kg	0.966	4.7 ± 0.5	4.74 ± 0.87	3.21	2.02	5.85	0.64
Ce	mg/kg	0.960	5.3 ± 1.6	1.80 ± 0.77	3.15	0.66	7.19	0.47
Sm	mg/kg	0.956	1.2 ± 0.1	0.63 ± 0.14	0.85	0.67	1.28	0.11
Eu	mg/kg	0.848	0.24 ± 0.06	0.12 ± 0.02	0.19	0.15	0.30	0.027
Yb	mg/kg	0.869	0.22 ± 0.07	0.38 ± 0.06	0.41	0.34	0.61	0.10
Lu	mg/kg	0.880	0.06 ± 0.01	0.07 ± 0.01	0.053	0.040		

1) Correlation against $CaCO_3$ in limestone deposits (Parekh et al., 1977)
2) Correlation against Al in surface sediments dumpsite (Peterson et al., 1986)
3) REE contents in $CaCO_3$ phase of surface sediments according to partitioning model of Peterson et al., 1986 (see section 3.6.4)
4) Cleaned Foraminifera (Palmer, 1985)
5) Calcite lattice in Foraminifera (Palmer, 1985)

$CaCO_3$ with acid is only 96% (PETERSON *et al.*, 1986, found 94% for surface sediments of the dumpsite). The concentration in the carbonate endmember can therefore more accurately be determined from a plot of the elemental concentration versus the residual weight, and extrapolation to 0% residual weight (Table 3.V). Since $CaCO_3$ content and residual weight are highly correlated ($r^2 = 0.993$), the resulting values are close to extrapolated values of the correlations against $CaCO_3$ to 96% $CaCO_3$.

This procedure shows that the Fe, K, Hf, Cr, and Sc contents of the carbonate phase are not significantly different from zero. The rare earth elements, however, have significant concentrations in the carbonate endmember. In Table 3.V these data are compared with similar analyses of surface sediments from the dumpsite (PETERSON *et al.*, 1986), with analyses of limestone deposits by PAREKH *et al.* (1977) and with REE analyses of Foraminifera tests by PALMER (1985). It has been pointed out by PALMER (1985) that only about 10% of REE in Foraminifera tests is present in the calcite lattice, the remaining 90% being associated with coatings (presumably oxyhydroxides) on the calcite skeletons. The diagenetic behaviour of hydroxyde-associated REE will be discussed in section 3.6.4.

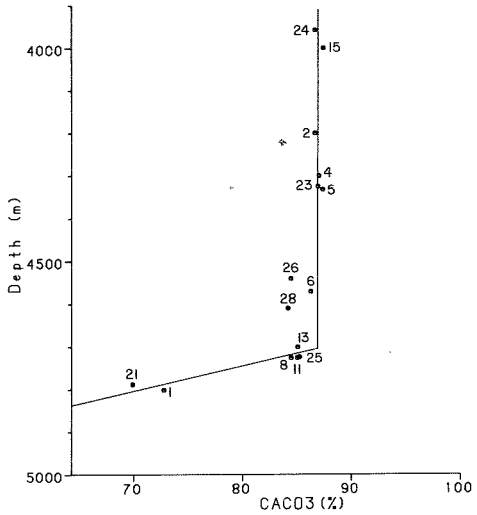

Fig.3.15. Boxcore-top calcium carbonate content as a function of water depth. station numbers are indicated.

A plot of boxcore-top carbonate contents as a function of water depth (Fig. 3.15) shows that the lysocline is situated at a depth of about 4700m at present. The factors affecting $CaCO_3$ dissolution are discussed in section 3.5.3.

From a bathymetric map of the dumping area (Fig. 2.1) and Fig. 3.15, a map could thus be constructed showing the distribution of $CaCO_3$ in surface sediments (Fig. 3.16). This same map can be used to show the distribution of other elements in surface sediments, using the correlations with $CaCO_3$ in Fig. 3.13 and in Table 3.IV.

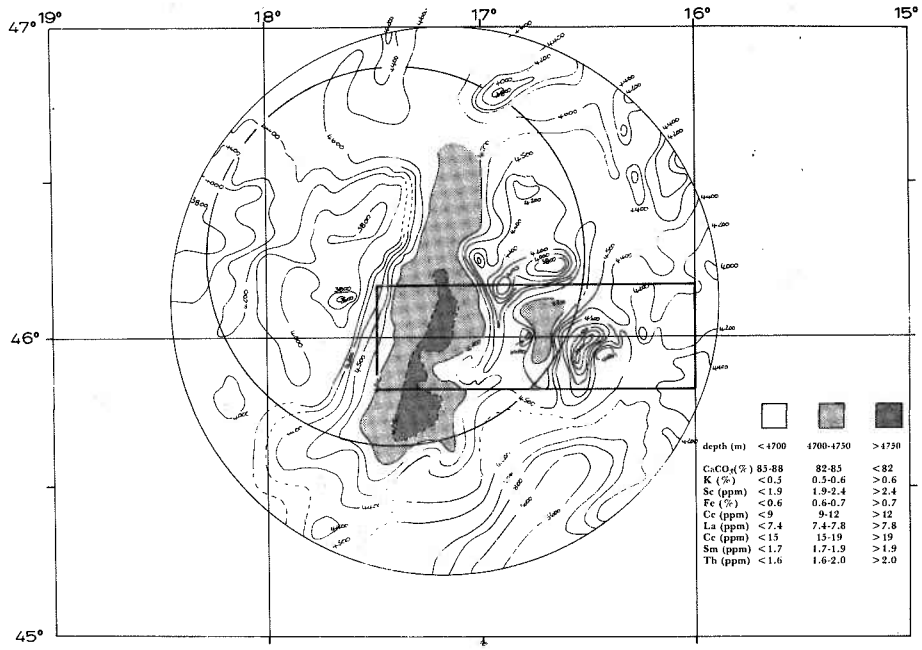

Fig.3.16. Distribution in surface sediments of the dumping area of $CaCO_3$ and of some of the elements that are well correlated with carbonate content.

3.5. EARLY DIAGENETIC REACTIONS IN THE SEDIMENT

Particles that have settled on the ocean floor are buried by bioturbation and new deposition, and become part of the sedimentary record. However, a suite of organic and inorganic reactions changes the composition of the material dramatically with time. The physical, chemical and biological processes taking place in the upper few hundred meter of the sediment (*i.e.* young enough to be unaffected by elevated temperatures or uplift above the sealevel) are collectively denoted by the term early diagenesis (BERNER, 1980). In the present study, only processes occurring in the upper few meters are of interest, and these are clearly all part of early diagenesis. In this section, we will discuss those diagenetic reactions that are known or can be expected to influence the behaviour and transport of trace elements and radionuclides. In the next section (3.6) this information will be used as a framework for the discussion of the diagenesis of trace elements.

3.5.1. MINERALIZATION OF ORGANIC MATTER

Organic matter settles continuously on the sediment surface. In section 3.7 it will be shown that the organic carbon content of freshly settled material is in the order of 40 $mg.g^{-1}$. Surface-deposit feeding organisms mix this material quickly down and start its decomposition, and consequently the organic carbon content of the surface sediment is already much lower: 2.8 $mg.g^{-1}$. Continued mineralization reduces this value further to

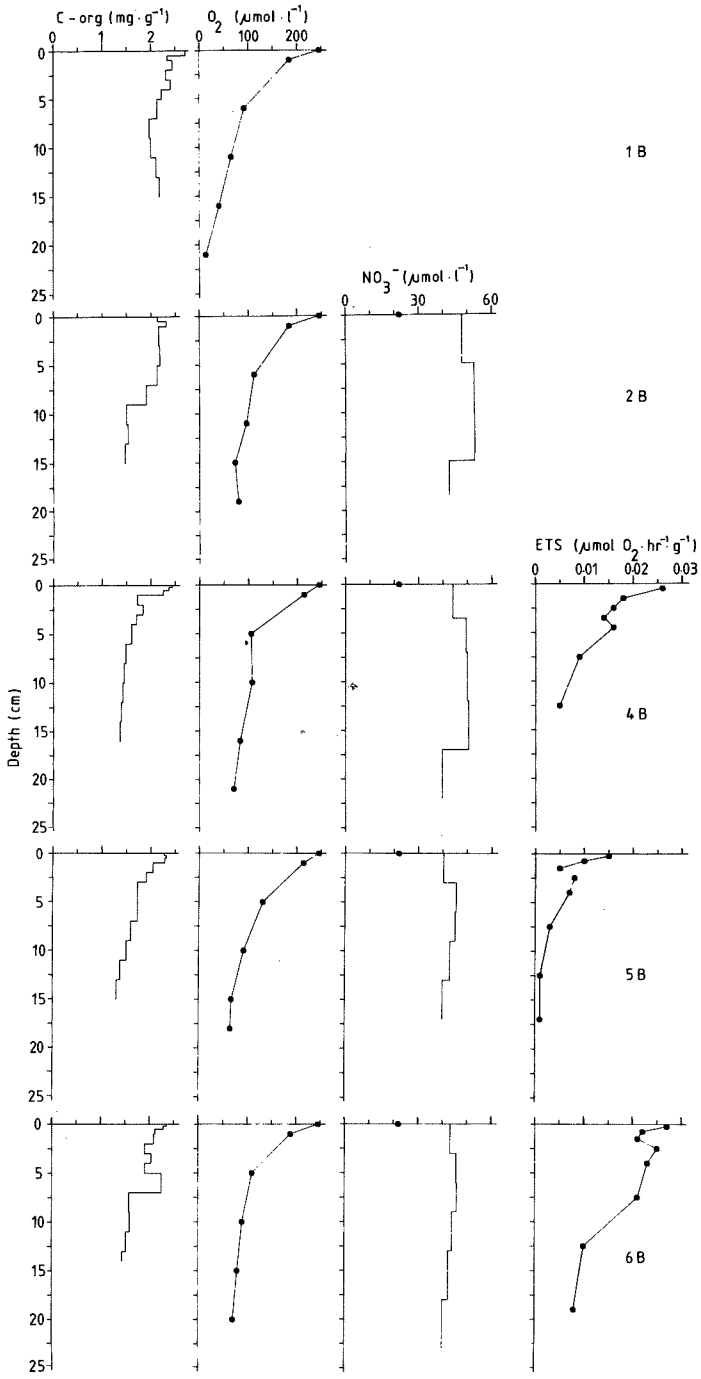

Fig.3.17. Depth distribution in boxcores of organic carbon in the sediment, of oxygen and of nitrate in the pore water, and of ETS activity (on a wet-weight basis) in the sediment.

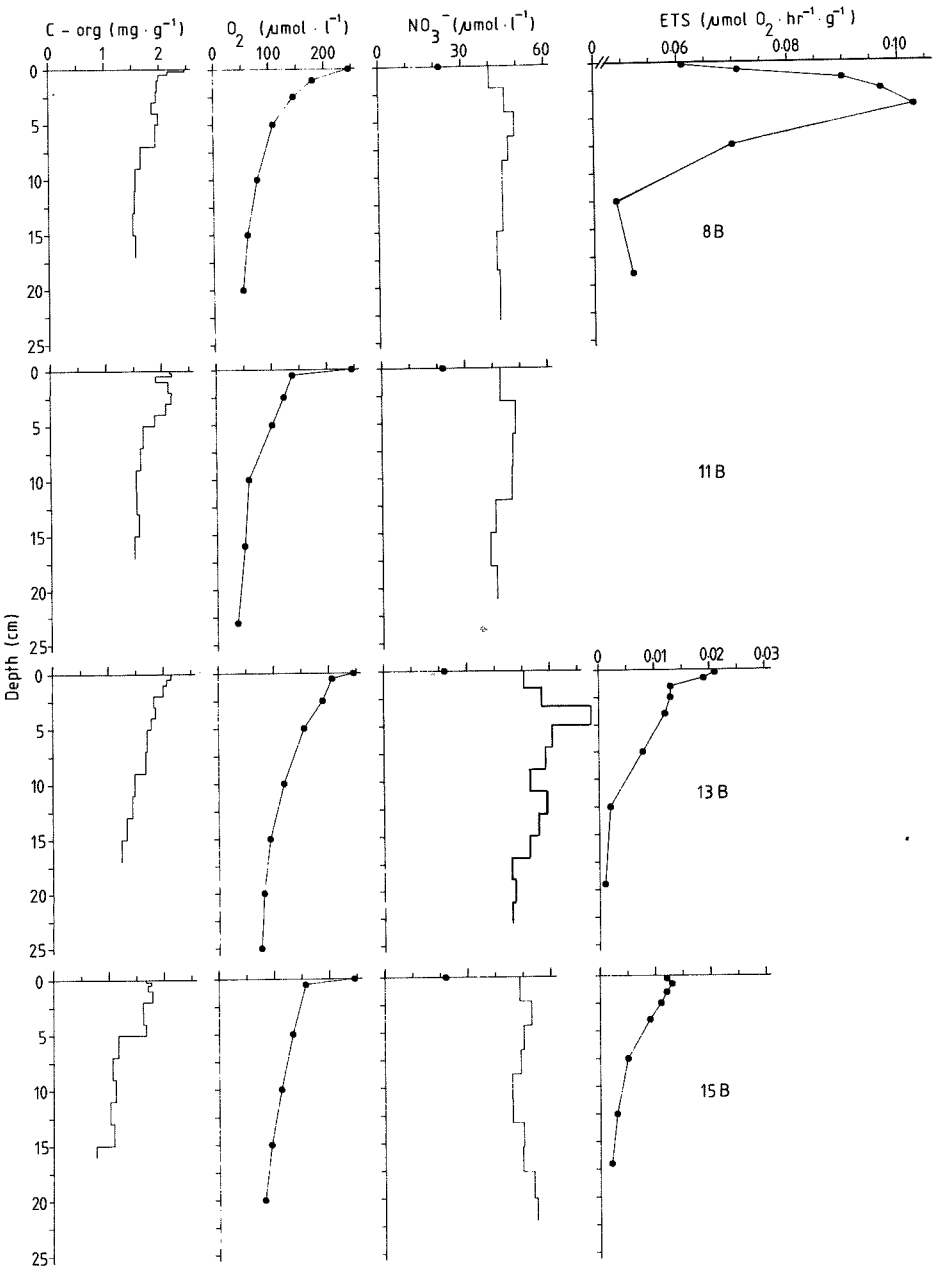

Fig.3.17. continued

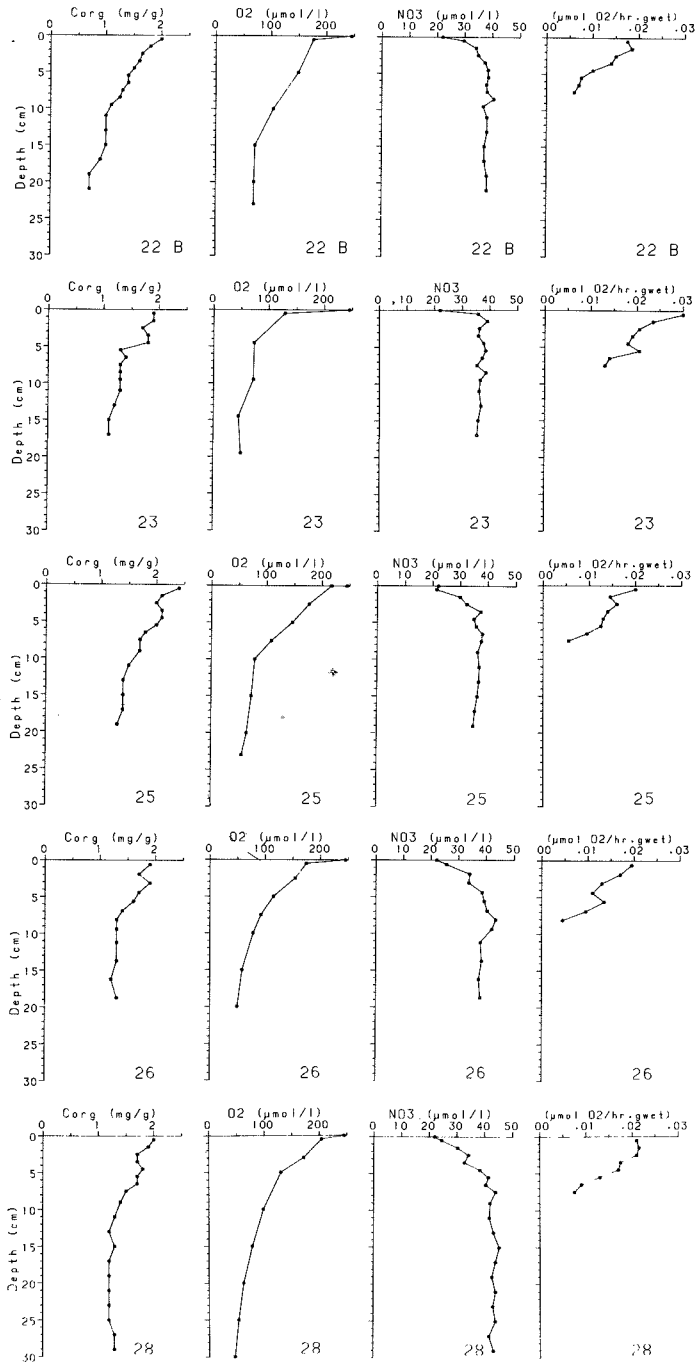

Fig.3.17. continued

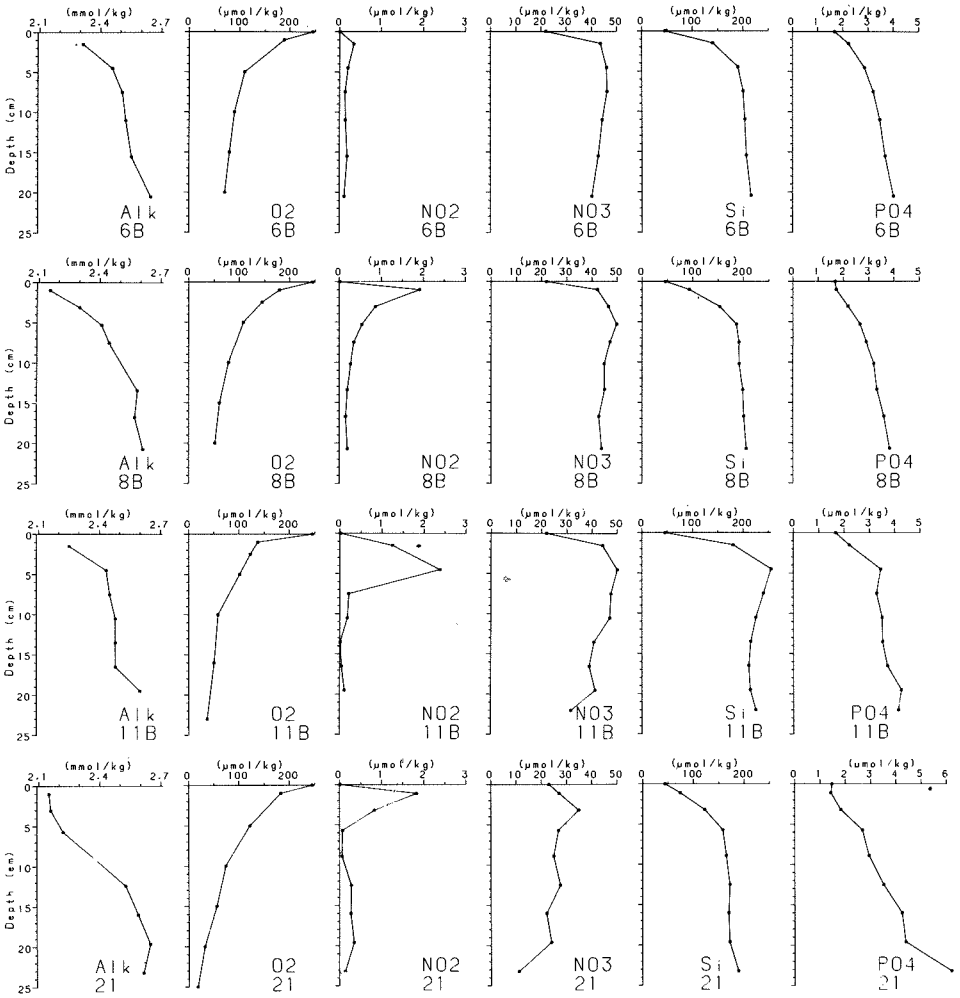

Fig.3.18. Depth distribution of alkalinity, oxygen and nutients in the pore water of boxcores 6B, 8B, 11B, and 21B.

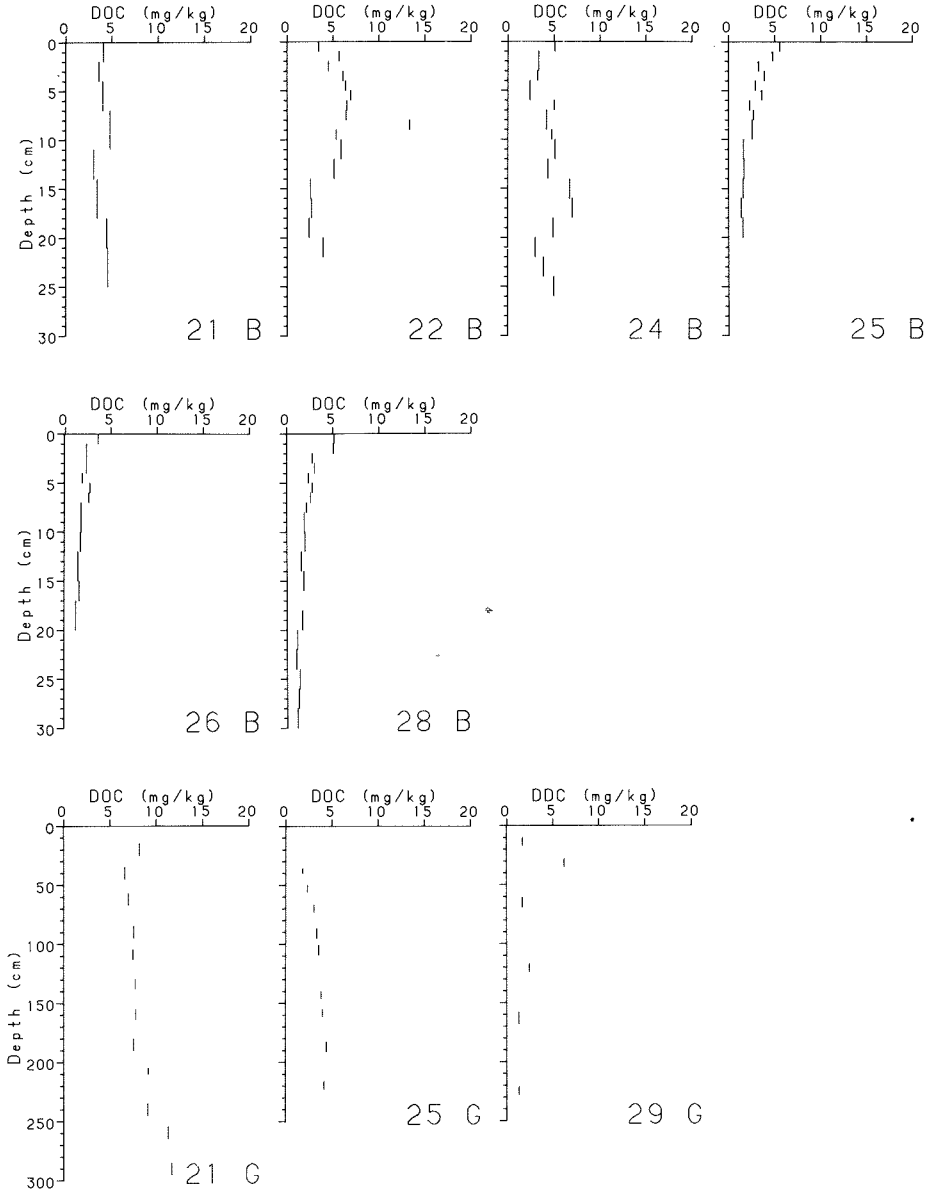

Fig.3.19. Depth profiles of dissolved organic carbon (DOC) in the pore water of boxcores and gravity cores.

about 1.5 mg.g^{-1} at 20 cm depth (Fig. 3.17). The decrease in organic carbon content with depth is associated with an increase with depth in the concentrations of nutrient elements and alkalinity in the pore water (Fig. 3.18).

During the second expedition, dissolved organic carbon (DOC) was measured in the pore water. Although the results are rather scattered, a trend of decreasing DOC concentration with depth in the boxcores was observed (Fig. 3.19). The concentrations are well above the bottom water concentration of 0.4 mg.l^{-1} (section 3.8).

The depth distribution of potential Electron Transport System (ETS) activity (Fig. 3.17) shows that mineralization activity is highest in the upper few cm, in accordance with the carbon and oxygen data. The subsurface maximum in organic carbon content and ETS activity observed in some boxcores at a depth of 2 to 6 cm is discussed in section 5 (bioturbation).

The mobilization of elements that are constituent of or bound to organic material, is inherent to the process of mineralization. Br and I are predominantly associated with organic matter (ULLMAN & ALLER, 1980), and their concentration in the sediment decreases with depth very much as organic carbon (Fig. 3.20) although WYTTENBACH (in RUTGERS VAN DER LOEFF *et al.*, 1985) pointed out that the half removal depths are different: 10 cm for Br and 25 cm for I compared to 8 cm for metabolizable organic C. The release of nutrients was shown above. Other elements released in this process are Ni, Cd (KLINKHAMMER *et al.*, 1982), Cu (KLINKHAMMER, 1980; CALLENDER & BOWSER, 1980), while the distributions of many more elements in sea water are correlated with those of the nutrients (reviewed by Quinby-Hunt and Turekian, 1983). In section 3.7 it will be shown how diagenetic modeling can be used to derive rates of mineralization and of trace element mobilization from measured concentration-depth profiles.

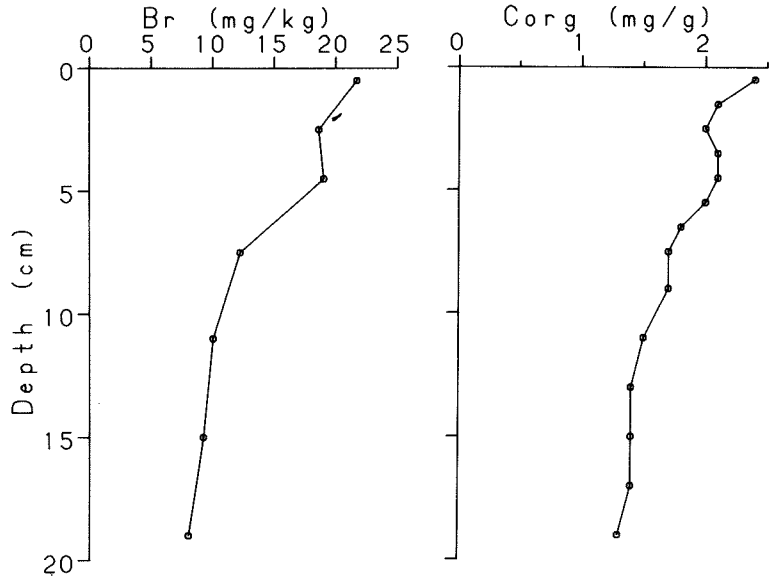

Fig.3.20. Depth profile of Br and organic C in the sediment of core 25B.

3.5.1.1. SEQUENCE OF ELECTRON ACCEPTORS AND CHANGES IN REDOX CONDITIONS

The consumption of electron acceptors for the mineralization of organic matter leads to a reduction of redox potential (Eh) with sediment depth. Redox conditions have a profound influence on distribution coefficients and transport of trace elements within the sediment. Because of problems in the quantitative interpretation of Eh readings with platinum electrodes (BRECK, 1974; WHITFIELD, 1974 VERSHININ & ROZANOV, 1982), the redox state of the sediment should preferably be studied by analysis of the concentrations of redox species involved. In deep-sea sediments poor in organic matter, like the sediments at the dumpsite, the zones of O_2, Mn, NO_3^-, Fe and sulfate reduction are distributed over a relatively wide depth range, and the successive depletion of these electron acceptors can be studied in detail (FROELICH *et al.*, 1979, EMERSON *et al.*, 1980).

Table 3.VI. (a) Stoichiometry of the organic matter oxidation reactions listed in the order in which they should occur (based on free energy released) in the environment, and of the calcium carbonate dissolution/precipitation reaction. (b) The relative changes in oxidants and alkalinity during organic matter degradation in the presence and absence of calcium carbonate. (after Emerson *et al.*, 1980, 1982).

(a) (C:N:P = 106:16:1)

(1) Oxygen reduction:

$$138\ O_2 + C_{106}H_{263}O_{110}N_{16}P + 18\ HCO_3^- = 124\ CO_2 + 16\ NO_3^- + HPO_4^{2-} + 140\ H_2O$$

(2) Nitrate reduction:

$$94.4\ NO_3^- + C_{106}H_{263}O_{110}N_{16}P = 13.6\ CO_2 + 92.4\ HCO_3^- + 55.2\ N_2 + 84.8\ H_2O + HPO_4^{2-}$$

(3) Mn^{4+} reduction:

$$236\ MnO_2 + C_{106}H_{263}O_{110}N_{16}P + 362\ CO_2 + 104\ H_2O = 470\ HCO_3^- + 8\ N_2 + 236\ Mn^{2+} + HPO_4^{2-}$$

(4) Fe^{3+} reduction:

$$212\ Fe_2O_3 + C_{106}H_{263}O_{110}N_{16}P + 740\ CO_2 + 316\ H_2O = 846\ HCO_3^- + 424\ Fe^{2+} + 16\ NH_3 + HPO_4^{2-}$$

(5) Sulfate reduction:

$$53\ SO_4^{2-} + C_{106}H_{263}O_{110}N_{16}P = 39\ CO_2 + 67\ HCO_3^- + 16\ NH_4^+ + 53\ HS^- + 39\ H_2O + HPO_4^{2-}$$

(6) $CaCO_3$ dissolution/precipitation:

$$CO_2 + H_2O + CaCO_3 = 2\ HCO_3^- + Ca^{2+}$$

(b) relative changes in oxidants, phosphate and alkalinity

	ΔO_2	ΔNO_3^-	ΔMn^{4+}	ΔFe^{3+}	ΔSO_4^{2-}	ΔP	Δ Alkalinity *	**	***
O_2 reduction (1)	-1	-	-	-	-	0.007	-0.12	1.68	1.50
NO_3^- reduction (2)	-	-1	-	-	-	0.011	1.0	1.29	1.15
Mn^{4+} reduction (3)	-	-	-1	-	-	0.004	2.0	-1.08	-0.96
Fe^{3+} reduction (4)	-	-	-	-1	-	0.002	2.0	-1.49	
SO_4^{2-} reduction (5)	-	-	-	-	-1	0.019	2.3	3.77	

* without reaction (6)
** assuming reaction (6) goes all the way to right or left to consume CO_2
*** considering reequilibration of reaction (6) (Emerson et al., 1982)

Electron acceptors are used in the order of the free energy change associated with the transfer of one electron from the organic matter to the electron acceptor. The sequence of reactions involved is given in Table 3.VI. The free energy change of reactions (2) and (3) is very similar: their order in the sequence depends on the phase in which MnO_2 occurs (FROELICH *et al.*, 1979). The table also gives the associated chemical shifts, and the shifts in alkalinity if all CO_2 produced is neutralized by the dissolution of an equivalent amount of $CaCO_3$ according to reaction (6) (EMERSON *et al.*, 1980, 1982). Equilibrium with $CaCO_3$ is a reasonable assumption since $CaCO_3$ is present at all depths, and pH had a constant value of 7.75 $\pm$ 0.05 in the boxcores, and did not decrease below 7.6 at greater depth. (note: pH values measured on-board ship are affected by $CaCO_3$ precipitation during decompression; *in situ* pH measurements are not available).

3.5.1.2. OXYGEN REDUCTION

As a result of the consumption of oxygen for the mineralization of organic matter, the dissolved oxygen concentration in the pore water decreases with increasing depth in the sediment. At the start of this study, no literature data were available on dissolved oxygen concentrations in deep Atlantic sediments. From Ca and alkalinity data of *in situ* sampled pore waters SAYLES (1981) concluded that oxygen respiration prevails down to about 30 cm in N.W. Atlantic carbonate oozes (depth range sampled: 3200-4300 m). In 1984, SØRENSEN & WILSON published oxygen profiles in a carbonate ooze in the equatorial Atlantic, indicating that half of the bottom water oxygen remains at 1m depth, and little consumption occurs between 1 and 2m (WILSON *et al.*, 1985). Similar profiles in the central equatorial Pacific (MURRAY & GRUNDMANNIS, 1980) and in the Angola Basin (RUTGERS VAN DER LOEFF, unpublished results) indicate that oxygen concentrations may level off at non-zero values in open-ocean carbonate oozes.

Dissolved oxygen measurements in sediments from the dumpsite show that oxygen declines most rapidly in the upper 5 cm, followed by a more gradual decrease (Fig. 3.17), in agreement with the ETS activity measurements. Oxygen is depleted at a depth of 60-100 cm. At slopes and topographic highs no anaerobic layers were reached in cores up to 2.5 m in length (Fig. 3.21, 3.22.b). The decreased oxygen penetration at increased water depth is also apparent from a plot of O_2 concentration at 20 cm sediment depth *vs.* water depth (Fig. 3.22.a). This relation contrasts with the usual trend of increasing oxygen penetration depth with increasing water depth that results from a decreasing supply of organic matter. The anomalous behaviour can be explained by winnowing of the sediment at local highs (KIDD, 1983), resulting in a net downslope transport of fine particles (see section 3.3). The accumulation of fine particles in the valleys could cause the shallower oxygen penetration through a higher organic matter content (Fig. 3.22.c) and a lower permeability of the sediment. In the valleys (core 11, 25, 27) the oxygen depletion is reached in a layer deposited during the last glaciation. This can be a coincidence and needs not to be related to a glacial to postglacial decrease in organic carbon burial as a result of the decrease in sediment accumulation rate (*cf.* THOMSON *et al.*, 1984). On slopes and topographic highs glacial sediments are oxidized throughout.

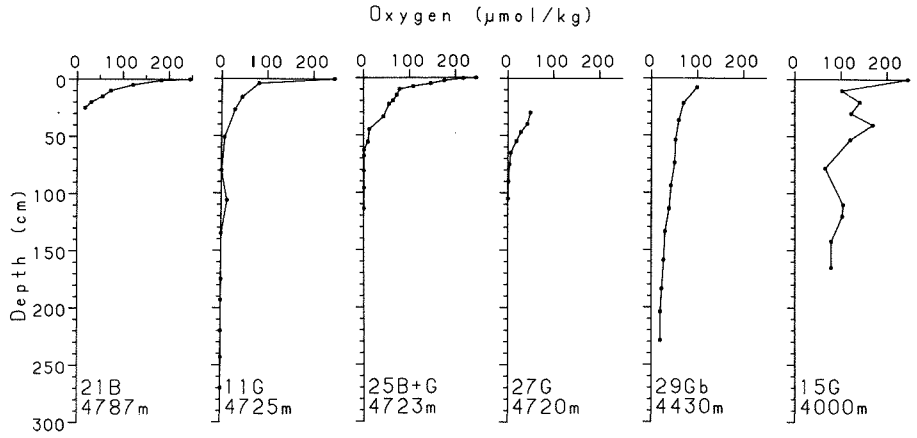

Fig.3.21. Depth profiles of dissolved oxygen in the pore water of gravity cores, in order of decreasing water depth.

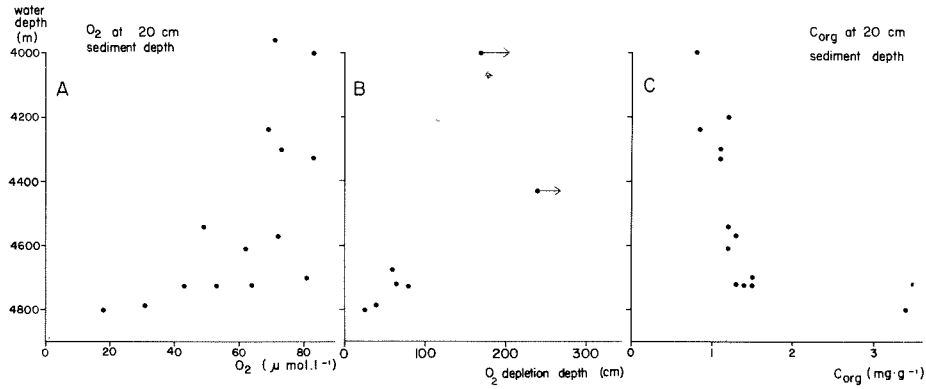

Fig.3.22. a: dissolved O_2 at 20 cm depth (bottom water value: 245 μmol.l^{-1}); b: O_2 depletion depth; c: organic carbon in the sediment at 20 cm depth *vs* water depth in dumpsite area.

The shallowest depth of oxygen depletion, about 25 cm, was observed in the Porcupine Abyssal Plain (core 1B and 21B, 4800 m, outside the dumping area). The colour of the sediment in the layer just above this depth suggests that pockets of oxygenated and oxygen-free sediment coexist here, which may cause a redistribution of trace elements between these phases (HARTMANN, 1979). The shallow oxygen penetration at this site is probably due to the oxygen demand of the buried turbiditic deposit (*cf.* WILSON *et al.*, 1985). It will be shown below that this turbidite is the only layer in the first few m of the local sediment where sulfate reduction plays a significant role. It can be expected that the same turbidite causes an equally shallow oxygen penetration in large areas of the Porcupine Abyssal Plain.

3.5.1.3. NITRATE, MANGANESE AND IRON REDUCTION

The succession of oxygen reduction by nitrate and manganese reduction is clearly seen in core 11G at 1 m depth (Fig. 3.23): Below 1 m, nitrate is depleted, and manganese is reduced and dissolves. Similar data were obtained at station 25, but the vertical resolution of the upper 22 cm was much improved by the use of boxcore samples. The results of the boxcore (0 to 22 cm) and the gravity core (25 to 250 cm) are presented together in Fig. 3.25. Although these cores (25B and 25G) were collected about 3 km apart, the sediment and pore water data fit very well into a single set of profiles. The mineralization of organic matter consumes first all oxygen (which is depleted at about 70-80 cm depth), and then reduces nitrate, Mn(IV) and Fe(III), and results in the dissolution of $CaCO_3$, the production of alkalinity and the release of Mn(II) and Fe(II) to the pore water.

The upward diffusion of manganese and its subsequent oxidation causes the well-known accumulation of Mn in the sediment in the aerobic zone (Figs. 3.24, 3.26, *cf.* FROELICH *et al.* 1979). Thermodynamics predict (Table 3.VI) that iron reduction starts at a lower Eh, and consequently at a greater depth, than manganese. Sample density is just enough to observe this offset in core 25G (Fig. 3.25). The Mn (and Co) increase starts between 40 and 55 cm; the Fe increase between 55 and 72 cm. A color transition at 61 cm marked the Fe(III)/Fe(II) transition (LYLE, 1983).

The reduction of manganese and iron oxides is also apparent from the analyses of reducible metals in the sediment (Figs. 3.24, 3.26). Below the depth of oxygen depletion, the HAM-extracted phase (the black area in the figures, representing all Mn oxides and part of the iron oxides) is practically absent, which means that the reduction of manganese is completed in a depth interval of less than 30cm. Nitrate reduction is probably limited to the same depth interval (*cf.* SØRENSEN *et al.*, 1984). Since a large amount of iron is left in the residual phase, and we have no data about its oxidation state, we can not determine whether iron reduction continues to greater depths.

3.5.1.4. SULFATE REDUCTION

Sulfate reduction is very limited in pelagic sediments. From the present sediment accumulation rate of 2 $cm.kyr^{-1}$ (KERSHAW, 1985) a rate constant for sulfate reduction of $3.3\ 10^{-7}\ yr^{-1}$ (BERNER, 1974; TOTH & LERMAN, 1977) or an initial sulfate gradient of only 0.2 $mM.m^{-1}$ (BERNER, 1978) can be estimated. No accurate results on the importance of sulfate reduction were therefore expected from dissolved sulfate, sulfide or particulate reduced sulfides measurements. Alkalinity measurements can be used to estimate the significance of sulfate reduction (HARTMANN *et al.* 1976). EMERSON *et al.* (1980) introduced the parameter potential alkalinity increase (PAI), which they calculated from the relations in Table 3.VI, taking due account of differences in diffusion coefficients. In core 25, the PAI after mineralization of organic matter with successively 245 μM O_2, 22 μM NO_3^-, 91 μM Mn(IV) and 27 μM Fe(III) as electron acceptors amounts to 0.68 mM. Added to the bottom water value of 2.46 mM, this gives an expected alkalinity of 3.15 mM below the Mn and Fe reduction zone. Measured values of alkalinity in pore water samples that have been obtained by squeezing on board ship are too low as a result of $CaCO_3$ precipitation during decompression (MURRAY *et al.*, 1980). The magnitude of this effect cannot be predicted from readjustment of the $CaCO_3$ equilibrium to 1 atm (EMERSON *et al.*, 1982), but can be estimated at about -0.20 mM from a systematic difference between alkalinity

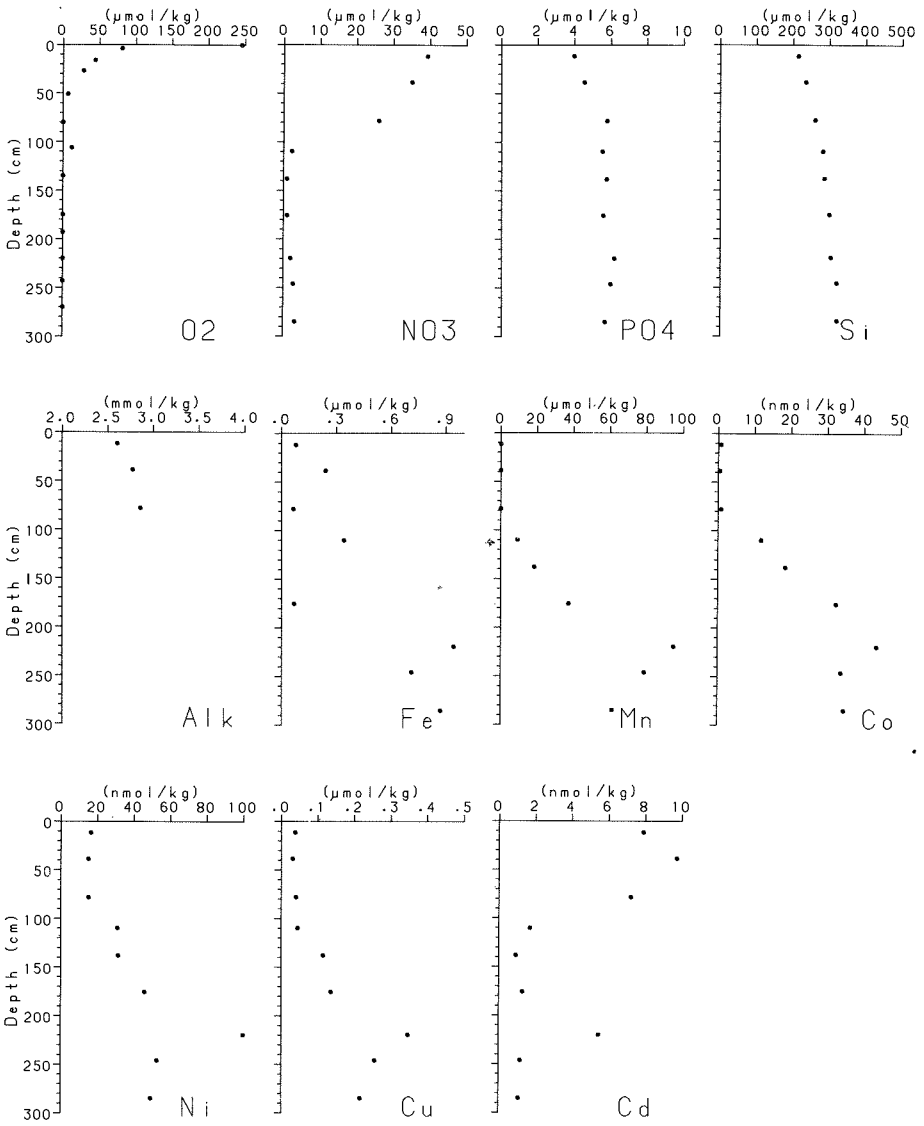

Fig.3.23. Depth profiles of oxygen, nutrients, alkalinity, and trace metals in the pore water of core 11G.

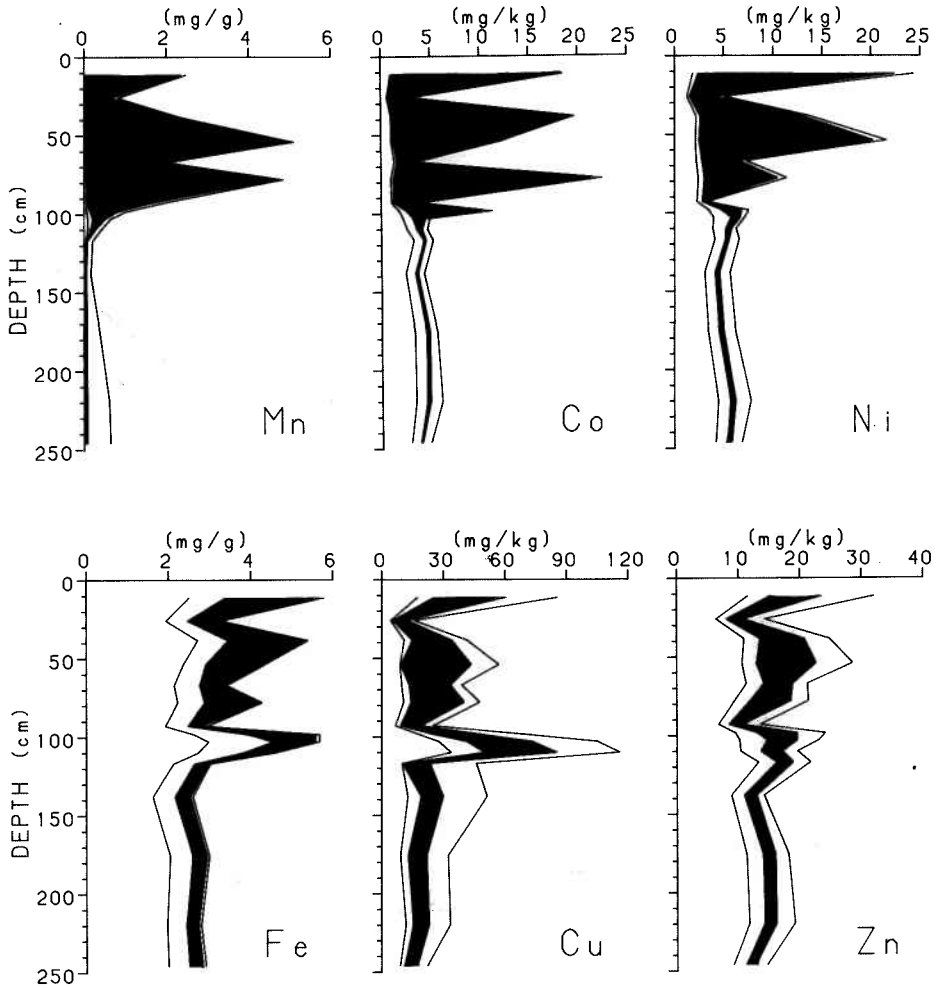

Fig.3.24. Partitioning of leachable trace metals in core 11G, expressed on a $CaCO_3$-free basis. Total extractable amounts (HAC + HAM + CH + HCl extracts) utmost right lines, and from right to left the extractable amounts remaining after the HAC, HAM, and CH extracts. Area representing HAM (reducible) extract coloured. Residual phase not analysed.

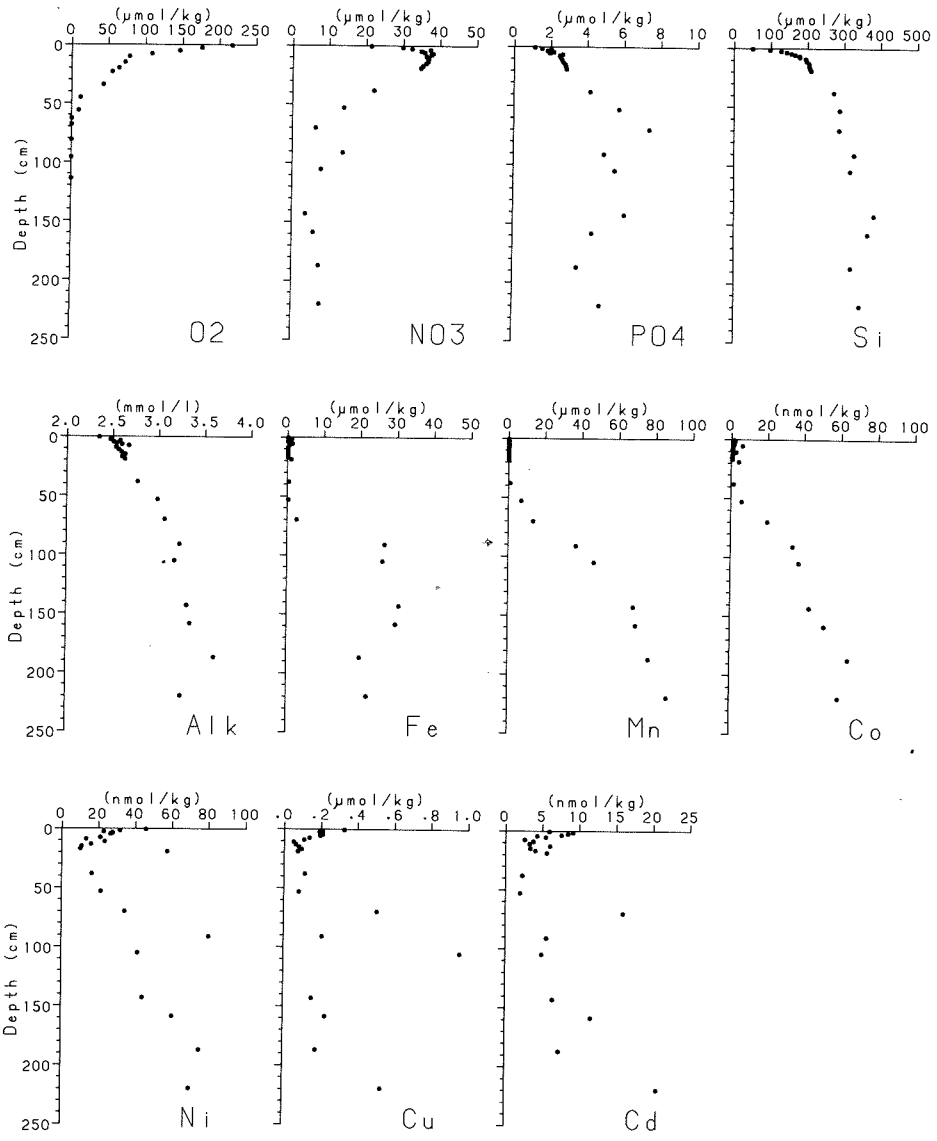

Fig.3.25. Depth profiles of oxygen, nutrients, alkalinity, and trace metal concentrations in the pore water of core 25(B + G).

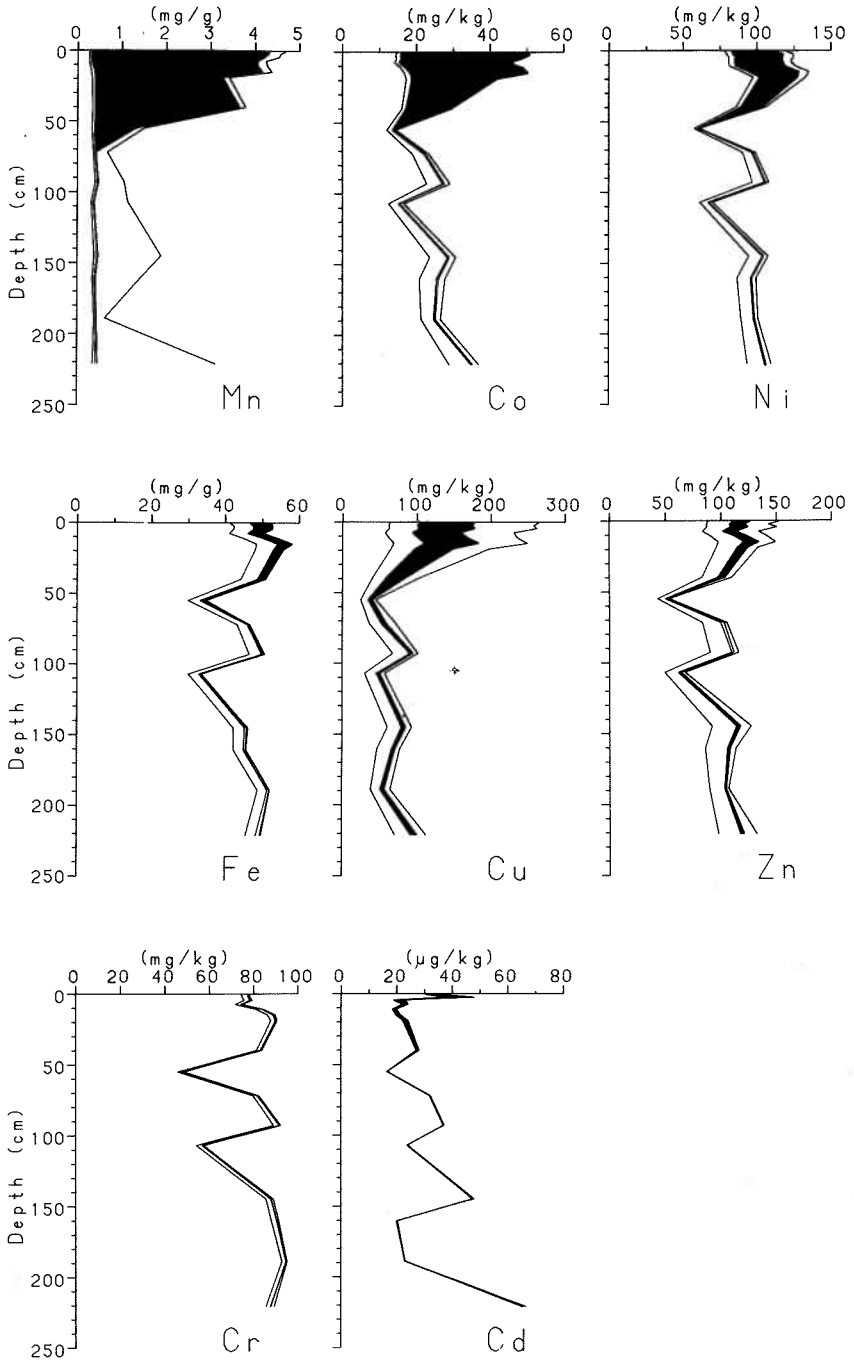

Fig.3.26. Partitioning of trace metals in core 25(B + G), expressed on a $CaCO_3$-free basis. Total amounts utmost right lines, and from right to left the amounts remaining after HAC, HAM, and HCl extracts. Area representing HAM (reducible) extract is coloured.

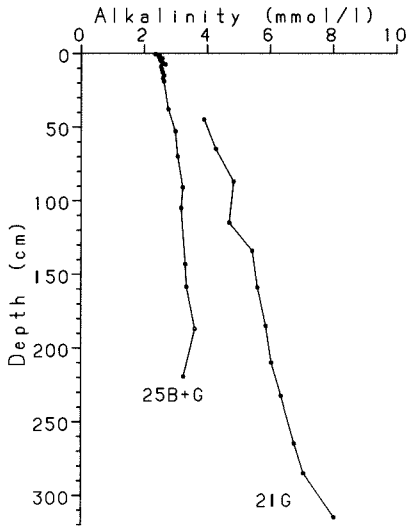

Fig.3.27. Depth profiles of alkalinity in the pore water of cores 25(B + G) and 21G.

values measured in the aerobic layer and predicted by a diagenetic model (section 3.7). Correcting observed alkalinity (Fig. 3.27) for this effect, we find an in-situ alkalinity at the bottom of core 25G of approximately 3.50 mM. We conclude that the contribution of sulfate reduction in core 25 is minor.

In core 21 alkalinity increases to 8mM (Fig. 3.27), which points at extensive sulfate reduction. This core does not fit the relationships found by TOTH & LERMAN and by BERNER. This suggests that organic matter is not only derived from pelagic sedimentation, but that additional material has been supplied by turbidites. Indeed, the core description, examination of the core with X rays and the $CaCO_3$ profile (Fig. 3.3) indicate that a 180 cm section of the core was a single turbiditic interval, presumably of continental origin (section 3.3). Oxidation of the top of such reduced turbiditic intervals is associated with significant diagenetic mobilization of trace elements (COLLEY *et al.*, 1984). It is presumably due to the high burial rate of organic carbon in the turbidite, that the concentration of dissolved organic carbon (DOC) is high in this core (Fig. 3.19).

From the above mentioned observations it can be concluded that sulfate reduction occurs in the Porcupine Abyssal Plain below a depth of 50 cm, but is of minor importance in the sediment at the dumpsite, and does not occur there above a depth of 1 meter.

3.5.2. CATION EXCHANGE

The cation exchange capacity (CEC) of the sediment is correlated with the non-carbonate fraction as could be expected:

$$CEC(mmol/100g) = 29.3 \times (1-(CaCO_3)) + 1.0$$

($r^2 = 0.86$; $n = 32$). When ammonia concentrations are built up in the pore water as a result of mineralization, ammonia will replace other cations from exchange sites leading to a remobilization of cations like K (HARTMANN *et al.*, 1976) and the same can be expected for Cs. In the aerobic sediment, ammonia is oxidized to nitrate, as evidenced by the increase of NO_3 above bottom water values (Fig. 3.17). In the anaerobic layer, ammonia levels increase, but since only little organic matter is left for anaerobic decomposition, no high levels are reached. Only in core 21, where appreciable sulfate reduction occurs in the upper few meters, ammonia increases to about 500 μM at 3m depth and may influence Cs mobility (SANTSCHI *et al.*, 1983 SHOLKOVITZ *et al.*, 1983).

3.5.3. DISSOLUTION OF CARBONATE

As a result of the pressure and temperature terms in the carbonate equilibrium (equation 6 in table 3.VI) and of the metabolic production of CO_2, deep waters are undersaturated with respect to calcite. Benthic mineralization produces an additional amount of CO_2, and as a consequence the very surface of the sediment is corrosive towards calcite at depths up to 1 km above the calcite saturation horizon in the bottom water (EMERSON & BENDER, 1981). The resulting $CaCO_3$ dissolution lowers the $CaCO_3$ content of the surface sediment below a depth called the lysocline, situated in the dumpsite at 4700 m (Fig. 3.15). In the NE Atlantic, the position of the lysocline is determined by the pressure term in the carbonate equilibrium, unlike in the W Atlantic, where the lysocline coincides with the transition between North Atlantic Deep Water (NADW) and Antarctic Bottom Water (AABW) (THUNELL, 1982). The CCD (carbonate compensation depth) is estimated at 5200 m in the NE Atlantic (BISCAYE *et al.*, 1976), which is beyond the actual depths in this ocean basin.

Within the sediment, dissolution due to the corrosiveness of bottom water is limited to the upper few mm of the sediment (SCHINK & GUINASSO, 1977). However, dissolution continues as a result of aerobic mineralization, and is therefore related to the consumption of organic carbon and molecular oxygen by equations (1) and (6). The decrease in C_{org} content with depth of 0.1 $mg.g^{-1}$ (Fig. 3.17) corresponds to a dissolution of only 0.08% in $CaCO_3$. However, in the upper 8 cm fresh organic material is continuously mixed down by bioturbation, the calcite dissolution continues, and the above estimate is therefore incorrect. Instead, the extent of dissolution can be estimated from the oxygen data. The initial oxygen gradient is approximately -50 μM $O_2.cm^{-1}$ (Fig. 3.17). The downward diffusive flux of O_2 is 5.10^{-6} $mol.cm^{-2}yr^{-1}$, corresponding to a $CaCO_3$ dissolution rate of 0.44 $g.cm^{-2}.kyr^{-1}$. In section 3.7 we will use a diagenetic model to make a second estimate of the O_2 flux, which does not depend on the risky determination of a concentration gradient across the sediment-water interface . There, we find a flux of metabolizable organic carbon or 8 $\mu mol.cm^{-2}.yr^{-1}$, corresponding to an O_2 flux of 10.4 $\mu mol.cm^{-2}.yr^{-1}$, and a $CaCO_3$ dissolution rate of 9.4 $\mu mol.cm^{-2}yr^{-1}$ or 0.94 $g.cm^{-2}.kyr^{-1}$. Above the lysocline, the $CaCO_3$ accumulation rate (sediment accumulation rate 2 $cm.kyr^{-1}$ porosity 0.70, mean density solids 2.65 $g.cm^{-3}$, $CaCO_3$ content 85%) is 1.34 $g.cm^{-2}.kyr^{-1}$. This implies that the $CaCO_3$ sedimentation rate is 1.8-2.3 $g.cm^{-2}.kyr^{-1}$, and that 25-40% of this amount dissolves in the bioturbated zone of the sediment, even above the lysocline. This value corresponds well with an earlier estimate of 20-50%, based by SAYLES (1981) on dissolved calcium measurements in the pore water.

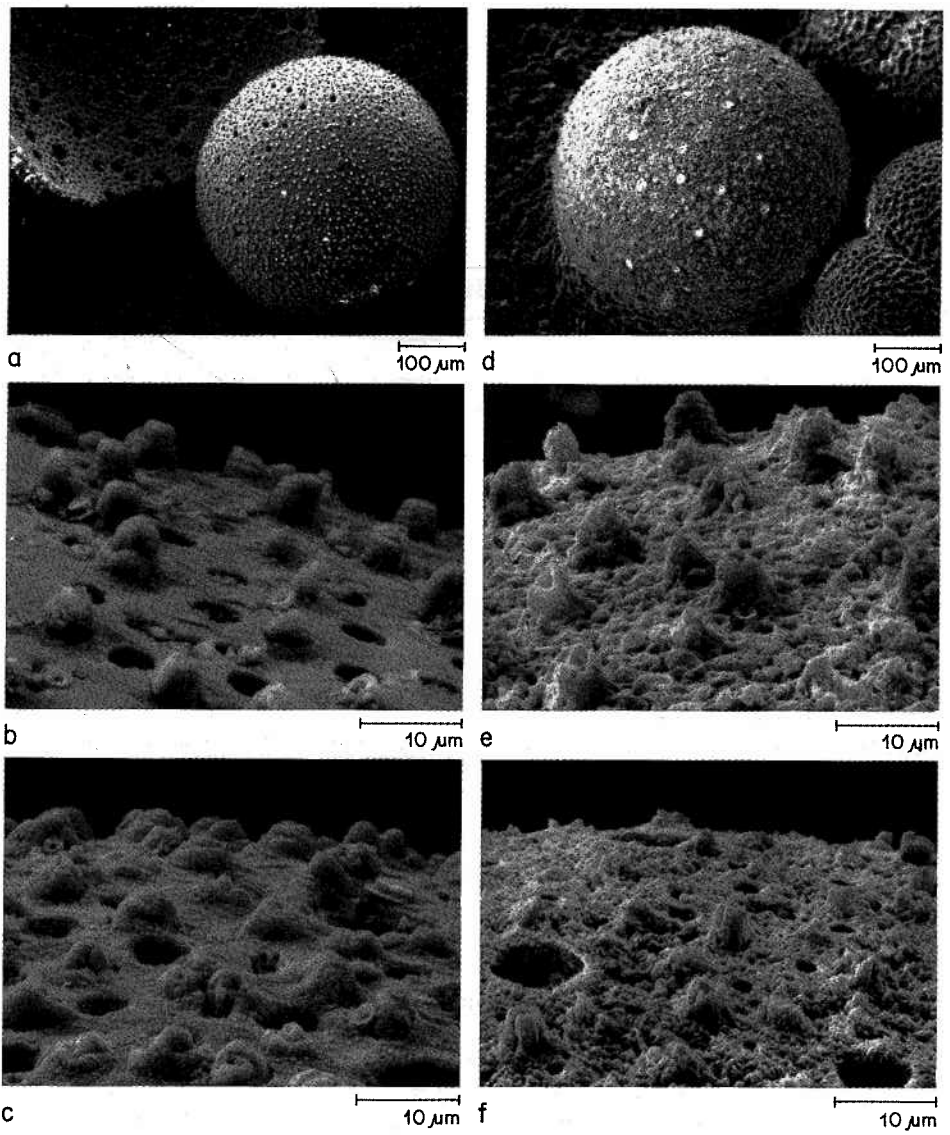

Fig.3.28. Scanning electron micrographs of tests of *Orbulina universa*, collected from boxcores 15B (left, water depth 4000 m), and 1B (right, water depth 4800 m). General view (a,d) and close-up (b,e) of shells collected in upper 2 cm; close up of shells collected at depth (c: 15 cm; d: 20 cm).

The corrosion of calcite is clearly visible on SEM photographs of *Orbulina universa* tests. Fig. 3.28 compares the state of corrosion of forams collected at the sediment surface and at 15 cm depth from two boxcores: one below (core 1B) and one above the lysocline (core 15B). The corrosion of the samples from the deeper station is evident. Additional corrosion during burial to 15 cm depth is not observed. In view of the calculated loss of $CaCO_3$, it is astonishing that the shells from the shallow station appear so little corroded, both at the surface and at 15 cm depth. Compared to other species of Foraminifera, *Orbulina universa* makes shells that are highly susceptible to dissolution (BERGER, 1968), and generally forams are less resistant than Coccoliths. Consequently, the 25-40% $CaCO_3$ that has disappeared can hardly have consisted of foram shells and Coccoliths. It is more likely that aragonite and small calcite particles like spines have dissolved. Indeed, EMERSON *et al.* (1982) showed that the pore water in the surface sediment of a deep-sea carbonate ooze (well below the aragonite compensation depth) was supersaturated with respect to calcite, and that the ion activity products fell within the range predicted for aragonite. If large enough, aragonite particles (mainly pteropods) will escape dissolution during sedimentation and reach the sediment surface. We found no aragonite (*i.e.* $<0.2\%$) in the surface sediment with X-ray diffraction, not even at station 15 (4000m depth). This observation does however not contradict the supposed role of aragonite dissolution in the carbonate budget of the surface sediment, since the dissolution after burial by bioturbation may be rapid enough to leave no measurable traces in the sediment. This argument is similar to the argument used to explain the discrepancy between the organic carbon content of the surface sediment and of the sedimenting material (sections 3.5.1 and 3.7).

$CaCO_3$ dissolution results in the release of Ca, HCO_3^- and the associated elements Sr and Mg to pore water and bottom water. Sr is also released as a result of the recrystallization of carbonates to low-Sr calcite (MANHEIM *et al.*, 1971; SAYLES *et al.*, 1973; BAKER *et al.*, 1981; ELDERFIELD *et al.*, 1982). This process proceeds on a timescale of millions of years, and is therefore not important for the behaviour of ^{90}Sr ($t_{0.5} = 28.5$ yr). Other elements that are present in trace amounts in the carbonate phase or in coatings on carbonate particles, like U and the rare earth elements (PAREKH *et al.*, 1977, PALMER, 1985 see section 3.6.4) will be released as well. It will be discussed below to what extent these trace elements released during carbonate dissolution are subsequently adsorbed on other phases like oxyhydroxides and clay minerals, or released to the bottom water and dispersed.

3.6. TRACE ELEMENT DIAGENESIS

The chemical composition of particles settling through the water column is changed by interaction with seawater. Both metal oxide coatings (GOLDBERG, 1954) and colloidal organic matter (NELSON *et al.*, 1985) and organic coatings (BALISTIERI *et al.*, 1981) on these particles offer good adsorption sites, and therefore the particles carry a load of elements which they have scavenged from seawater. Measurements of Th isotopes in seawater and on particles (BACON & ANDERSON, 1982) indicate that adsorption equilibrium exists for these isotopes in the entire water column, and it may be expected that the same holds for other particle reactive elements as well, including many of the waste radionuclides.

The diagenetic reactions described in the previous section cause a release of trace elements by the decomposition of their carrier phase (organic matter, hydroxides or $CaCO_3$) and change the chemical environment of the particles (pH, Eh, and concentration of ligands in the pore water) which in turn shifts the adsorption equilibria. The resulting behaviour of trace elements has been studied by measurements of their concentrations in pore water and in sequential extracts of the sediment. It should be borne in mind that any selective extraction technique only distinguishes operationally defined phases, and does not allow quantitative conclusions to be drawn about the actual distribution among the phases in the sediment. Vertical changes in the observed distributions, however, can without doubt be considered as indications that diagenetic changes have occurred.

3.6.1. TRACE METALS

Diagenesis of trace metals in pelagic sediments has received much interest in relation to the formation of manganese nodules, and the best information currently available is from the MANOP (Manganese Nodule Program) sites in the eastern equatorial pacific (KLINKHAMMER *et al.*, 1980, 1982). It turns out to be practical to distinguish at least two groups of metals: Fe, Mn, and Co on one hand are strongly hydrolized and very little soluble in oxidized seawater (KNAUER, *et al.*, 1982). Cu, Ni, Cd, and Zn on the other hand are more soluble, and their concentrations change in correlation with those of the nutrients both in the water column (BRULAND, 1980) and in the aerobic pore water (KLINKHAMMER *et al.*, 1982). The opposing behaviour of the two groups was clearly demonstrated in *in-situ* measurements of metal fluxes through the sediment-water interface of a coastal sediment (SUNDBY *et al.*,1986 WESTERLUND *et al.*, 1986).

3.6.2. Mn, Fe, Co

Fe and Mn data for pore water and sediment of two gravity cores from the dumpsite (cores 11G and 25G) fit well with established models (section 3.5.1.3). Pore water data are presented in Figs. 3.23 and 3.25, and results of the sequential extraction of the sediment are given in Figs. 3.24 and 3.26 for core 11 and 25, respectively. The diagenetic behaviour of Co is very similar to that of Mn. This agrees with literature data on Co concentrations in pore water, which have only recently become available for coastal (MARTIN, 1985; SUNDBY *et al.*, 1986) and deep-sea (HEGGIE & LEWIS, 1984) sediments. As in the water column, the dissolved concentrations of Fe, Mn, and Co are very low in the oxic sediments.

When oxygen is depleted, at approximately 80 cm in core 11G and at 70 cm in core 25G, first Mn, and then Fe are reduced from resp. the (IV) and the (III) to the (II) oxidation state. Since the reduced forms are much more soluble, the metals are released to the pore water, and dissolved concentrations increase with depth. Diffusion along the resulting concentration gradients transports the metals upward, and at the bottom of the aerobic layer they are oxidized again and precipitate. This cycle results in the accumulation of the metals, especially Mn, in the oxic layer, and thus prevents or retards the burial of Mn. We observed a similar enrichment of Co in the oxic layer, in agreement with HEGGIE & LEWIS (1984). Mn, Co and also Ni occur here predominantly in the HAM extract, corresponding to the Mn oxyhydroxide phase, whereas the much smaller amounts in the

reduced layer occur in the HAC extract (Mn probably as mixed carbonate overgrowths on Foraminifera tests, BOYLE, 1983) and in the HCl extract (Co and Ni). The low concentrations at 26 and 93 cm in core 11, and at 55 and 105 cm in core 25, result from dilution by much ice-rafted material (section 3.3; Fig. 3.7). Since only a small fraction of total Fe is mobile, the diagenetic Fe flux is small relative to the accumulation rate (approx. 1.6 *vs* 9.4 $\mu g.cm^{-2}yr^{-1}$, based on data of core 25), and a surface enrichment is difficult to detect. However, the diagenetic flux compares better with the rate at which HAM-reducible Fe is buried below the aerobic layer: 1.0 $\mu g.cm^{-2}yr^{-1}$

In environments where Mn reduction occurs closer to the sediment surface than in the present study as a result of a higher input of organic matter, Mn and associated elements escape the oxidation trap and diffuse into the bottom water (SUNDBY *et al.*, 1981). This is not likely to occur at the dumpsite where the aerobic layer is at least 70 cm thick. (A fresh turbidite would reduce this thickness, as it happened in the Porcupine Abyssal Plain, but even then the sediment surface would remain oxidized). Oxidation is rapid enough to prevent any release of Fe, Mn and Co through the oxidized layer towards the bottom water. This was already expected by ELDERFIELD (1976) for pelagic sediments with thick oxidized layers, but is even true in coastal sediments with an oxygen penetration depth of only about 1mm, provided that the sediment surface is well oxidized (SUNDBY *et al.*, 1986). In fact, a flux into the sediment of these metals (and of Ce, see section 3.6.4), similar to the fluxes contributing to the hydrogenous growth of ferromanganese nodules and encrustations, is more likely. Elements remobilized by reduction in the anaerobic layer could however be released to the bottom water during slides or slumps, or by deep burrowing organisms (see section 5: Biology and WEAVER & SCHULTHEISS, 1983a). This pathway applies in principle to Co, but can not be of any significance for the radioisotope ^{60}Co (half-life 5.3 yr).

3.6.3. Cu, Ni, Cd, Zn

Unlike the former group, these metals are released by oxic mineralization of organic matter in the surface sediment. As in the water column, their behaviour in the pore water is closely linked to that of the nutrients: Ni to silicate, Cd to nitrate (KLINKHAMMER *et al.*, 1982). Just as in case of the nutrients , appreciable fluxes towards the bottom water exist. Regeneration of Cu at the seafloor was concluded by BOYLE *et al.*, (1977) from Cu data in the water column. Fluxes of Cu, Ni and Cd from sediments were predicted from pore water data of deep-sea sediments (CALLENDER & BOWSER, 1980; KLINKHAMMER *et al.*, 1982) and shown experimentally by flux chamber studies in a coastal sediment with oxidized surface (WESTERLUND *et al.*, 1986).

Within the aerobic layer, dissolved Cu decreases with depth (Fig. 3.29) as a result of the decomposition of organic matter in the surface sediment and subsequent adsorption below (CALLENDER & BOWSER, 1980; KLINKHAMMER *et al.*, 1982; SAWLAN & MURRAY, 1983). Nickel concentrations in the pore water (Fig. 3.30) are also above bottom water values (around 10 $nmol.kg^{-1}$). A near-surface maximum, as observed for Cu, is less pronounced for Ni, and is even doubtfull if we consider that the upper one or two segments may well be contaminated by the boxcorer. Release of organic-bound metals explains the Ni and Cd concentrations in pore water of the surface sediment, but is not sufficient to explain the Cu results. An additional effective scavenging and release cycle exists near

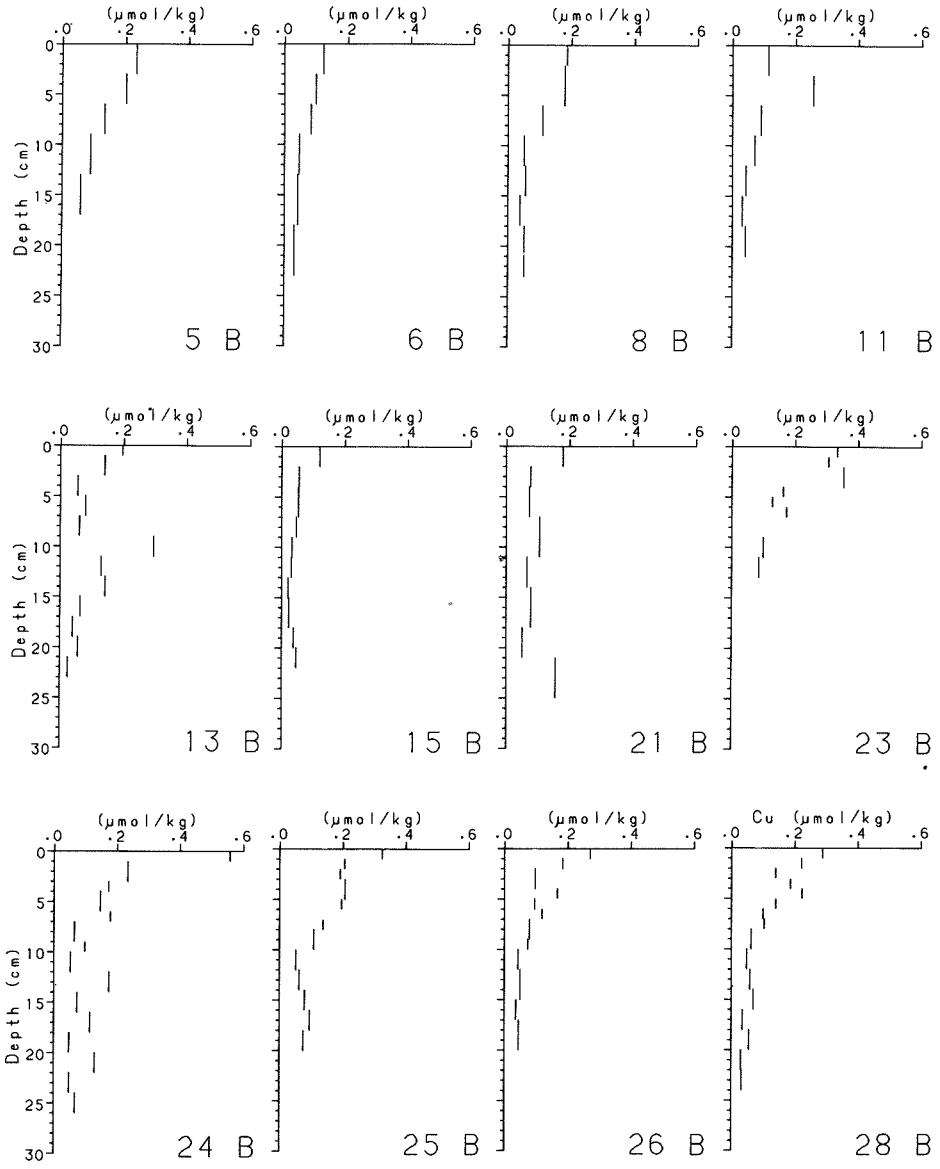

Fig.3.29. Depth profiles of copper concentrations in the pore water of the boxcores.

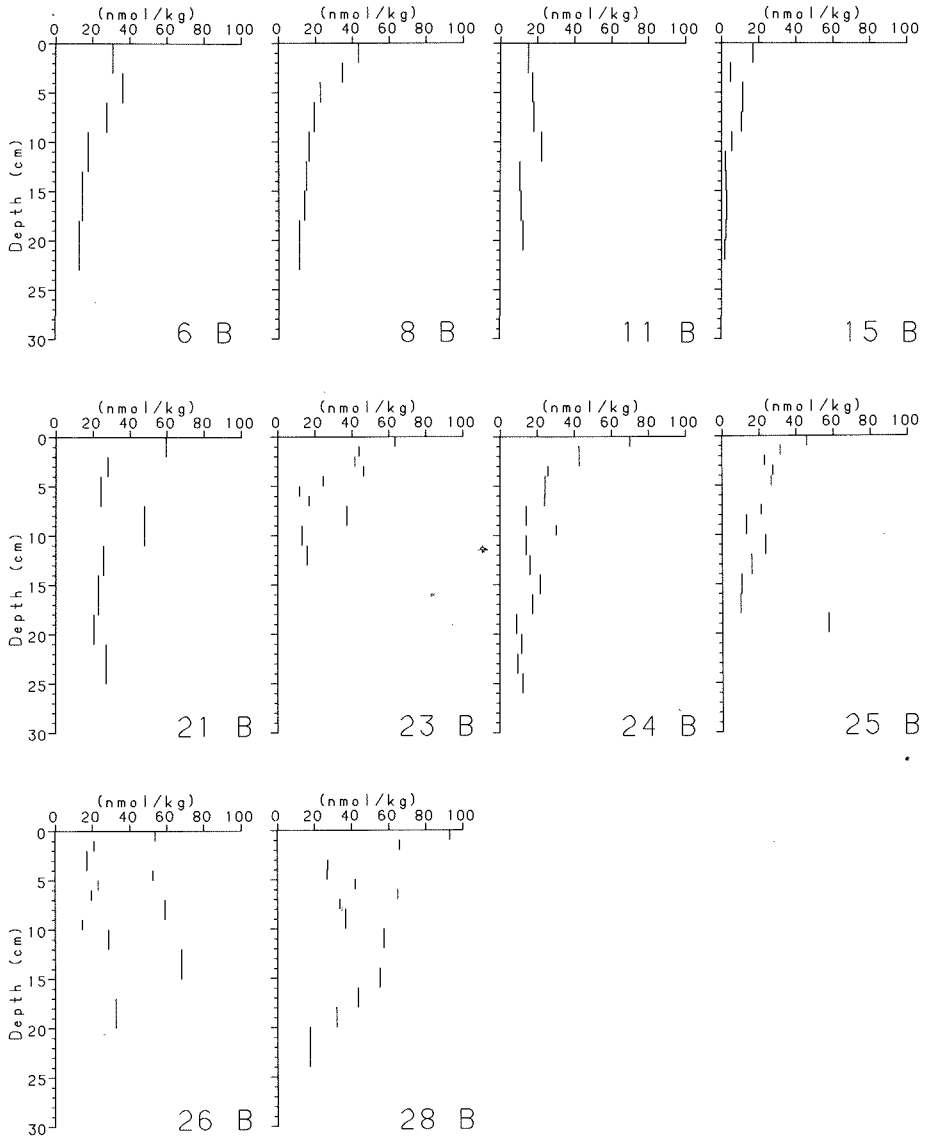

Fig.3.30. Depth profiles of nickel concentrations in the pore water of the boxcores.

the sediment-water interface (KLINKHAMMER *et al.*, 1982). Cu is recycled from a highly enriched veneer at the sediment-water interface at a much higher rate than the decomposition rate of the bulk organic matter. Apparently, Cu adsorbs on organic coatings that are preferentially broken down after deposition. The oxic trace metal diagenesis is further discussed in the section on diagenetic modeling.

The results of selective extraction experiments (Fig. 3.24, 3.26) show the dominance of the HAM-reducible phase in the aerobic layer for Ni, similar to Mn and Co, and to a lesser extent for Cu and Zn, similar to Fe. We conclude that Ni, in agreement with SAWLAN & MURRAY (1983), and Co are primarily associated with the manganese hydroxide phase, whereas Cu and Zn are also associated with Fe.

All metals associated with the Mn and Fe hydroxide phase must be released upon reductive dissolution of this phase. This causes an increase in the pore water concentrations of Cu and Ni (Fig. 3.23, 3.25), similar to the increase observed for Fe, Mn, and Co. The resulting concentration gradients in the pore water transport these metals upwards. Upward diffusive transport associated with the Mn redox pump has been demonstrated previously for Ni (KLINKHAMMER, 1980). As Mn, both Ni and Cu are enriched in the sediment in the aerobic layer.

The high contents of Cu, Ni, Mo and Zn at the lower surfaces of manganese nodules have been explained by diagenetic enrichment from the underlying sediment of metals associated with the manganese phase (CALVERT & PRICE, 1977; ELDERFIELD *et al.*, 1981). The nodules are supposed to grow by metal fluxes originating both from the decomposition of organic matter and from the reduction of hydroxides. The two maxima in the pore water profiles of Ni, Cu, (and Cd) show that the same two processes occur in the dumpsite sediment, although separated in space. Hydrogenous growth, the third source for the nodules, accumulates preferentially the first group of metals: Fe, Co, and also REE, especially Ce (ELDERFIELD *et al.*, 1981). It is due to the relatively rapid accumulation of $CaCO_3$ at the dumpsite that the fluxes do not form nodules here, but that the metals accumulate in a dispersed way in the oxic layer.

It should be noted that all metals studied here are far more mobile in the suboxic sediments at the dumpsite than they are in reduced sediments. In nearshore marine sediments, sulfate reduction occurs at shallow sediment depth, and the sulfide produced keeps the concentrations of dissolved metals at very low levels (MARTIN, 1985). Especially Fe and Cu sulfides are very little soluble. The absence of sulfate reduction in the dumpsite allows these metals to accumulate in the pore water, and consequently to be mobilized and transported by diffusion, to a greater extent than in coastal sediments.

3.6.4. RARE EARTH ELEMENTS

Our understanding of the behaviour of REE in seawater has increased considerably in the last few years (ELDERFIELD & GREAVES, 1982; DE BAAR *et al.*, 1985). REE are well correlated with the nutrients: their concentrations increase with depth in the water column, and in deep ocean waters they increase from the Atlantic to the Pacific. An exception is formed by Ce, which is the only of the series forming a 4+ instead of a 3+ valence state under earth surface conditions. Ce(IV) is more strongly hydrolysed than the other REE,

is less soluble and adsorbs more readily on particle surfaces. In this respect Ce behaves very much like Mn, Fe and Co. Similar to Co(II), Ce(III) is oxidized to valence (IV) on particle surfaces (especially MnO_2), and subsequently adsorbed.

The first data of dissolved REE in an anoxic basin (DE BAAR, pers. comm.) show that REE are mobilized in a reducing environment: Ce as a result of reduction to Ce(III), the other REE through dissolution of the hydroxides to which they were adsorbed. Preliminary results of pore water analyses (ELDERFIELD, pers. comm.) indicate that the same mobilization occurs in anoxic sediments. Such a diagenetic mobilization could be expected to deplete suboxic layers in REE, relative to the oxic surface layers. Although the distribution of REE among the carbonate and non-carbonate phase does change with depth, measurements of REE in bulk sediment above and below a redox boundary did not reveal any diagenetic enrichment of REE (MARCHIG *et al.*, 1985), suggesting that diagenetic fluxes are negligible compared to the sediment accumulation rate.

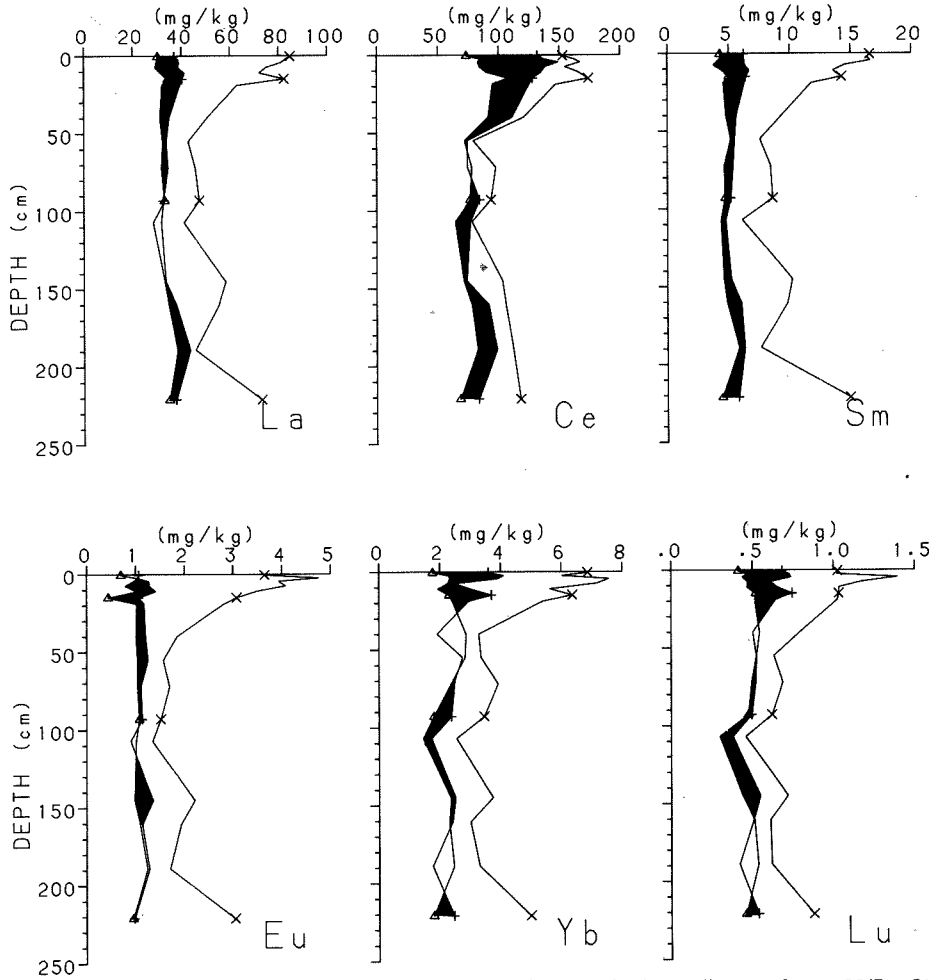

Fig.3.31. Depth profiles of concentrations of rare earth elements in the sediment of core 25(B + G) expressed on a $CaCO_3$-free basis. Total amounts (×), and the amounts remaining after HAC (+) and HAM (△) extracts. Area representing HAM (reducible) extract is coloured.

In analogy with the trace metal study, we expected that a selective extraction procedure could tell us whether the rare earths were affected by a redox transition. We applied the same extraction technique that we used for the trace metals to 16 samples from core 25B + G, in which oxygen was depleted at 70 cm (Fig. 3.25.).

The amounts of REE in the original samples, and the amounts left after the sequential extraction with first HAC and then HAM (Table 3.I) are shown in Fig. 3.31 on a $CaCO_3$-free basis. Theoretically, the lines should not intersect. They sometimes do, however, as a result of the cumulative error introduced by REE analysis, determination of weight loss, and inhomogeneity of the samples. In this presentation, the rightmost profiles (total contents) reflect the influence of the large variation in $CaCO_3$ content: from 88% at the top down to 9.2% at 200cm depth. This influence is much more pronounced than in the case of the trace metals (Fig. 3.26) because the dissolution of $CaCO_3$ removes relatively more trivalent REE than trace metals (with the exception of Cd). According to PALMER (1985), only about 10% of REE in Foraminifera is a constituent of the calcite lattice, the remaining part being associated with coatings (presumably hydroxides) on the calcite surfaces. Lattice-bound REE concentrations are three orders of magnitude lower than average concentrations in shale, and must therefore be negligible in Fig. 3.31. The appreciable amounts of REE released by the HAC attack (acetic acid/acetate, pH 5) were evidently no part of the calcite lattice, but were rather part of the coatings. This is why, just as in Fig. 3.26, we expressed in Fig. 3.31 all REE contents, including the REE mobilized by the acetic acid attack, on a $CaCO_3$-free basis by normalizing the REE contents in the fractions remaining after the various sequential extractions to the weight remaining after the HAC attack.

The REE content in the residual fraction is constant throughout the core, and is not affected by the redox transition, the change in $CaCO_3$ content, nor even by the admixture of ice-rafted material rich in Si (quartz) and Mg (dolomite), but depleted in Al and most other elements (Fig. 3.7, 3.26, 3.32). The other fractions, however, change markedly with depth. The transition between the oxic and anoxic sediment layers is illustrated in Fig. 3.33c and d respectively. These figures show the partitioning of REE (expressed on a $CaCO_3$-free basis and shale-normalized) over the phases that are distinguished by the selective extraction method. The normalization to concentrations in average shale (HASKIN & HASKIN, 1966; PIPER, 1974) yields the so-called REE patterns. Because REE form a very coherent group of elements, such patterns give more information than the concentrations of individual REE alone. The behaviour in the oxidized $CaCO_3$-rich, holocene surface sediment (Fig. 3.33.c) is clearly different from the behaviour in the sediment below 50 cm depth (Fig. 3.33.d), which is reduced and contains less calcite.

WYTTENBACH & TOBLER (1984) investigated the partitioning of REE among the carbonate, the hydroxide and the residual phase in oxidized samples from the dumpsite. Surface samples from 7 stations and a profile (0 to 22 cm, 10 sections) at station 6 were analysed for 31 elements by neutron activation analysis. Some samples were also analysed after removal of carbonates with 1n HCl. From these data and from correlation analysis against Th they calculated the partitioning of elements between the phases $CaCO_3$, silicates (the undissolved fraction, assumed to contain all Th) and a third phase that dissolved during acid treatment along with $CaCO_3$ and that was assumed to consist mainly of Fe-Mn-oxyhydroxides. 79% of Co, 50% of Ce, and 25-40% of other REE, V, U, and As in these oxidized sediments was present in this oxyhydroxide phase. These results compare rather well with our results for the aerobic layer (Figs. 3.26, 3.31, 3.32).

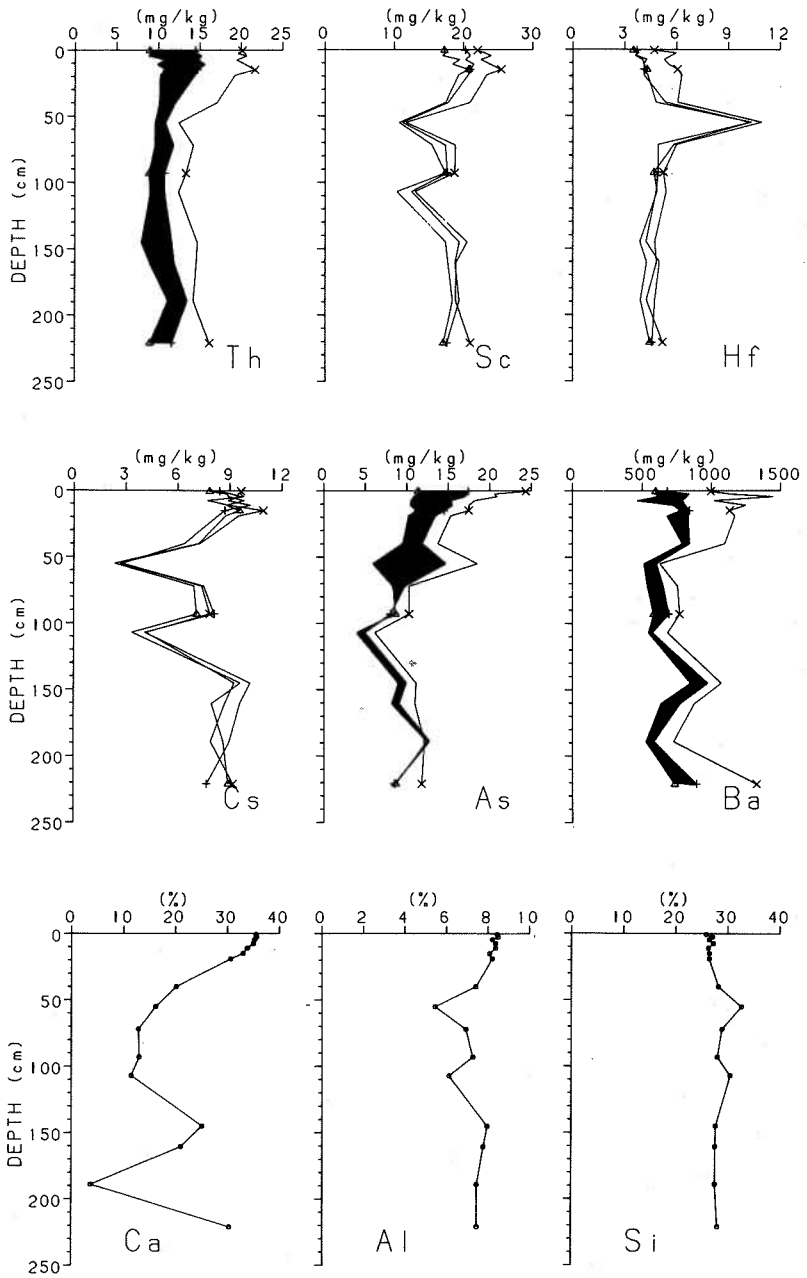

Fig.3.32. Depth profiles of concentrations of other trace elements in the sediment of core 25(B + G) expressed on a $CaCO_3$-free basis. Total amounts (x), and the amounts remaining after HAC (+) and HAM (Δ)extracts. Area representing HAM (reducible) extract is coloured for Th, As and Ba. Below, depth profiles of Ca concentration in total sediment and of Al and Si concentration in the material left after HAC + HAM + HCl extraction.

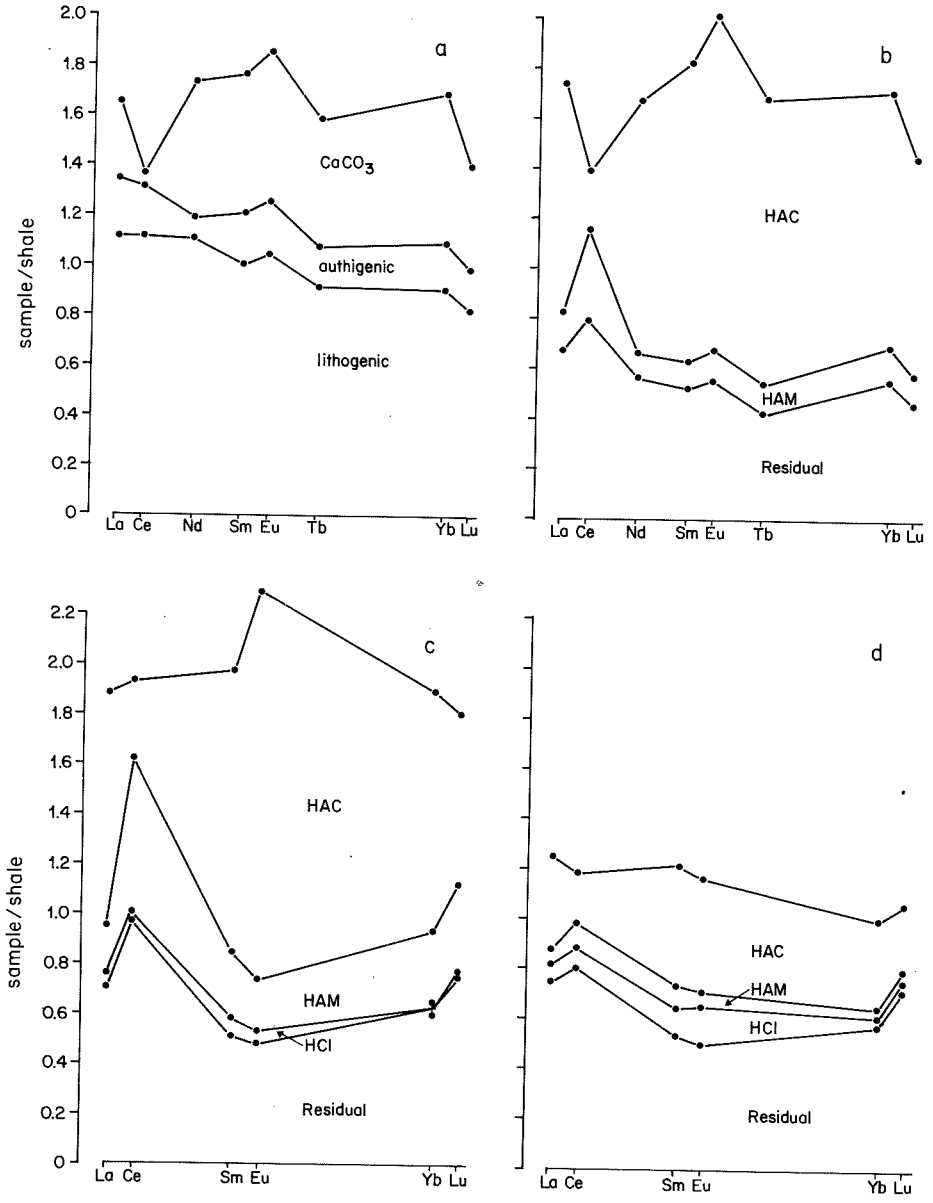

Fig.3.33. Patterns of cumulative REE concentrations in dumpsite sediments. Model (a) and selective extraction (b) results for oxic (0-20 cm) sediments from PETERSON *et al.*, (1986); Selective extraction results of oxic (c: 0-22 cm) and suboxic (d: 55-250 cm) section of core 25 (B + G).

Recently, the same team published additional results obtained on the same samples (PETERSON *et al.*, 1986). In stead of Th, they used Al as the element specific for the lithogenic phase. This appears to be a more suitable choice, since Th adsorbs on oxyhydroxides and is clearly affected by the various extractants (Fig. 3.32). Moreover, they included leaching experiments using extraction techniques very similar to ours. Results from their leaching experiments (Fig. 3.33.b) were similar to those predicted by their partitioning model based on interelement correlations (Fig. 3.33.a), although the extraction procedure overestimated the $CaCO_3$ fraction on the expense of the oxyhydroxide- and residual fractions. Comparison with our results for the oxidized boxcore (Fig. 3.33.c) suggests that this overestimation was less in our extraction procedure.

REE patterns in the residual phase are rather flat, and the REE contents in this phase are similar in the oxic and in the suboxic layer. In the extractable phase however, the $CaCO_3$-rich surface sediment contains more than twice as much REE as the deep layer (Fig. 3.33c,d), as a result of the REE associated with the abundant $CaCO_3$ phase. Extraction with HAC removes from 25% in the deep layer to over 50% in the surface layer of all REE present, except for Ce which is strongly depleted in the HAC extract. Since only 10% of REE in Foraminifera is part of the calcite lattice, this means that HAC removes not only the REE in the calcite lattice, but also most of the REE that are present as coatings on these particles. And since Fe and Mn are not released by the HAC attack (Fig. 3.24, 3.26), this means that either the binding of REE to the FeOOH and MnOOH phase is too weak to keep the trivalent REE adsorbed during this treatment, or REE are adsorbed to the calcite surfaces in a different way. This holds both for the heavy REE, known to form stable complexes with carbonate ion - which is of course abundant in the HAC extract - and for the light REE La. The strong binding of Ce (IV) to the hydroxide phases in the oxidized sediments prevents its release during the HAC treatment.

The succeeding reductive extract (HAM) is strongly enriched in Ce. As we know from the trace metal results, the HAM reducible fraction is negligible in the suboxic sediment. This holds also for the REE (Fig. 3.33.d). In the oxic sediment, however, an appreciable part of REE is released by reduction of the hydroxides (Fig. 3.33.c). The additional amounts of REE extracted by 1M HCl are quite low.

In conclusion, more than half of the trivalent REE in the surface sediment is bound to $CaCO_3$ surfaces. In a gentle dissolution with HAC (pH 5), these REE are set free and do not readsorb on oxyhydroxides. REE released during dissolution of $CaCO_3$ at the sediment surface and in the bioturbated zone may therefore be released to the bottom water. Such a release was predicted by ELDERFIELD & GREAVES (1982) from REE gradients in deep ocean waters. An additional but smaller amount of trivalent REE is released to the pore water after reduction of the oxyhydroxide phase. Ce is depleted in the $CaCO_3$ phase and enriched in the hydroxide phase. Dissolution of $CaCO_3$ will not release Ce. Instead, a flux of Ce into the sediment, similar to Fe, Mn, and Co is more likely. Ce is released by reduction to Ce(III) at the depth of oxygen depletion.

3.6.5. FACTORS AFFECTING TRACE ELEMENT MOBILITY

a. adsorption control: the concept of distribution coefficients (K_d)

In radiological assessment studies, the behaviour of radionuclides has often been described in terms of distribution coefficients. From a modelers' point of view, it is very practicle when the distribution of a nuclide between the dissolved and particulate phase

can be predicted by constant coefficients. This approach was stimulated by the great similarity of K_d values found in laboratory experiments of the same nuclide with a variety of natural sediments (DUURSMA & EISMA, 1973). However, as explained in the introduction (section 3.1), distribution coefficients are by no means physical constants, and it is not generally justified to apply K_d values measured in the laboratory or in a particular environment to a different environment. Especially in the sediment-pore water system, with large variations in pH, Eh and ligand concentrations, the applicability of the K_d approach should be checked by *in-situ* measurements of sediment- and pore water concentrations. In this section, the measurements of trace elements in sediment and pore water, described in the previous section, will be used to calculate *in situ* K_d coefficients, and to discuss the suitability of the K_d approach to predict radionuclide mobilities.

The change from oxidized to suboxic conditions has a large impact on the distribution of most of the elements investigated: The distribution coefficients of trace metals, expressed as cumulative extractable concentrations (all steps up to the HCl extract) divided by concentrations in the pore water, and the ratios between K_d in the oxic and K_d in the suboxic layers, are given in Table 3.VII. The K_d of Fe, Mn, and Co decreases dramatically with depth. A less pronounced difference exists for Ni, Cu, and Cd. A single K_d value for each element is clearly not appropriate but could the behaviour of these elements be described by a two-layer model with two sets of K_d values?

In the aerobic layer, the pore water concentrations of Fe, Mn and Co are similar to bottom water values (where they are higher it is difficult to exclude contamination as a source), and may well be controlled by adsorption equilibria (BALISTIERI & MURRAY, 1984). The concentrations of Ni, Cu and Cd are constant below about 20cm, and can there also be assumed to be governed by adsorption. In the surface layer, however, the latter metals are released as a result of decay of organic matter, and higher concentrations are built up. Their concentrations are apparently determined here by a dynamic equilibrium between release and adsorption (removal rate constant in the order of 0.5-15 yr^{-1} according to SAWLAN & MURRAY, 1983; see also section 3.7), and cannot be predicted from distribution coefficients.

Table 3.VII. Concentration of trace metals in sediment (HAC + HAM + HCl extracts, $\mu g.g^{-1}$) and in pore water ($\mu g.kg^{-1}$); and distribution coefficients in the aerobic and the suboxic layer of core 25.

		Fe	Mn	Co	Ni	Cu	Cd
aerobic:	sediment ($\mu g.g^{-1}$)	1500	600	5.5	8	30	0.4
	pore water ($\mu g.kg^{-1}$)	5	0.7	0.03	0.6	4	0.4
	K_d	$3\ 10^5$	$9\ 10^5$	$2\ 10^5$	$1.3\ 10^4$	$8\ 10^3$	1000
suboxic:	sediment ($\mu g.g^{-1}$)	2000	500	3.5	5.5	18	0.2
	pore water ($\mu g.kg^{-1}$)	1500	4500	3.5	3.5	15	0.6
	K_d	1300	110	1000	1570	1200	330
	$\frac{Kd\ aerobic}{Kd\ suboxic}$	225	7700	180	8.5	6.2	3

After the depletion of molecular oxygen, oxyhydroxides are reduced and dissolve, and all associated elements are set free. Since oxyhydroxides have strong binding properties their disappearance after the depletion of oxygen means a decrease in available binding sites and a competition for the remaining sites, mostly on clay minerals, by the released elements, including Fe^{2+} and Mn^{2+}. As long as the concentrations in the pore water are controlled by adsorption equilibria, these concentrations increase as a result of the reduction in number and in strength of available binding sites. Below the depth of this mobilization, sulfide may be produced if sufficient organic material is left for sulfate reduction to occur (at the dumpsite only to be expected in turbidites). Due to these concentration changes the solubility of some mineral phases is reached.

b. solubility control

Dissolved Mn has been shown to be controlled in reduced pore water by the formation of authigenic carbonate minerals like rhodochrosite ($MnCO_3$)(Li *et al.*, 1969; Holdren *et al.*, 1975; Balzer, 1982) or a mixed Ca/Mg/Mn carbonate (Suess, 1979). In calcareous sediments a mixed Ca/Mn carbonate forms on the surface of Foraminifera tests (Boyle, 1983). With a CO_3^{2-}-ion concentration from pH and alkalinity data, we obtain an ion concentration product in excess of the stoichiometric solubility constant of rhodochrosite (Johnson, 1982), but an accurate calculation to determine whether Mn is in equilibrium with a (Ca,Mn)CO_3 phase cannot be made (Sawlan & Murray, 1983). Such a solubility control would fit with our observation that a large part of particulate Mn in this layer is associated with the HAC-leachable or "carbonate" phase. Since appreciable amounts of other elements are also present in this phase (Fig. 3.26, 3.31), and since sulfate reduction is usually unimportant in these sediments, the solubility of carbonates may control the dissolved concentrations of other elements as well. Where concentrations are controlled by solubility rather than by adsorption equilibria, it is not justified to use the K_d approach to describe the behaviour of the elements involved, since the dissolved concentration is regulated irrespective of the concentration in the particulate phase.

c. complexation

Pore water concentrations, and consequently mobilities, of trace elements may be increased by complexing ligands in the pore water. Concentrations of such ligands change with depth: Dissolved organic carbon concentrations first decrease and then appear to increase again in the suboxic sediment (Fig. 3.19). Polysulfides can be quite soluble, but only at sulfide concentrations that are not reached in the sediments under investigation. Carbonate ions form complexes with U and REE.

d. conclusions

It was shown above that diagenetic processes reduce the abundance of three important carrier phases of trace elements: hydroxides, organic matter, and carbonates. The dissolved concentrations of many trace elements in equilibrium with the remaining phases have been shown to increase. In situ K_d values for REE in the sediments of the dumpsite are not available, but the recent data on dissolved REE in anoxic basins and pore waters suggest that the mobility of REE may likewise increase after reduction of the sediment.

The general nature of mobilization resulting from a reduction in binding sites, the absence of sulfide, and the analogies between the chemistry of transuranic elements and

of trivalent REE (*e.g.* BOUST, 1986) suggest that Am and Pu nuclides become likewise more mobile in the suboxic layer at the dumpsite. This contrasts with the reduced mobility of Pu in reduced, and sulfide containing, sediments, that was demonstrated in the Irish Sea (NELSON & LOVETT, 1980). Although Eh does not decrease in the suboxic layer of core 25G below 0.12 V (Fig. 3.34), we would expect the stable form of Pu to be the less soluble Pu(IV) at that Eh (EDGINGTON, 1981; SKYTTE JENSEN, 1982, see however warning in 3.5.1.1). There is not sufficient information to determine which effect is more important: reduction of mobility through reduction to Pu(IV), or increase of mobility through decreased availability of binding sites.

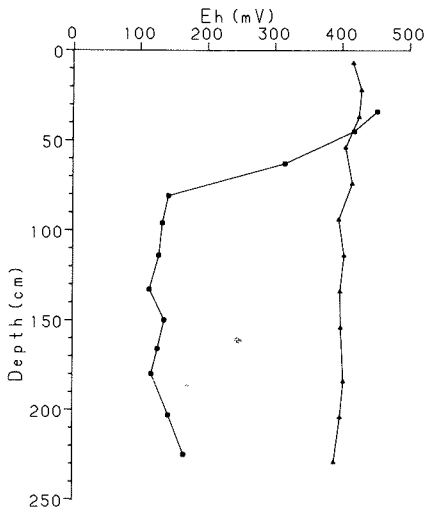

Fig.3.34. Redox potential in cores 25G (o) and 29G (▵).

3.7. DIAGENETIC MODELING

In the discussion of the early diagenetic reactions in the sediment, it has already been emphasized that all these processes are closely linked to each other. The driving force is the supply of organic carbon to the sediment. The decomposition of this carbon, mainly by oxygen diffusing downwards from the bottom water, controls the redox state of the sediment, the dissolution of $CaCO_3$, and also ion exchange. Since sediment trap data are not available for this ocean area, we must find another way to estimate the incoming flux of organic matter. Diagenetic modeling provides an excellent tool to estimate the carbon flux to the sediment and to understand the interrelationships between the various diagenetic processes.

An appreciable part of the mineralization of organic matter takes place close to the sediment surface. Estimates of the resulting fluxes from pore water gradients are therefore dependent on the accuracy with which we can determine the *in situ* gradients across the sediment-water interface. In practice, this means that they rely heavily on measurements in the upper few mm of the sediment, a section that is most easily affected

Table 3.VIII. Diagenetic equations describing the behaviour of alkalinity and copper in the pore water, and parameter values used in the diagenetic model. Other equations and parameters as in JAHNKE *et al.* (1982).

$$\frac{\partial(\phi AlK)}{\partial t} = \frac{\partial}{\partial z}\left(\frac{D_A}{F}\frac{\partial AlK}{\partial z}\right) + \gamma_4 K_1 C(1-\phi)\delta + \gamma_5 K_2 C\, NO_3^- (1-\phi)\phi(1-\delta)$$

$$\frac{\partial(\phi\, Cu)}{\partial t} = \frac{\partial}{\partial z}\left(\frac{D_c}{F}\frac{\partial Cu}{\partial z}\right) + \gamma_6 K_1 C(1-\phi)\delta + \gamma_6 K_2 C\, NO_3^- (1-\phi)\phi(1-\delta) - K_c(Cu-Cu_e)\phi$$

Boundary conditions:

at z=0 Alk = AlK (bottom water): 2.46 mmol.l^{-1}

Cu = Cu (bottom water): 5 nmol.l^{-1}

at z=20 cm $\partial Alk/\partial z=0$

$\partial Cu/\partial z=0$

AlK Alkalinity (moles/cm^3_{pw})

Cu Copper concentration (moles/cm^3_{pw})

Cu_e Copper concentration at adsorption equilibrium (50 nmol.l^{-1})

D_A Molecular diffusion coefficient of HCO_3^- (5.4 10^{-6} $cm^2.s^{-1}$)

D_c Molecular diffusion coefficient of Cu^{++} (3.6 10^{-6} $cm^2.s^{-1}$)

F Formation factor (fig. 3.35)

γ_4 AlK/C ratio during oxic respiration (1.50 x 138/106)

γ_5 AlK/C ratio during denitrification (1.15 x 94.4/106)

γ_6 Cu/C atomic ratio (1.9 10^{-4})

K_1 Oxic respiration rate constant (s^{-1})

K_2 Denitrification rate constant (1 10^{-4} $cm^3.mol^{-1}.s^{-1}$)

K_c Cu adsorption rate (5 10^{-8} s^{-1})

δ Oxygen respiration zone: δ =1
Denitrification zone: δ =0

K_z Sediment mixing coefficient: z=0 to 6 cm: 1 10^{-8} $cm^2.s^{-1}$
z=6 to 15 cm: decreasing linearly to 0

ω Sediment accumulation rate: 2 cm. kyr^{-1}

ϕ porosity

by mixing and diffusion during recovery of the core (REIMERS *et al.*, 1984). With the aid of diagenetic modeling we can also use data that have been obtained for larger sediment depths, and check our various estimates for interconsistency. Moreover, it enables the calculation of rates that could not otherwise be calculated.

The diagenetic equations describing the organic matter decomposition in a marine sediment have been given by BERNER (1980). JAHNKE *et al.* (1982) formulated the equations describing carbon, oxygen and nitrogen diagenesis in a deep-sea sediment with nitrification and denitrification, taking into account both sediment accumulation and bioturbation. They obtained the steady-state solution numerically. Using their approach, we have modeled the diagenesis of organic matter in the upper 20 cm of the sediment at the dumpsite. We used the same equations for C, N, and O diagenesis, but added equations describing production and consumption of alkalinity and dissolved copper. These equations, boundary conditions and parameter values selected based on data from core 25B are given in Table 3.VIII. Bioturbation was assumed to be constant in the upper 6 cm, and to decrease linearly to zero at 15 cm depth. Bioirrigation was assumed to be negligible compared to molecular diffusion (*cf.* EMERSON *et al.*, 1982).

The formation factor F increased from 1.4 at the sediment surface to 2.7 at 20 cm depth (Fig. 3.35). Formation factor and porosity (φ) are related by the equation

$$F = \varphi^n \qquad (7)$$

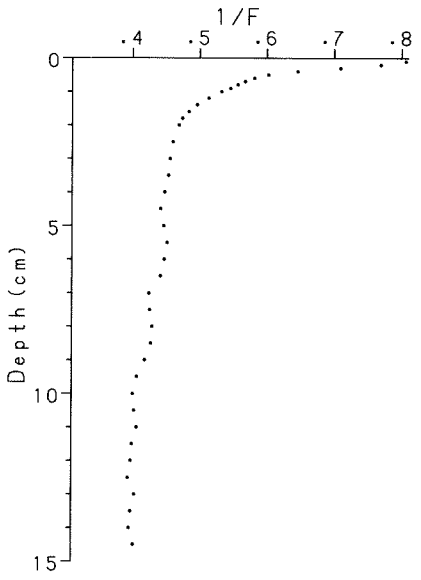

Fig.3.35. 1/F (F = Formation factor) versus depth in boxcore 25B.

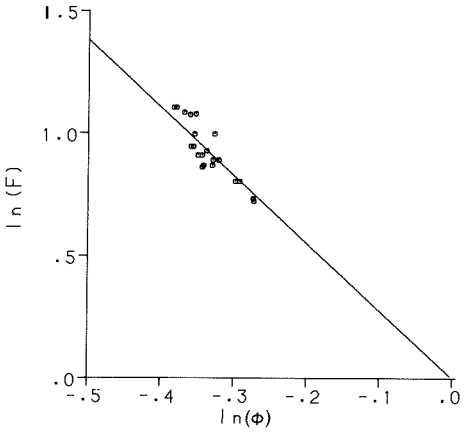

Fig.3.36. Relation between formation factor (F) and porosity (φ). Straight line corresponds to n = -2.76 in eq.(7).

(BERNER, 1980), with n = -2.76 for dumpsite sediments (Fig. 3.36). Since we know the profile of F near the sediment-water interface more accurately than the profile of porosity, we used in the model the measured profile of F and calculated the porosity at each depth from the above relationship. Porosity thus decreased from 88% at the interface to 70% at 20 cm depth.

As observe by JAHNKE *et al.*(1982), the oxygen profile is rather insensitive to the rate of oxidation of organic matter, since the organic matter concentrations adjust to the decomposition rate. The oxygen profile is however very sensitive to the supply of organic matter to the sediment surface. It is therefore in principle possible to derive through curve fitting the supply of organic matter from the observed oxygen profile, and the decomposition rate constant from the observed organic carbon profile.

It turns out to be impossible to fit the model to the experimental carbon data of the dumpsite: if reasonable organic carbon values at the surface are to be obtained, all organic matter is depleted at about 12 cm depth, whereas the data indicate that aerobic carbon mineralization continues down to 80 cm. In order to obtain a better fit of the model to the organic carbon data, we had to distinguish, apart from a refractory pool constituting about 1 $mgC.g^{-1}$ (Fig. 3.17), two pools of organic carbon with different decomposition rates. A so-called 'multi-G model has been used earlier by BERNER (1974) to describe the differences in decomposition rates of organic matter between various electron acceptors and organic matter components. Experimental support for a multi-G model comes from the data on ETS activity, which decreases more rapidly with depth than does organic carbon (Fig. 3.17).

We obtain the best fit to the observed oxygen profile with an organic carbon sedimentation rate of 8 $\mu mol.cm^{-2}yr^{-1}$ (Fig. 3.37.a). The introduction of two organic matter fractions that differ a factor 12 in decomposition rate improves the fit to the experimental organic carbon data (Fig. 3.38.b), but a discrepancy remains in the upper few cm. This implies that either a fraction of yet higher decay rate is present in the surface sediment (as confirmed by the copper data, see below), and/or that the bioturbation is not ade-

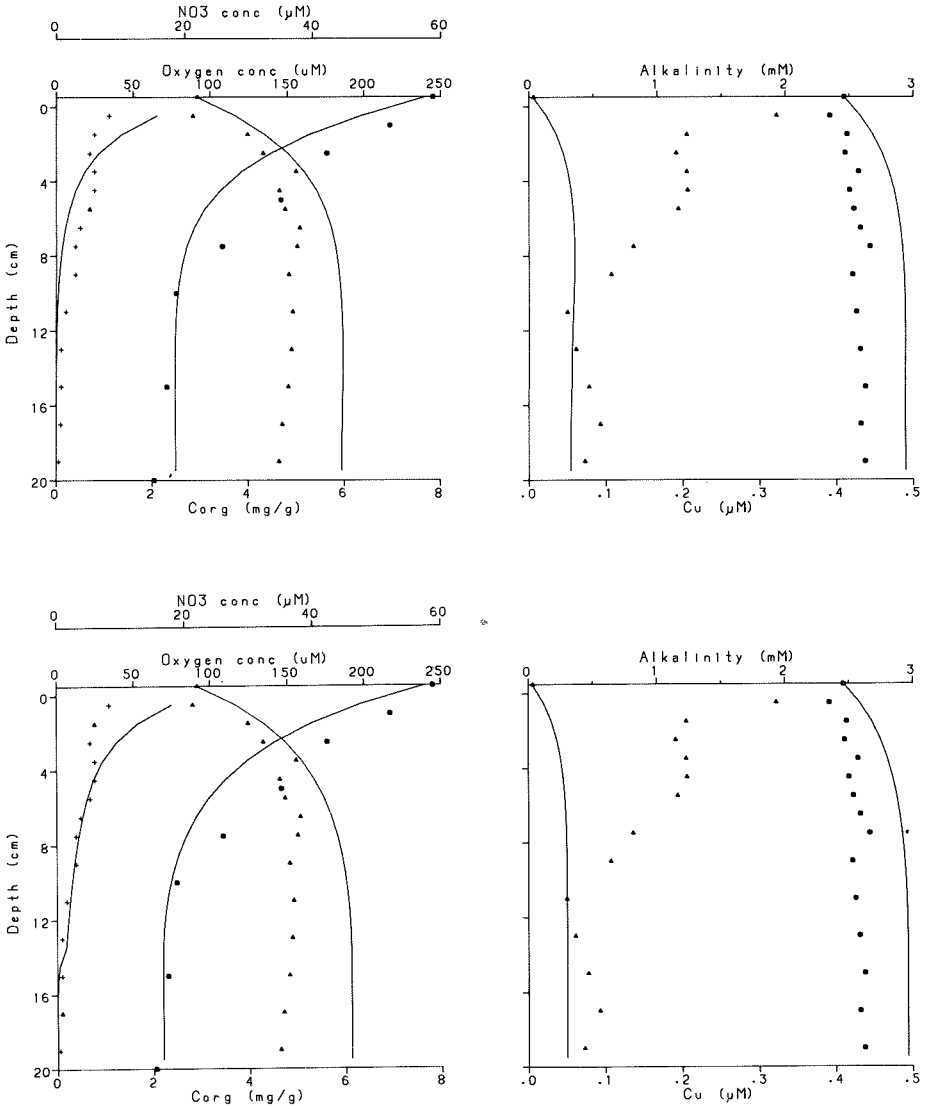

Fig.3.37. Model results and experimental data (core 25B) for oxygen, nitrate and copper concentrations and alkalinity in the pore water and organic carbon concentration in the sediment, with carbon flux = 8 μmol.cm^{-2}.yr^{-1} and above: K_1 = 1.5 $10^{-9}s^{-1}$, below: K_1 = 2.5 $10^{-9}s^{-1}$ and 20% of sedimenting organic matter is decomposed at a rate of 2 $10^{-10}s^{-1}$.

quately described by a homogeneous sediment mixing in the upper 10 cm (BOUDREAU, 1986b). The value adopted for the decomposition rate of the main part of the organic carbon corresponds to a residence time of 13 years, which is within the range of values given by EMERSON *et al.* (1985).

SUESS (1980) presented an empirical relationship between organic carbon flux as measured with sediment traps, and surface productivity. From this equation, we expect that 0.9% of the organic matter produced at the ocean surface reaches the seafloor at 4500m depth. With our data for the primary productivity in this part of the Atlantic (section 4.5) this corresponds to an organic carbon supply to the sediment of 8 (4-10) μmol.cm^{-2}.yr^{-1}, in good agreement with the results of the diagenetic model.

It is now possible to calculate the composition of the material that settles on the seafloor. The rate of accumulation of sediment below the zone of bioturbation is 1.58 mg.cm^{-2}.yr^{-1}, of which 85 % or 1.34 mg.cm^{-2}.yr^{-1} is $CaCO_3$ and approx. 13% or 0.20 mg.cm^{-2}.yr^{-1} is detrital siliceous matter. In section 3.5.3 it was shown that an additional .4- .9 mg.cm^{-2}.yr^{-1} $CaCO_3$ dissolves within the bioturbated zone. The diagenetic model shows that the supply of organic matter (with 40% C) amounts to 0.24 mg.cm^{-2}.yr^{-1}. The fluxes and composition of the freshly settled material are summa-

Table 3.IX. Composition (in %) and fluxes (in μg.cm^{-2}.yr^{-1}) of the material settling on the seafloor.

	$CaCO_3$		organic matter		detrital material	
	flux	%	flux	%	flux	%
supply to ocean floor	2.27	84	0.24	9	0.20	7
burial rate						
above lysocline:	1.34	87	0.004	.2	0.20	13
at 4800 m :	0.43	68	0.002	.2	0.20	32

rized in Table 3.IX. These values must be regarded as average values. It is likely that these fluxes vary seasonally, but any supporting data from this ocean area are lacking.

Some more conclusions can be drawn from comparison of the model results with other data: From the accumulation rate and organic carbon content of the sediment we know that the burial rate of organic carbon below the bioturbated zone is 0.13 μmol C.cm^{-2}.yr^{-1}. From the nitrate gradient in the pore water a downward diffusive flux of nitrate of 1.63 10^{-15} mol.cm^{-2}.s^{-1} is calculated, corresponding (with equation (2), disregarding advection) to a carbon mineralization rate with denitrification of 0.057 μmol C.cm^{-2}.yr^{-1}. As usual in open ocean sediments (BENDER & HEGGIE, 1984) oxygen is by far the most important electron acceptor: 98.4% of the carbon supply is mineralized with oxygen, 0.7% with nitrate, leaving only 0.07 μmol C.cm^{-2}.yr^{-1} (0.9%) at about 80 cm depth for further decay (by Mn(IV), Fe(III), and sulfate), and burial. At that depth, however, steady state assumptions are no longer valid since the accumulation rate and organic carbon content of the sediment were different during the last glaciation.

The measured potential activity of the electron transport system (ETS), integrated over the top 20 cm of the sediment, amounts on the average to 2.2 mmol $O_2.cm^{-2}.yr^{-1}$, corresponding to 1.7 mmol $C.cm^{-2}.yr^{-1}$. This implies that the potential activity exceeds the actual activity by a factor of 200.

Model and experimental results for Cu and alkalinity are compared in Fig. 3.37. For copper, we used the parameters of SAWLAN AND MURRAY (1983) to describe the adsorption of Cu in the sediment. The model results do not predict any near-surface maximum in dissolved copper, in clear contrast to the observations. The explanation must be that, as pointed out by KLINKHAMMER *et al.* (1982), Cu is released in a very thin surface layer as a result of preferential decomposition of its highly reactive organic carrier phase.

The offset between measured and predicted alkalinities is largely due to $CaCO_3$ precipitation during decompression. MURRAY *et al.* (1980) have tried to calculate the maginitude of this effect from reequilibration with $CaCO_3$ at 1 atm pressure, but unfortunately the effect is variable, and in carbonate oozes it is larger than predicted from thermodynamical considerations. From Fig. 3.37 it can be estimated at -0.20 mM.

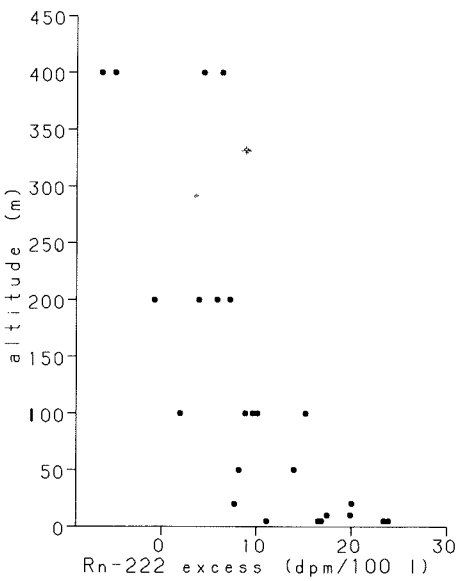

Fig.3.38. Excess-^{222}Rn in bottom water (dpm/100 l) *vs.* height above seafloor. Composite plot of results from stations 25, 27, 28 and 29.

3.8. MEASUREMENTS IN THE NEPHELOID LAYER

Mixing in the bottom water was studied using ^{222}Rn as a tracer. A composite plot of results from 4 stations from approximately 4700 m shows the enrichment of ^{222}Rn near the ocean floor (Fig. 3.38). Although the data show appreciable scatter, a half removal height in the order of 50 m can be estimated. In a one-dimensional mixing model this would correspond to a vertical eddy diffusion coefficient in the order of 100 $cm^2.s^{-1}$. This value is larger than the value of 22 $cm^2.s^{-1}$ reported by GURBUTT & DICKSON, 1985, but is still within the range given by SARMIENTO *et al.*, 1976. The scatter in the data suggests however that the ^{222}Rn distribution is influenced by horizontal advection of water masses that have been in contact with the sediment surface on hill sides, and cannot be simply modeled by one-dimensional eddy diffusion. Similar observations have been made earlier by ARMI & D'ASARO (1980) and by GURBUTT & DICKSON, and are in accordance with the data on BNL structure (NYFFELER *et al.*, 1985).

We faced a similar problem when interpreting data produced by V. Noshkin on $^{239+240}Pu$ in bottom water samples that had been collected during our cruises to the dumpsite. The Pu level in samples collected within 10 m from the seafloor was on the average significantly higher than above that depth. In view of the problems in interpreting the ^{222}Rn data, it is not certain whether it is justified to calculate Pu fluxes from these data. Moreover, we cannot yet distinguish whether the increased levels are the result of leaching from waste canisters, or from a remobilization of fall-out Pu, similar to the behaviour of Cu.

The suspended matter concentration, as measured by weighing, increases from 9 $\mu g.l^{-1}$ at mid-depth to values up to 28 $\mu g.l^{-1}$ in the nepheloid layer, in agreement with the data of NYFFELER *et al.*, (1985). Particulate organic carbon (POC) forms 20 $\pm$ 10% of the suspended particles within 200 m from the bottom, which means that 50 $\pm$ 25% of this suspended matter is organic. The filtration procedure gives the concentration of the abundant fine particles, not of the rare large particles. The fine suspended particles contain apparently more organic matter than the large particles that contribute most to the sedimentation flux (*cf.* section 3.7). Dissolved organic carbon is much more abundant in the bottom water than POC: its concentration is aproximately 0.4 $mg.l^{-1}$.

3.9. CONCLUSIONS ON THE BEHAVIOUR OF EACH OF THE RADIONUCLIDES OF MAJOR CONCERN:

$^{239+240}Pu$, ^{241}Pu and ^{241}Am

These nuclides are bound to both the organic phase and to the oxyhydroxides (including the coatings on the $CaCO_3$ phase). According to NELSON *et al.*, (1985) the binding strength of colloidal organic matter and sediment is in lakes approximately equal. To our knowledge no data exist to estimate the ratio of organic to oxyhydroxide sites in the fluff at the ocean floor, but BALISTIERI & MURRAY (1984) stress the importance of trace metal organic interactions in interfacial sediment from the deep sea. Predictions of diagenetic behaviour of these nuclides have to be based primarily on their supposed similarity to trivalent REE. The organically bound nuclides should thus be released during decomposition of organic matter. Since most of the Pu and Am in the waste is not incorporated in the organic matter, but rather adsorbs on it in the deep water, we can expect that the organically bound Pu and Am behave similar to copper, a metal that is known to form stable organic complexes.

The organic coatings that adsorb copper are decomposed at the interface much faster than the average decomposition rate of organic matter (half-life approximately 10 years in the bioturbated zone). A part of the released nuclides is trapped by oxyhydroxide surfaces, the remainder is released to the bottom water, in the same way as Cu and REE. Since Am is more strongly bound to oxyhydroxides than Pu, the percentage released to the bottom water would be higher for Pu than for Am, but it is difficult to estimate the actual percentages. The nuclides are transported downwards in the sediment by bioturbation and new deposition. Upon depletion of oxygen at 80 cm depth, mobility may increase, which would retard burial to depths beyond the reach of deep-burrowing organisms.

^{226}Ra

Radium (K_d in the order of 10^4) is more soluble than Pu and Am and therefore less efficiently scavenged from the bottom water. Release may increase the ^{226}Ra flux from the sediment locally some 200% above the flux from the natural U decay series (*cf.* Table 1.I).

^{3}H

Most ^{3}H is discharged as HTO, and it is assumed to be released quickly from the waste packages. It will be dispersed and transported in the water phase and reactions in the sediment are of no importance.

^{14}C

Occurs mainly as bicarbonate or incorporated in organic matter. The deepest part of the site is situated below the lysocline, but even just above the lysocline precipitation of fresh calcite can not be expected. Bicarbonate-^{14}C is transported in the water phase. Organic matter will be subject to degradation at the sediment surface. The percentage degraded at or near the surface without leaving measurable traces in the sediment or pore water is not known: REIMERS & SUESS (1983) mention 35-85%, but according to EMERSON *et al.* (1985) the percentage is negligible. The correspondence, noticed in section 3.7, between carbon fluxes predicted by our diagenetic model and by primary productivity, suggests that only a minor part of the sedimenting organic matter is decomposed at the very surface. Although Cu data indicate that the most reactive organic coatings are rapidly decomposed at the sediment surface without leaving any trace in the sediment (KLINKHAMMER *et al.*, 1982), this needs not be a significant fraction of the organic matter. Sediment trap data to check the situation at the dumpsite are lacking. From diagenetic modeling we know, however, that the major part of the organic matter is mineralized at an average rate of about $2.5\ 10^{-9}s^{-1}$ (decomposition halflife 10 years), about 20% decays some 10 times slower, and only 0.9% is buried. Since the organic matter in the waste has not been through the same mineralization process during descent through the water column, the percentage of decomposable material is probably even higher. Thus, the major part of ^{14}C in discharged organic matter, is released to the pore water and subsequently to the bottom water on a time scale of decades. Hence, part of ^{14}C will temporarily reside on the seafloor and be incorporated in the food chain, but the major part will ultimately be transported by water currents in the form of bicarbonate ion. Since the isotopic composition in sedimentary calcite, even in thin calcite layers, is very well preserved over the lifetime of ^{14}C, it appears unlikely that an appreciable part of waste-derived ^{14}C would be incorporated in the sedimentary calcite by isotope exchange.

^{90}Sr

is relatively soluble (K_d in the order of 10^2), and the major part will be transported with the bottom water. No new calcite precipitation will incorporate ^{90}Sr at the seafloor, but through cation exchange ^{90}Sr may become associated with clay and calcite particles (DUURSMA, 1973). Some release of Sr occurs as a result of $CaCO_3$ dissolution. Release due to the recrystallization of $CaCO_3$ occurs at a much longer time scale than the radioactive decay of ^{90}Sr, and is therefore insignificant.

^{137}Cs

is relatively soluble (K_d in the order of 10^3), and a large part is transported with the bottom water. Also within the sediment, Cs is more mobile than e.g. Pu (Santschi *et al.*, 1983). Adsorbed Cs is bound to or protected by organic and hydroxide coatings, and some release occurs in the suboxic sediment after the breakdown of these coatings (MCKAY & BAXTER, 1985). Remobilization continues in the sulfate reduction zone (only present in turbidites) as a result of ion exchange with NH_4^+. The release processes in the suboxic and sulfate reduction zones are of no radiological significance in view of the relatively short half-life (30.1 yr).

^{60}Co

Cobalt adsorbs strongly on hydroxides at the sediment surface. It is ingested by fauna together with these particles. Mobilization in the digestive system as a result of low pH and Eh can be expected, but Co is not accumulated by the organisms. The release of Co to the pore water occurs only in the suboxic zone, *i.e.* below 80 cm depth, and is therefore of no significance for ^{60}Co (halflife 5.3y).

4. BIOLOGY

4.1. INTRODUCTION

Our knowledge of the deep-sea bottom fauna of the NEA-dump site has been very small so far. FELDT *et al.* (1981) mentioned the occurrence of the sea-anemone *Actinauge abyssorum*, and with traps fish *Coryphaenoides armatus* and Amphipoda *Eurythenes gryllus* were caught near the bottom (PENTREATH, 1983 & WICKINS, 1983). Recently GEIDAROV *et al.* (1983) gave far more information about the benthos. They found 70 different species of invertebrates and also presented a figure for the biomass. For the meiofauna no data at all were available, but in the neighbourhood of the dumpsite, in the Iberian deep sea, THIEL (1972), RACHOR (1975) and DINET & VIVIER (1977) collected some data on this group. It was only during the project reported here that more information became available about the megafauna from FELDT *et al.* (1985). Their annual trawling surveys since 1980 in the dumping area showed the presence of the following megafaunal groups: Porifera, Actiniaria, "Vermes", Crustacea, Gastropoda, Asteroidea, Holothuroidea and fishes. Besides, they provided estimates for density and biomass of these groups.

Because of this lack of data and the need, formulated by CRESP, to get site-specific information about the NEA-dumpsite, the biological program of the DORA-project was focussed on the benthos of the site. Determination of the composition, density, biomass, horizontal and vertical distribution in the sediment of the meio- and macrobenthos not only gives us a better general knowledge of the area, but it also provides information about processes that can influence the transport of radionuclides. These data can give us an explanation for the (bio)turbation that is known to exist there from measurements of 239 + 240 Pu and 210 Pb (see chapter 5).The vertical distribution will indicate the maximum penetration of bioturbation. Data on composition, density, biomass and trophic structure will give a better understanding of the deep-sea foodweb, which is a first requirement to get an idea of the importance of these animals as accumulators of radionuclides and as a food source for mobile predators connecting the benthic region with levels higher in the watercolumn. Finally measuring diversity provides not only the relative ecological value of the fauna, but is also a potential tool to determine a disturbance of the fauna in the future, e.*g.* by radioactivity.

4.2. METHODS

4.2.1. MEIOFAUNA

From the boxcore samples of the 1982 expedition several subcores were taken with perspex tubes of 24,6 cm^2 to study the meiofauna. These subcores were cut horizontally into slices (Above 5 cm depth: 1 cm slices; below 5 cm depth: 2.5 cm slices; below 10 cm depth: 5 cm slices), which were then preserved in buffered formalin 4%. During the 1984 expedition 10 subcores of 10 cm^2 were taken from 6 boxcore samples to determine the horizontal distribution of the meiofauna within a boxcore. Now only the upper 6 cm, cut into two horizontal slices of 3 cm, were studied. In the lab the samples were coloured with rosebengal added with phenol (THIEL, 1966). Because of the phenol, rosebengal will give an optimum colouring in a wider range of the Ph, but to our experience it also has a remarkable effect on the sticky clay. It makes the sediment "softer", with the consequence that the colour

will penetrate better and, moreover, it makes the sieving or elutration much easier and quicker. The samples of 25 to 125 cm^3 were fractioned by elutration (UHLIG, THIEL & GRAY, 1973) in a 5 liter glass jar by a tapwater current of 1 l/min. until the water in the jar was clean. A second fraction was obtained by a current of 2 l/min. All fractions were sieved over 50 μm and the residu of the sample also over 200 μm gauze (Fig. 4.2). To calibrate the effect of a smaller screen-size on the number of "meiofaunal" animals retained, in some samples a 31 μm gauze was used in addition. This screen-size is smaller than those used in most other meiofaunal studies. Contamination with *e.g.* fresh water Nematoda in the tapwater used was avoided by a 10 μm sieve, which was cleaned regularly. The 4 different fractions were sorted under a stereomicroscope (20x) and always checked by a second person. Checking increased the number of animals found by 10 - 25%. Most animals were concentrated in the very small 1 $l.min^{-1}$ fraction. The animals were picked out and mounted in lactophenol, but later on in glycerin because of its better long-term conservation properties. The measuring and counting was done with a microscope (100-400x). The individual Nematoda biomass was calculated by the method of ANDRASSY (1956), with the formula $G = 0.665 * a^2b$. For the Nematoda with a short and thick body, *e.g.* the family Desmoscolecidae, we used the following formula: $G = 0.436 * a^2b$. In both formulae G = wet weight, a = the largest diameter and b = the body length of a nematode. For the conversion of wet weights to dry weights we used a ratio of 0.25 (see *e.g.* WITTE & ZIJLSTRA, 1984). This method of Andrassy has the advantage above real weighing with a balance, that the material is not ruined by drying and that instead of a total biomass for Nematoda, also the weight of individuals is measured. So, studies on diversity, trophical levels and taxonomy are still possible. Besides, these data can be coupled with biomass data. So, for example, the biomass of all deposit feeding Nematoda can be calculated. We do not think that real weighing would have given a more accurate value for the Nematoda biomass, as used balances have an accuracy of 1 μg (PFANNKUCHE, 1985), which means, apart from errors made by handling the samples (cleaning, drying), an error of 25 to 50 Nematoda for the dumping area. The volume of Copepoda and nauplii was calculated in a similar way by breaking up the animal in cones, cilinders etc. For the calculation of the dry weight we used a factor derived from 100 copepods of the North Sea. No attempt has been made to estimate the biomass of the other less important meiofauna taxa. The results of 1 (station 1 - 15) or 5 subcores (station 21 - 26) of each boxcore are reported here.

4.2.2. MACROFAUNA AND LARGE MEIOFAUNA

Of the same boxcore sample used for subcoring during the 1982 expedition, we skimmed off approximately the upper 3 centimetre of the remaining surface area (1864-2046 cm^2), while the perspex subcores were still in the sediment. This upper 3 cm layer and the remaining part were sieved on board seperately over 1 mm to collect the macrofauna, which was stored in formalin. For the study of the larger meiofauna a sieve of 200 μm screen-size was used in addition. To prevent contamination with plankton we sieved the used seawater over 50 μm. The macrofauna was identified to the level of higher groups. Since too few animals were available to get reliable dry weights by normal weighing, we measured the volume of each animal in a similar way as with the meiofauna. With a value of 1 for the specific gravity (which is, of course, an underestimate) and with the conversion table of ROWE (1983) for wet weights to dry weights for the different deep-sea animals, the shell-free dry weight was calculated. For Tunicata and the indeterminanda we had to estimate

a factor (0.25 and 0.10, respectively) and for Bivalvia we used the factor derived from Rowe's carbon data. During the 1984 expedition we used an additional sieve of 0.5 mm screen-size for the study of the large meiofauna. Also during this second expedition some box-core samples were cut horizontally into slices for a more detailed study of the vertical distribution of the macrofauna in the sediment. Slice thickness depended on the surface relief of the bottom sample.

During the 1984 sampling we also tried to collect larger meiofauna (> 0.5 mm) and macrofauna in larger numbers than recovered by a boxcore, with help of a bottom sledge with a closing device and a net of a sreen-size of 0.5 mm. However, after one successful catch, the sledge was lost, and no results are given in this report.

4.2.3. MEGAFAUNA

There is no internationally accepted definition for megafauna. We defined as megafauna those animals that have a diameter of more than 1 centimetre and/or a wet weight of more than 50 mg, because those animals can be caught, more or less quantitatively with our fishing gear, which had a net of a meshsize of 1 cm.

The megafauna was sampled with a 3.5 m Agassiz trawl with a net of 1 cm screen-size. When the net was lowered and heaved, the catch was inevitably contaminated with pelagic organisms, since the trawl was not equiped with a closing mechanism. We obtained very poor catches, and suspected that this was due to the use of the light-weight synthetic wire (Kevlar), which apparently resulted in a poor bottom contact of the trawl. In 1984 we used a steel wire instead, and indeed obtained far richer catches. Moreover, the contamination by pelagic organisms was effectively prevented by the use of a mechanical closing device on the trawl.

Part of the catches was frozen for chemical and radionuclide analyses and a part was preserved for identification. Dissection of the frozen animals for chemical and radionuclide analyses was done as cleanly as possible with scalpels of tantalum or teflon coated steel. Plastic equipment and storage jars were thoroughly cleaned with a HCL solution and bidistilled water. Contamination with the sediment on the skin and in the gut of the animals was avoided as much as possible. The thawing period was kept short and after dissection the samples were freeze-dried.

4.2.4. DIVERSITY OF NEMATODA

The diversity of the Nematoda fauna in the meiofaunal subcores of stations 11, 13 and 15 has been measured in 3 different ways:

1. Species richness (SR) with the formula according to MARGALEFF (1958); $SR = (S - 1)/\ln N$, in which S = the number of species in the sample and N = the number of individuals in the sample.
2. Shannon species diversity index (H) following PIELOU (1966):

$$H = -\sum_{i=1}^{S} P_i(\ln P_i)$$

In which P is the percentage of the species i of the total number of nematodes in the sample and S is the total number of species in the sample. The parameter J, called evenness or equitability, gives the ratio between the measured diversity (H) and the maximum

Table 4.1. Number of specimens per m^2 of the different meiofauna groups in the boxcore samples. Data have been derived from 1 subcore of 24.6 cm^2 (stations 1 to 15) or from 5 subcores of 10 cm^2 (stations 21 to 26). Data of the 1984 expedition for Nematoda, Copepoda and nauplii have been corrected (see section 4.3.1.4), because they were derived from subcore samples of only 6 cm depth.

Station	1	2	4	5	6	8	11	13	15	21	22	23	24	25	26	mean	%
Nematoda	321.6	100.7	246.4	385.7	300.4	373.1	401.5	595.2	989.0	314.9	403.1	534.0	560.0	621.6	720.2	457.8	86.78
Foraminifera	22.8	6.1	1.2	37.8	13.8	19.1	7.3	7.3	34.1	12.6	4.2	22.8	6.8	4.6	11.2	14.1	2.68
nauplii	2.4	2.4	2.4	11.8	6.5	4.9	6.5	20.3	28.0	5.4	1.9	10.1	10.6	4.5	5.6	8.2	1.56
Copepoda	3.3	7.3	9.3	4.9	8.9	8.1	6.1	11.8	20.7	5.1	2.0	6.4	8.7	11.6	6.4	8.0	1.52
Polychaeta		0.4		1.2			0.8	1.2	5.7	1.2	0.8	3.2	1.4	1.8	2.0	1.3	0.25
Ostracoda	0.4	0.8	0.8	2.0	0.4	0.4	0.8	0.4	2.4	0.6	1.2	2.0	0.8	0.6	0.6	0.9	0.18
Kinorhyncha						0.8			1.2	0.2		1.0	0.2		0.2	0.2	0.05
Tardigrada			0.8		0.4				0.4			0.6				0.1	0.03
Oligochaeta		0.4		0.4					0.4							0.1	0.02
Bivalvia			0.4						0.8		0.2		0.2	0.2		0.1	0.02
Tanaidacea							0.4	0.4	0.4					0.2		0.1	0.02
Ectoprocta													1.2			0.1	0.02
Sipunculida	0.4													0.2			0.01
Porifera							0.4										0.01
Loricifera								0.4									0.01
Komokiacea											0.4						0.01
Isopoda											0.2		0.2				0.01
Nemertini											0.4						0.01
Xenophyophorea															0.2		
Acarina															0.2		
Eggs & Spheres	3.3	0.8	0.8	1.2	6.1	8.1	2.0	16.3	6.1	4.8	1.6	4.6	4.0	8.4	8.2	5.1	0.96
Indeterminanda	2.0	2.5	1.2	18.3	11.0	9.3	5.3	32.5	37.8	34.2	39.2	87.2	40.2	60.0	84.8	31.0	5.88
Total	356.2	131.4	263.3	463.3	347.5	423.8	431.1	685.8	1127.0	379.0	455.2	671.9	634.3	713.7	839.6	527.1	

possible diversity in a sample with S species: $J = H / H_{max}$ and $H_{max} = \ln S$.
3. Simpson's index of diversity (D) following PLATT *et al.* (1984): 1 - D = (Runs - 1)/N, in which N is the number of Nematoda individuals in a sample. With "Runs" we mean the number of recordings that a specimen picked out from the randomized Nematoda sample is taxonomical different from the specimen picked out just before. See for an explaining figure PLATT *et al.* (1984). The higher the number of runs (high diversity), the lower the value for D.

Most of the Nematoda species in the abyssal sea are still undescribed. Therefore we recognized a nematode specimen as a different species when it was morfologically clearly different from the other specimens. Drawings of head, tail and habitus were used to make comparisons easier. This method will most likely give an underestimate of the real diversity, as differences between nematode species are sometimes only recognized after a careful morfological study of the specimens. On the other hand, males and females of the same species have sometimes greatly different habiti, and they may thus have been counted as different species.

4.2.5. TROPHIC STRUCTURE OF NEMATODA

Using the microscopical slides, made for calculating the biomass and diversity, we studied the trophic structure of the Nematoda fauna of stations 11, 13 and 15. According to mouth structures Nematoda can be divided into four trophic levels (WIESER, 1953), *viz.*: selective (1A) and non-selective-depositfeeders (1B), grazers or epistrate feeders (2A) and carnivores (2B) (Fig. 4.10). That mouth structure and feeding types are actually correlated has been confirmed by analyses of the gut contents (PERKINS, 1958; TIETJEN, 1969; BOUCHER, 1973 and LEVY & COULL, 1977), and by nutritional studies (TIETJEN & LEE, 1977; TIETJEN, 1980 and ALONGI & TIETJEN, 1980).

4.3. RESULTS AND DISCUSSION

4.3.1. MEIOFAUNA

The meiofauna ($> 50\ \mu m$ and < 1 mm) consisted mainly of Nematoda, Foraminifera, nauplii and Copepoda and several less important groups (Table 4.1, Figs. 4.1 and 4.2).

All these groups are known to occur on those water depths, except for the Loricifera, a new phylum described recently by KRISTENSEN (1983) and until 1984 only known from rather shallow water. The indeterminanda consisted mainly of wormlike bodies, probably chiefly Foraminifera.

4.3.1.1. DENSITY

As expected from most other deep-sea meiofaunal studies the Nematoda have the highest density (87% of the total meiofauna) with a mean of 457 800 per m^2. The density varies between 100 700 and 989 000 per m^2 (Table 4.1).

These figures are rather high compared with other studies in the Atlantic from the same depth (Table 4.2), but not exceptional. A density of almost 1 million per m^2 in station 15

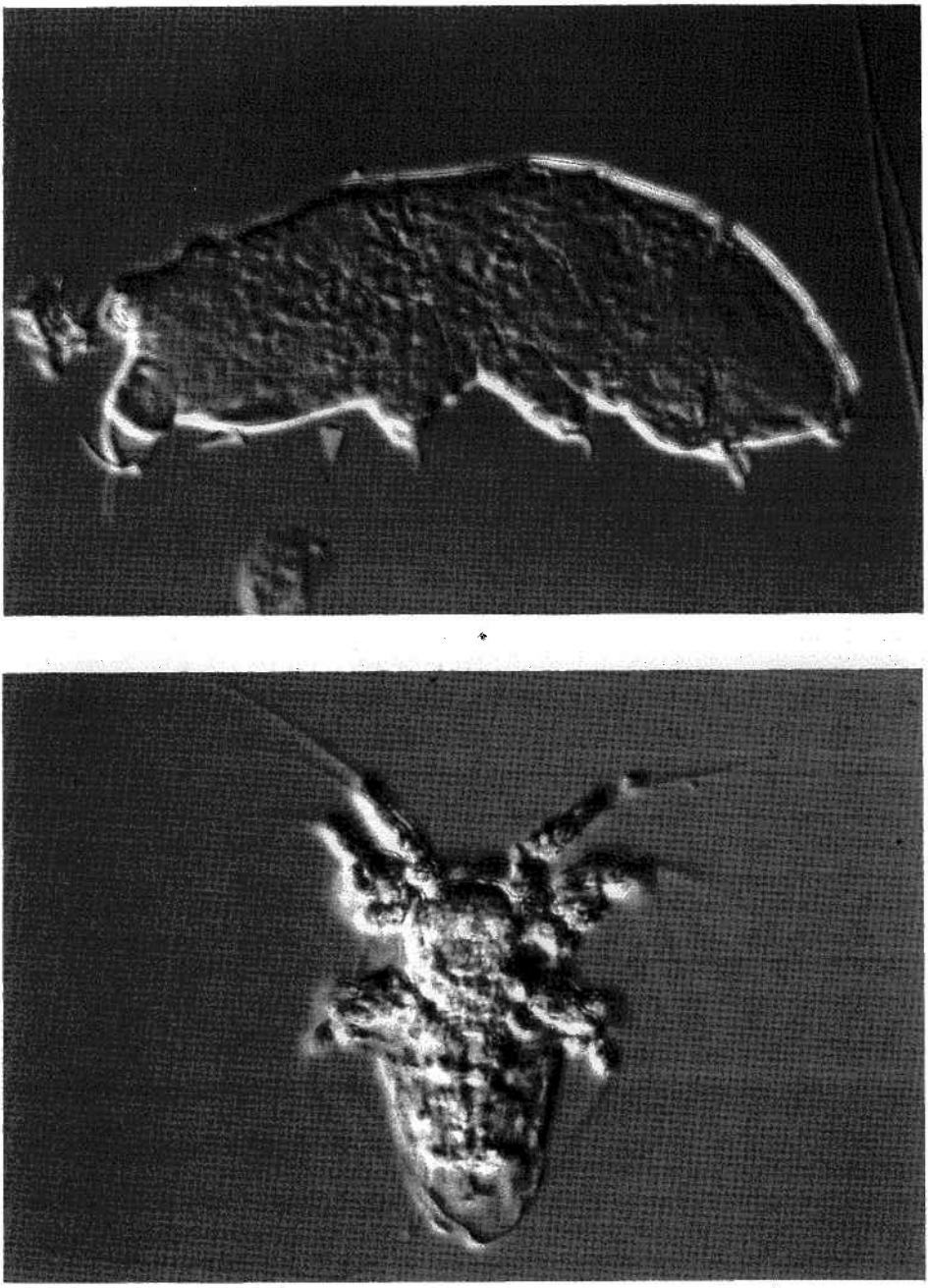

Fig. 4.1. Meiofauna from the boxcore samples. Above: Specimen of the phylum Tardigrada, length 240 μm (core 4B). Below: Nauplius, length 86 μm (core 6B).

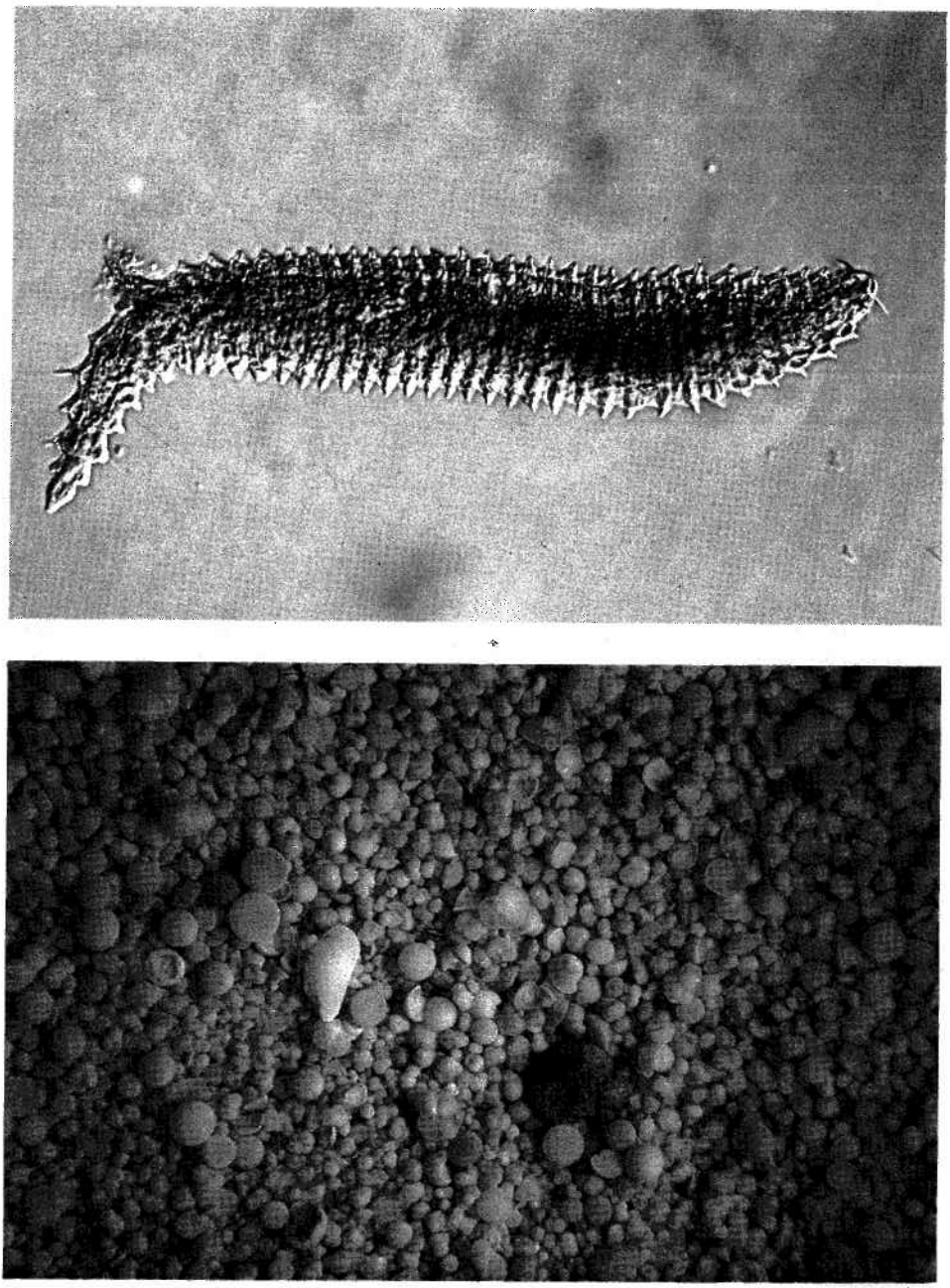

Fig. 4.2. Above: Meiofauna from the boxcore samples. Nematode belonging to the family Desmoscolecidae, length 330 μm (core 5B). Below: coarse fraction (> 200 μm) of sediment from the boxcore 8B, containing for the larger part tests of pelagic Foraminifera. The sphere shaped tests are from *Orbulina universa* d'Orbigny, 1839. Length of photo 14 mm.

Table 4.2. Density and biomass of Nematoda, Copepoda and nauplii from different quantitative studies on the benthos of the Atlantic ocean below 4000 m.

	depth	area	Nematoda			Copepoda and nauplii		Screen-size in µm
			Density[1]	mean	Biomass[2]	Density[1]	Biomass[2]	
Thiel, 1972	5272-5340m	Iberian deep sea	156 -278	219	150 mg	4.7	1.9 mg	42
Rachor, 1975	4878-5510m	Iberian deep sea	15.5- 76	46	5.9mg	11.6	1.5 mg	50
Dinet & Vivier, 1977	4096-4725m	Bay of Biscay	86 -383[3]	243		20.5		50
Dora expedition, 1982	4000-4800m	Iberian deep sea	101 -989	413	16.4mg	18.4	10.0 mg	50
Dora expedition, 1984	4000-4800m	Iberian deep sea	315 -720	473	11.1mg	11.4	8.6 mg	50
Pfannkuche, 1985	4167-4850m	Porcupine Seabight	272 -462	345		45		42
Dinet, 1973	4100-5170m	South Atlantic	294 -504	364		14.7		40

1 Density in thousand per m^2.
2 Biomass in dry weights per m^2.
3 Leaving out two probably biased samples with densities of 5 to 12 thousand per m^2.

must, however, be considered as a new record for those depths. It cannot be immediately concluded that the dumping area is richer than the other areas studied, because part of the differences can be explained by differences in methods. The elutration method will concentrate the meiofauna better and to our opinion will work, because of the slow water stream, more gently than the normal sieving method used by THIEL (1972) and RACHOR (1975). The use of a smaller screen-size (31 µm) in addition to a 50 µm raised the total nematode density on average by only 8% (Table 4.3). The effect of this smaller screen-size on densities of other meiofaunal groups and on the nematode biomass was negligi-

Table 4.3. Number of Nematoda (of 10 subcore samples of 10 cm^2) passing through a sieve of 50 µm screen-size and retained by a sieve of 31 µm screen-size.

Station / Subcore	25	26
1	34	41
2	107	45
3	141	18
4	29	19
5	25	11
Mean	67.2	26.8
Stand. deviation	53.3	15.2
$\frac{N_{31\mu m}}{N_{50\mu m}} \times 100\%$	12.0	4.1

$N_{31\mu m}$ = number of Nematoda passing through a 50 µm screen and retained by a 31 µm screen.

$N_{50\mu m}$ = number of Nematoda retained by a 50 µm screen.

ble. We agree with THIEL (1983) that decantation before fixation of the sediment samples can be the explanation of the low figures of RACHOR (1975), because fixation makes the animals stiffer and less fragile, with the consequence that fewer animals will be broken up and/or pressed through the sieve. Extraction of meiofauna from sediments by using a solution of high specific gravity (*e.g.* Ludox) too, must give higher losses of nematodes, if the same screen-size is used, because the sample is thoroughly sieved before and after the procedure (see *e.g.* HEIP *et al.*, 1985). We, therefore, recommend a smaller screen-size than 50 μm, when the normal sieving method or Ludox technique are used. However, we have to realize that we do not want to calculate the density of all Nematoda or all metazoans, but only of the meiofaunal representatives. If we wanted to study all Nematoda or metazoans, we do not need the arbitrary terms meio- and macrofauna. Another point of difference is that most studies only investigated the upper centimetres of the sediment. If only the upper 6 cm are studied, which is common practice, densities of Nematoda, Copepoda and nauplii are underestimated by 10, 10 and 15 %, respectively, according to our data from the dumpsite.

Two other important groups are the Copepoda and the nauplii with densities varying from 3900 to 48 700 with a mean of 16 200 per m^2 (Table 4.1). They constitute together 3.1% of the total number of meiofauna animals (Table 4.1). Figures of comparable studies in the Atlantic (Table 4.2) are of the same order.

Foraminifera constitute 2.7% (Table 4.1), but for this group it is difficult to get reliable data. In spite of the colouring with rose bengal it is often difficult to decide whether a foraminifer was alive at the time of collection. Tests with one to all chambers coloured were found. If only one or two chambers were coloured, these were not always the last chambers as would have been expected. On the other hand, pelagic Foraminifera known to be living only in the upper 100 m of the sea and expected to be dead, sometimes coloured, which can partly be due to naked Foraminifera inhabiting the empty test (A.J.Gooday, IOS, Wormley, UK., personal communication).

4.3.1.2. BIOMASS

Nematoda biomass varied from 8.2 to 28.2 mg dry weight per m^2, with a mean of 14.4 mg per m^2 (Table 4.24). Few data from the area are available for a comparison with these figures (see Table 4.2). The low figures of RACHOR (1975) are explained by his low values for the densities, but still they overlap our data. THIEL (1972) gives much higher figures, notwithstanding his lower values for densities. Rachor already noted and later on THIEL (1983) agreed that these numbers were probably too high, because the mean individual weight used for Nematoda was derived from a study of a much shallower area (290-2500 m). Our much smaller estimates of the individual weights for Nematoda (Table 4.4) agree relatively well with the value of 0.072 μg given by DINET *et al.* (1985) for nematodes from the abyssal Atlantic, as it falls just within our range. Our individual weights for deep-sea nematodes differ from values for intertidal Nematoda (see *e.g.* WITTE & ZIJLSTRA, 1984) by almost an order of magnitude (Table 4.4).

The correlation between biomass and density of Nematoda in our samples is not very great (0.657 with $n = 15$). Within a boxcore this correlation coefficient varies between -0.158 and 0.881 ($n = 5$) for station 21 to 26. Calculated for all 30 subsamples of stations 21 to 26, it is only 0.505. Furthermore, we found a large difference (almost a factor 2) between the values for mean individual nematode weight of the 1982 and 1984 expedition (Table

Table 4.4. Mean individual biomass of Nematoda in μg dry weight.

	depth	mean dry weight in μg
DORA expedition, 1982	4000-4800 m	0.040 (0.029-0.081)
DORA expedition, 1984	3958-4787 m	0.023 (0.017-0.031)
Thiel, 1972	290-2800 m	0.27-1.9
Witte & Zijlstra, 1984	littoral	0.28 (0.23-0.42)
Dinet et al., 1985	abyssal Atlantic	0.072

4.4). For a part this difference may be explained by a different way of mounting the nematodes in slides that could have caused a slight flattening of the nematodes of station 2 to 8. Those stations have indeed a higher mean individual nematode weight than the other stations of the first expedition (0.058 and 0.033 μg, respectively). Yet, the average individual nematode weight of stations 1, 11, 13 and 15, is still markedly higher than that of the 1984 expedition (0.033 and 0.023, respectively). From these data it can be concluded that the use of a mean individual weight for nematodes leads to inaccurate calculations of the biomass in our area. If a mean individual weight derived from one deep-sea area is used for an other deep-sea area, the errors can be much larger. So for instance, the mean individual weight measured by Dinet *et al.* (1985) for the Iberian deep sea below 4000 m is a factor 2 higher than for the NEA-dumpsite, while the individual weight derived from data given by TIETJEN (1984) for the Venezuela basin (> 3600 m) is even larger.

From samples of the boxcore stations of both DORA-expeditions 23 336 Nematoda were measured. The mode of the individual Nematoda biomass is 0.007-0.0100 μg and the mode of the Nematoda length is 300-350 μm (Figs. 4.3 and 4.4). Probably because of the high diversity there is no good correlation (0.55 with n = 23 336) between body length and biomass. This correlation does not improve if large Nematoda and/or Desmoscolecidae are discarded.

The biomass of Copepoda and nauplii varied from 1.1 to 32.9 mg/m^2 dry weight, with a mean of 9.8 mg/m^2 (Table 4.24). Compared to the Nematoda the biomass is much more variable, which is caused by the lower densities and the high diversity in body sizes. On average the biomass is lower than that of the Nematoda. Because of the high average individual weight of Copepoda, the copepode biomass is, inspite of their low densities, not negligible. Only RACHOR (1975) calculated the biomass of Copepoda in a similar way. For stations deeper than 4000 m in the Iberian deep sea he found wet weights from 0 to 16.4 mg/m^2, with a mean of 5,9 mg/m^2. This means an average biomass of only about 1.5 mg/m^2 dry weight (if calculated with the conversion factor 0.25). An explanation may be that large Copepoda have a higher specific weight, so that these animals are not collected quantitatively by the decantation method used by Rachor. This argument seems reasonable, as in our elutration method the larger Copepoda were always found in the residue. The

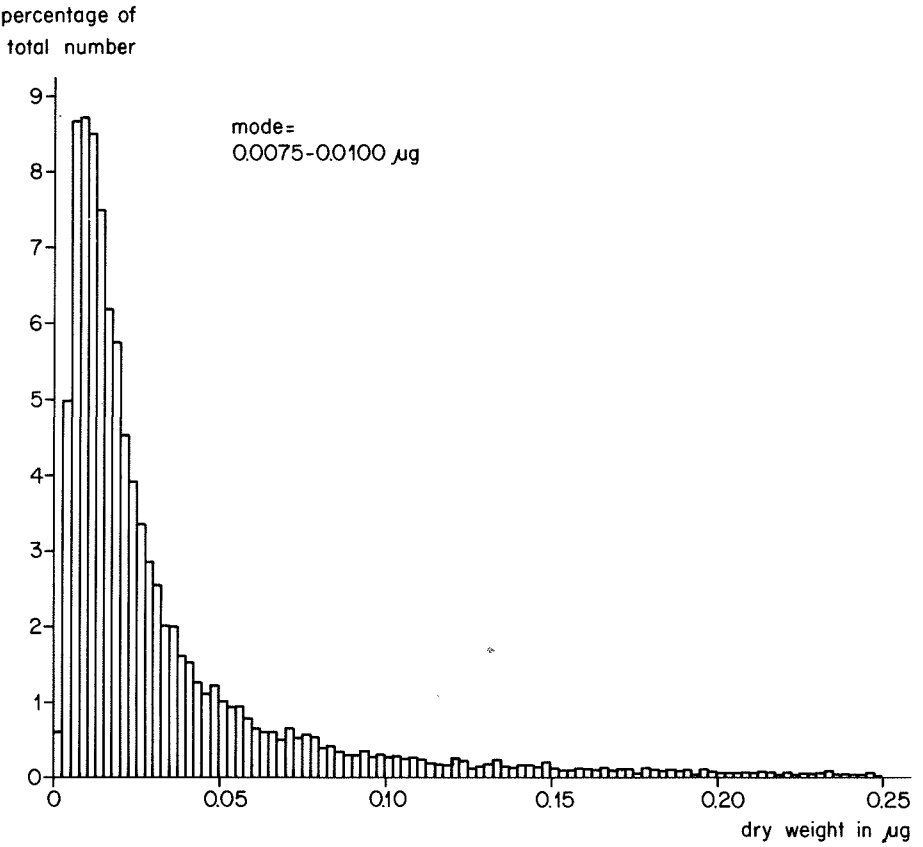

Fig. 4.3. Frequency distribution of the individual biomass (dry weight) of 23 336 Nematoda from stations 1 to 26.

rough estimate for wet weights of Copepoda given by THIEL (1972) for wet weights of Copepoda by assuming that the mean individual weight was 2 µg (Table 4.2) seems to be reasonable.

The total biomass of the meiofauna given in Table 4.24 does not include other meiofauna groups than Nematoda, Copepoda and nauplii. The contribution of these other groups is estimated to be very small, and no attempt has been made to calculate it.

4.3.1.3. HORIZONTAL DISTRIBUTION

Density and biomass for Nematoda, Copepoda and nauplii from 5 subcores of 10 cm^2 of boxcores of stations 21 to 26 are given in Tables 4.5 - 4.8. These data point to an even distribution for Nematoda densities within a boxcore. Density and biomass estimates for Nematoda from our first expedition, derived from one subcore with a diameter of 24.6 cm^2, are statistically less accurate than those derived from 5 subcores of 10 cm^2 (more samples and larger total surface), and probably because of that they have a larger range. Data for subcores 23-3, 24-2 and 25-1 show that densities can be actually much higher or lower than the average density in a boxcore (Table 4.5).

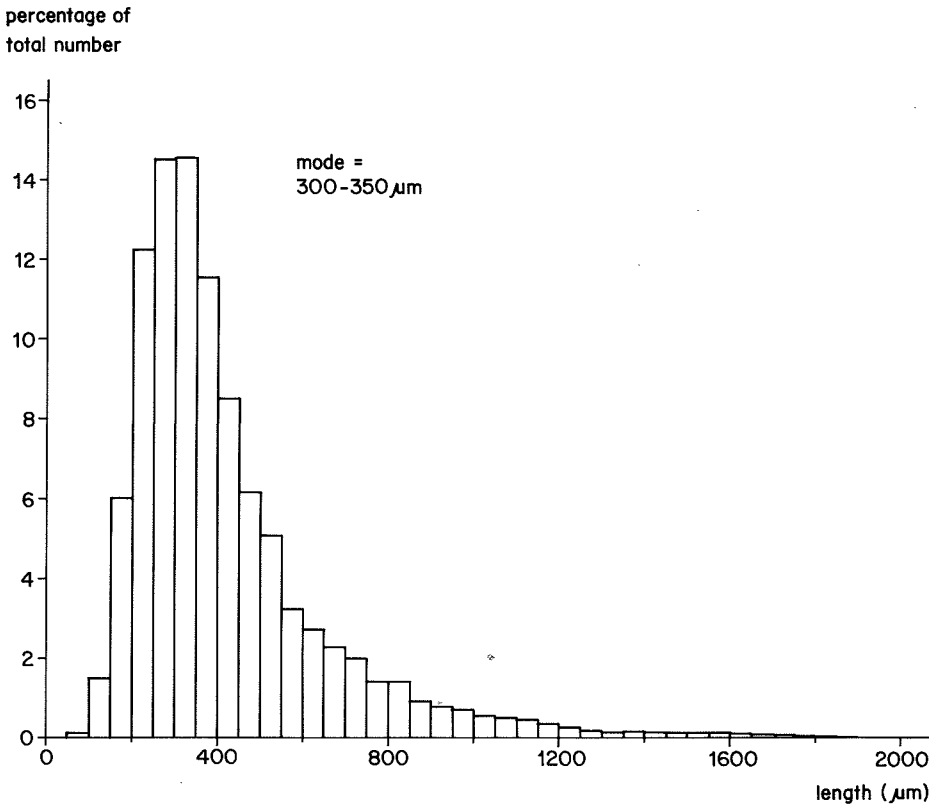

Fig. 4.4. Frequency distribution of the body length of 23 336 Nematoda from stations 1 to 26.

Table 4.5. Number of Nematoda in 5 subcores of 10 cm^2 from one boxcore sample of each of the stations 21 to 26.

CORE \ BOX	21B	22B	23B	24B	25B	26B
1	289	382	436	458	318	700
2	318	380	456	654	659	592
3	257	343	597	429	550	649
4	269	390	469	452	604	669
5	284	319	445	529	666	631
MEAN	283	363	481	504	559	648

Table 4.6. Biomass of Nematoda from 5 subcores of 10 cm^2 from one boxcore sample of each of the stations 21 to 26, in $\mu g/10\ cm^2$ dry weight (= mg/m^2).

CORE \ BOX	21B	22B	23B	24B	25B	26B
1	12.5	9.1	12.3	12.3	9.6	14.7
2	7.2	10.3	16.6	20.4	13.4	10.2
3	10.0	5.3	12.1	11.5	17.9	8.5
4	6.6	8.5	9.8	13.1	12.8	10.5
5	8.4	8.4	8.0	11.6	10.9	10.7
MEAN	8.9	8.3	11.8	13.8	12.9	10.9

Table 4.7. Number of Copepoda and nauplii in 5 subcores of 10 cm^2 from one boxcore sample of each of the stations 21 to 26.

CORE \ BOX	21B	22B	23B	24B	25B	26B
1	9	2	13	16	19	13
2	14	4	16	21	17	11
3	4	3	19	15	10	6
4	2	1	14	13	17	6
5	17	7	10	19	8	17
MEAN	9.2	3.4	14.4	16.8	14.2	10.6

Table 4.8. Biomass of Copepoda and nauplii from 5 subcores of 10 cm^2 from one boxcore sample of each of the stations 21 to 26, in μg dry weight/10 cm^2 (= mg/m^2).

CORE \ BOX	21B	22B	23B	24B	25B	26B
1	7.3	1.6	1.6	9.5	6.0	7.8
2	15.3	1.0	7.0	9.3	6.1	30.4
3	1.8	0.6	3.0	10.6	6.2	1.5
4	2.3	0.7	28.7	8.3	6.7	1.3
5	5.1	3.2	4.8	12.6	4.9	50.9
MEAN	6.4	1.4	9.0	10.1	6.0	18.4

Nematoda biomass, however, varies much more within a boxcore (Table 4.6), and even within a boxcore there is no good correlation between densities and biomass.

Due to the lower densities and the larger size range of the Copepoda and nauplii, their densities and especially their biomass show large fluctuations within a boxcore (Tables 4.7 and 4.8). When densities become higher, however, fluctuations are lower (see stations 23 and 24). From these data it is clear that a good estimate of densities and biomass for Copepoda and nauplii can only be derived from larger samples than needed for Nematoda.

If we compare meiofauna data of different boxcores, some relationships are found between stations that are situated near each other and have the same depths. It is obvious that densities for Nematoda for station pairs 1 and 21, 13 and 25, 8 and 11, and less clearly in 5 and 23, differ only slightly from each other (2, 4, 7 and 28%, respectively) (Fig. 4.5). However in areas in which, during our first expedition the lowest (station 2) and the highest (station 15) densities were found, highly different results were obtained during the second expedition (stations 22 and 24, respectively). If we assume that the numbers of Nematoda found in the subcores of station 2 and 15 are not representative for those stations, than the data of the other station pairs, mentioned above, suggest a fairly even distribution for Nematoda on a much larger scale than a boxcore. Data for Nematoda biomass and for Copepoda and nauplii are much more scattered and do not allow such a generalisation. As the input of terrigenous material at the dumpsite is relatively small, because of the distance to the continent, the main input being caused by remains of pelagic organisms (chapter 3), such large differences in animal densities and biomass as on the continental slope are not likely to be found. Yet sediment characteristics are variable within the area studied here. The deeper areas in the western part of the dumpsite and around stations 1 and 21 are different from the top and the slopes of the sea-mounts in the area. So dif-

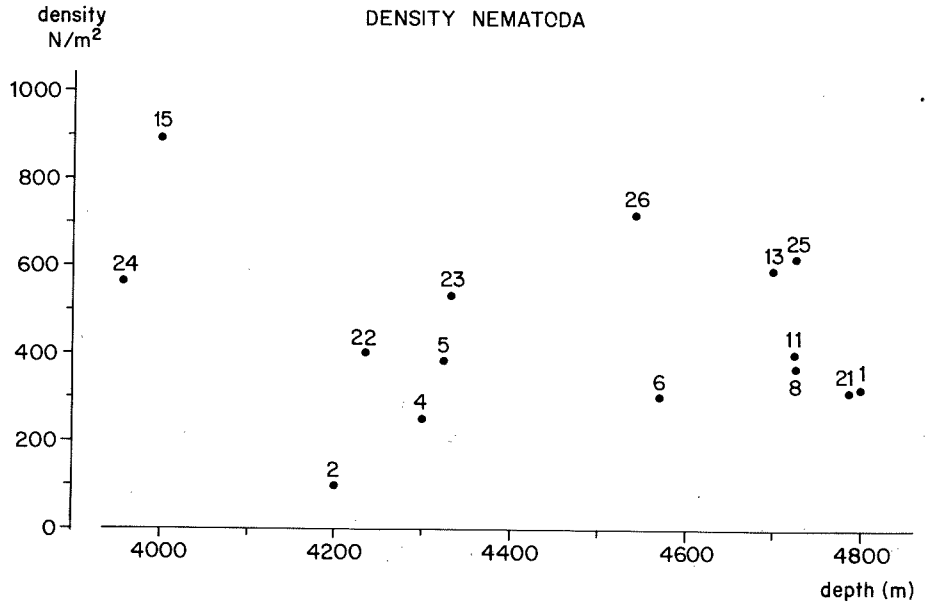

Fig. 4.5. Distribution of Nematoda density with depth. The numbers refer to station numbers.

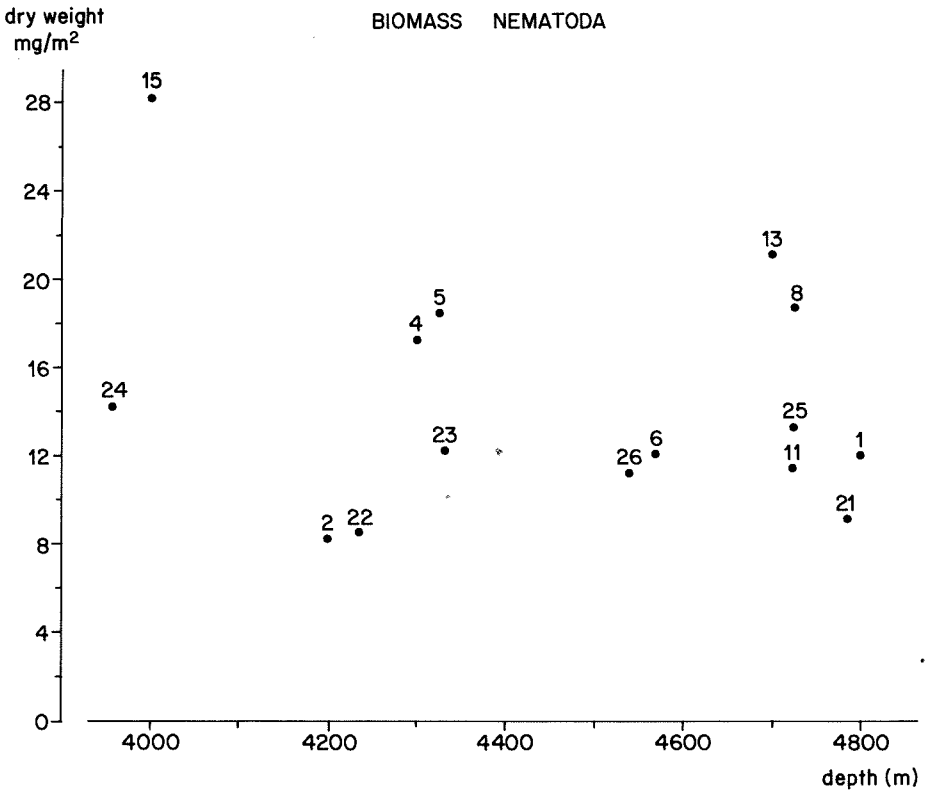

Fig. 4.6. Distribution of Nematoda biomass with depth. The numbers refer to station numbers.

ferences could have been expected, but no significant correlation of Nematoda densities and biomass with water depth was found (Figs. 4.5 and 4.6). The correlation coefficient is -0.23 and -0.24, respectively, with n = 15. However, if we plot nematode densities in the area, it is striking that stations with high nematode densities, *viz.* station 13, 15, 24, 25 and 26 (Fig. 2.1), are all situated near to each other in the eastern part of the actual dumpsite, with relatively steep hills. This does not hold for biomass data.

4.3.1.4. VERTICAL DISTRIBUTION

At all 1982 stations except for station 15, the highest density as well as the highest biomass for Nematoda is found in the upper centimetre (Figs. 4.7 and 4.8). As a mean, 76% of the Nematoda biomass occurs in the upper 3 cm (Table 4.9). In general, the other taxa are also concentrated in the upper layer of the sediment. The density of Nematoda declines very rapidly with depth in the sediment. It is estimated from data of both expeditions that below 6 cm only 10% of the total number of Nematoda is found. Below 10 cm the density is very low, but nematodes were found down to 20 cm depth. The vertical distribution of biomass is similar, but at some stations we can detect a weak subsurface maximum at 4-5 or 5-7.5 cm (see station 2, 4, 8 and 13 in Fig. 4.8). This corresponds approximately with the border between the soft upper layer and the more solid clay underlayer. The nematode biomass below 6 cm is estimated to be only 3% of the total nematode biomass.

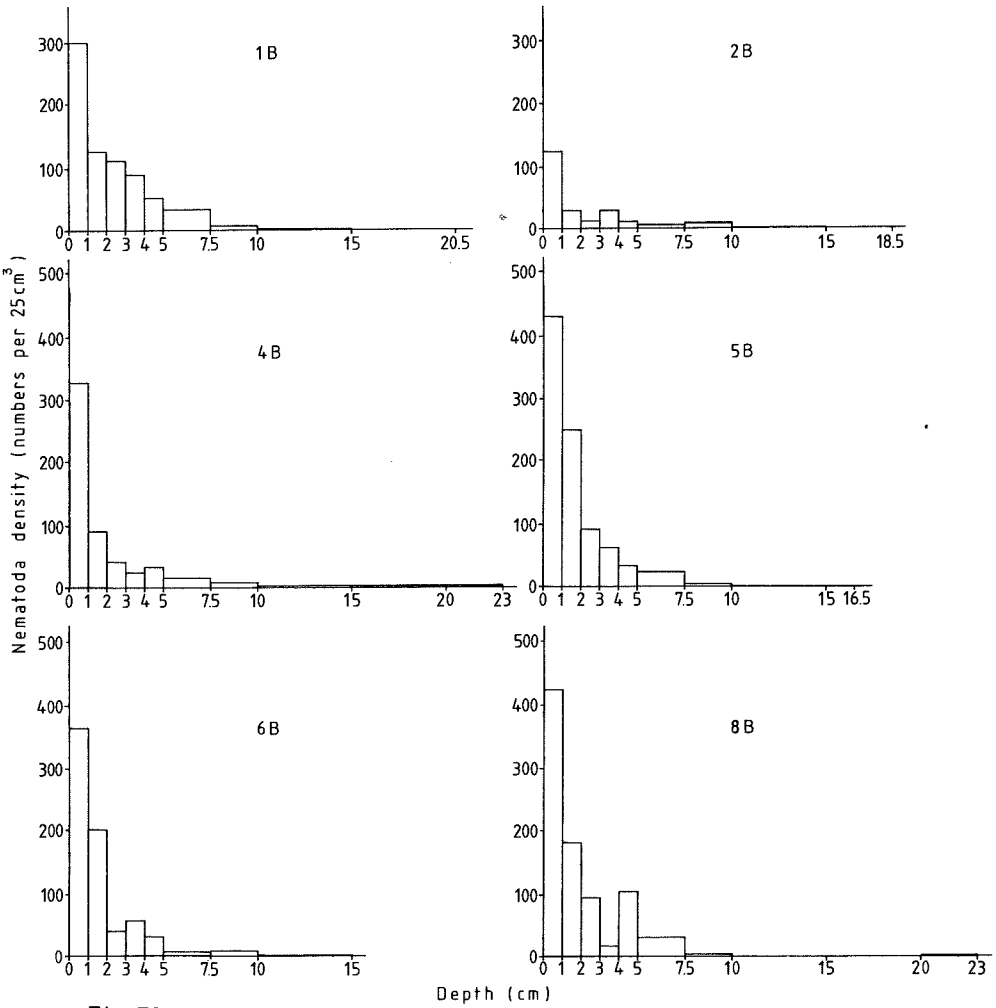

Fig.7[a]

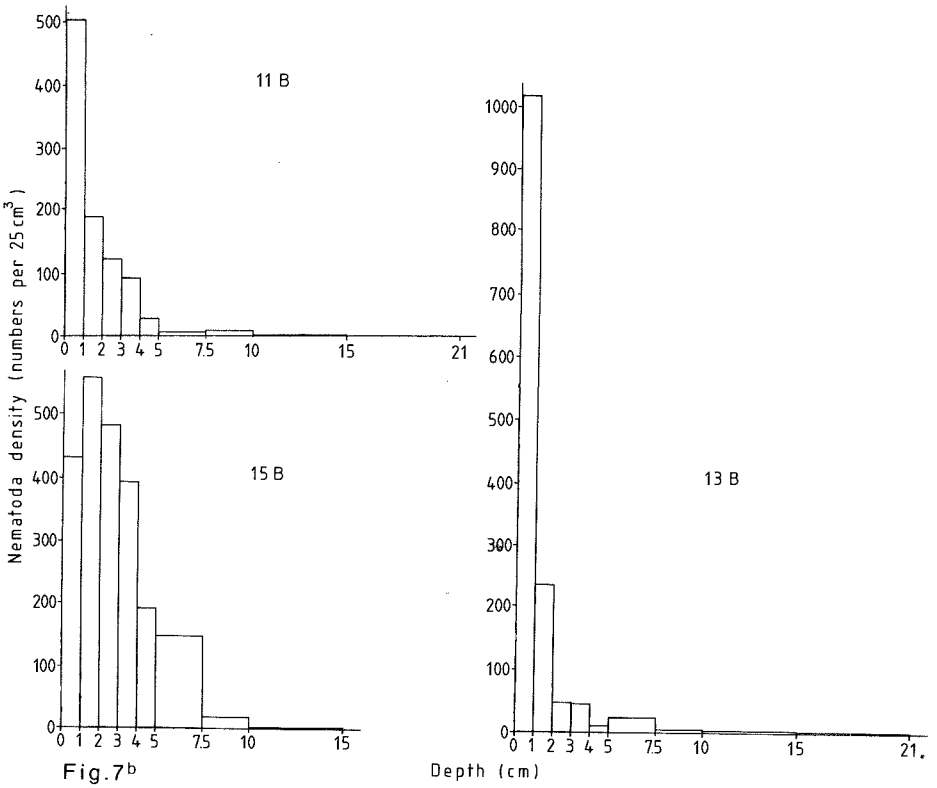

Fig. 4.7. Vertical distribution of the density of Nematoda (number per 25 cm^3) in each of the boxcore samples.

Table 4.9. Biomass of Nematoda in the upper 3 cm, the rest and the total of one subcore (24.6 cm^2) of each boxcore sample of the first DORA-expedition, in μg dry weight/10 cm^2 (= mg/m^2).

Station	1	2	4	5	6	8	11	13	15	MEAN	%
0 - 3cm	8.5	5.0	12.8	16.0	10.8	16.1	9.7	15.5	19.3	12.6	76.4
3 - ±20cm	3.6	3.2	4.4	2.4	1.4	2.8	1.8	5.6	8.9	3.8	23.6
Total	12.1	8.2	17.3	18.4	12.2	18.9	11.5	21.1	28.2	16.4	

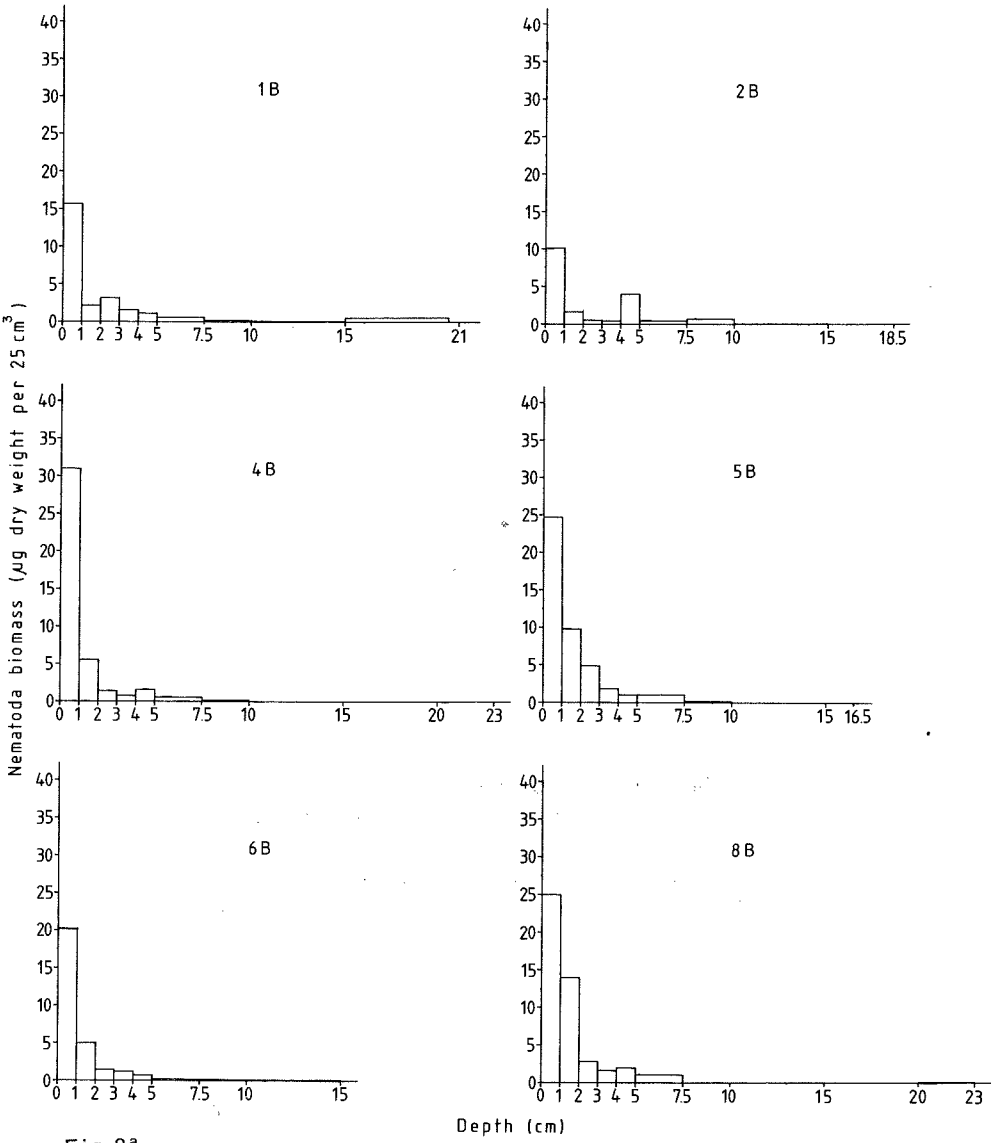
1B
2B
4B
5B
6B
8B
Nematoda biomass (µg dry weight per 25 cm³)
Depth (cm)

Fig.8[a]

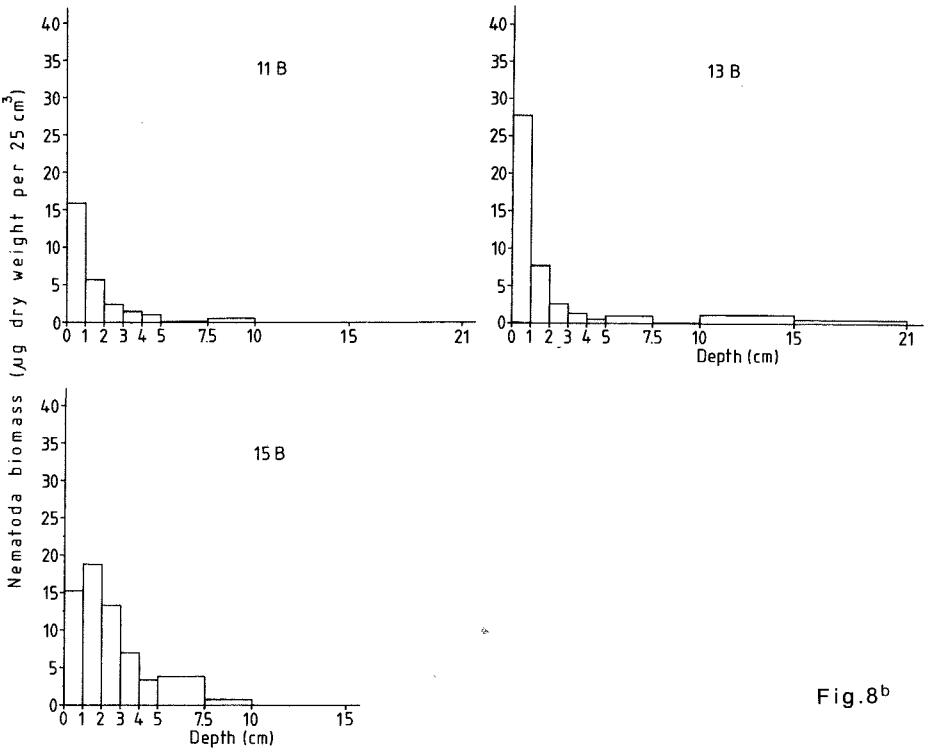

Fig. 4.8. Vertical distribution of biomass of Nematoda (µg dry weight per 25 cm^3) in each of the box-cores.

Because of the low densities of Copepoda and nauplii we cannot say much about their vertical distribution, but on the average, 70% of their biomass is present in the upper 3 cm (Table 4.10). They penetrate as deep as the Nematoda in the sediment. It is estimated from data of both expeditions that yet 10% of the Copepoda and at least 15% of the nauplii are present below 6 cm. For Copepoda + nauplii biomass this is estimated to be 16%.

75% of the biomass of the meiofauna (Nematoda, Copepoda and nauplii) is situated in the upper 3 cm of the sediment (Table 4.11).

Table 4.10. Biomass of Copepoda and nauplii in the upper 3 cm, the rest and the total of one subcore (24.6 cm^2) of each boxcore sample taken during the first DORA-expedition, in µg dry weight/10 cm^2 (= mg/m^2).

Station	1	2	4	5	6	8	11	13	15	mean	%
0 - 3cm	0.4	1.2	1.4	1.6	4.5	18.0	3.3	14.5	18.7	7.1	70.0
3 - ±20cm	0.7	1.7	2.0	0.2	1.5	0.4	0.7	5.1	14.2	2.9	30.0
Total	1.1	2.9	3.4	1.8	6.0	18.4	4.0	19.6	32.9	10.0	

Table 4.11. Biomass of meiofauna (Nematoda, Copepoda and nauplii) in the upper 3 cm, the rest and the total of one subcore (24.6 cm^2) of each boxcore sample taken during the first DORA-expedition, in μg dry weight/10 cm^2 (= mg/m^2).

Station	1	2	4	5	6	8	11	13	15	mean	%
0 - 3cm	8.9	6.2	14.2	17.6	15.2	34.1	13.5	30.0	38.0	19.7	74.5
3 - ±20cm	4.3	4.9	6.5	2.6	2.9	3.1	2.6	10.7	23.2	6.8	25.5
Total	13.2	11.1	20.7	20.3	18.1	37.2	16.1	40.7	61.2	26.4	

4.3.1.5. COMPOSITION AND TROPHIC STRUCTURE OF THE NEMATODA FAUNA

Based on drawings of head, tail and general habitus, 69 taxa could be distinguished among 376 Nematoda of stations 11, 13 and 15. Twenty-six taxa were common to all 3 stations. The percentage abundance of the different taxa is given in Fig. 4.9. The two most abundant taxa belong to the family Desmoscolecidae and constitute more than 13% of the total. Other important families are *e.g.* the Halalaimidae and Monhysteridae.

A high percentage (62%), with a range of 59-67% for station 11, 13 and 15 is in the juvenile stage. The ratio male-female is varying between 1.2 and 0.8, and is not significantly different from 1.

The four different nematode feeding types, according to WIESER (1953), are distinguished by the mouth structures (Fig. 4.10). The deposit feeders (types 1A and 1B) have no buccal armature and ingest whole particles by the sucking power of the oesophagus. The animals belonging to the group with mouth structure type 1A have relatively small mouth diameters (Fig. 4.10) and can devour only small particles, and so they are called selective. Those with the type 1B mouth structure can also swallow larger

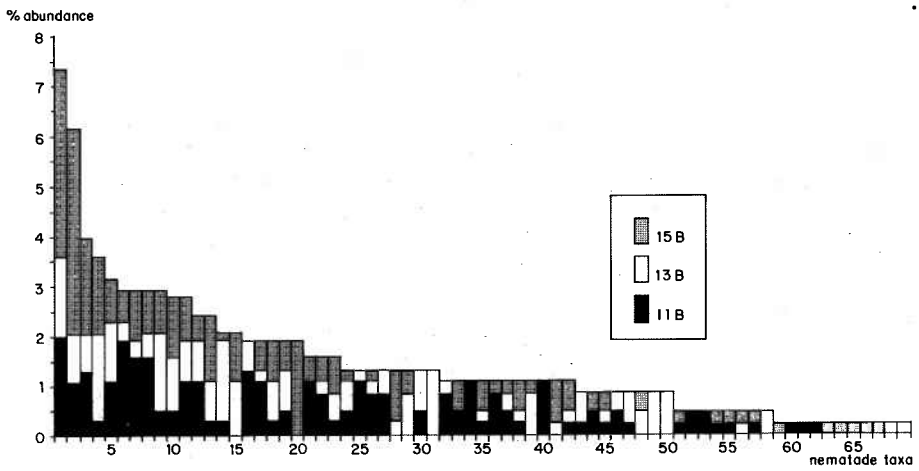

Fig. 4.9. Cumulative percentage abundance of the different Nematoda taxa for subcore samples of station 11, 13 and 15.

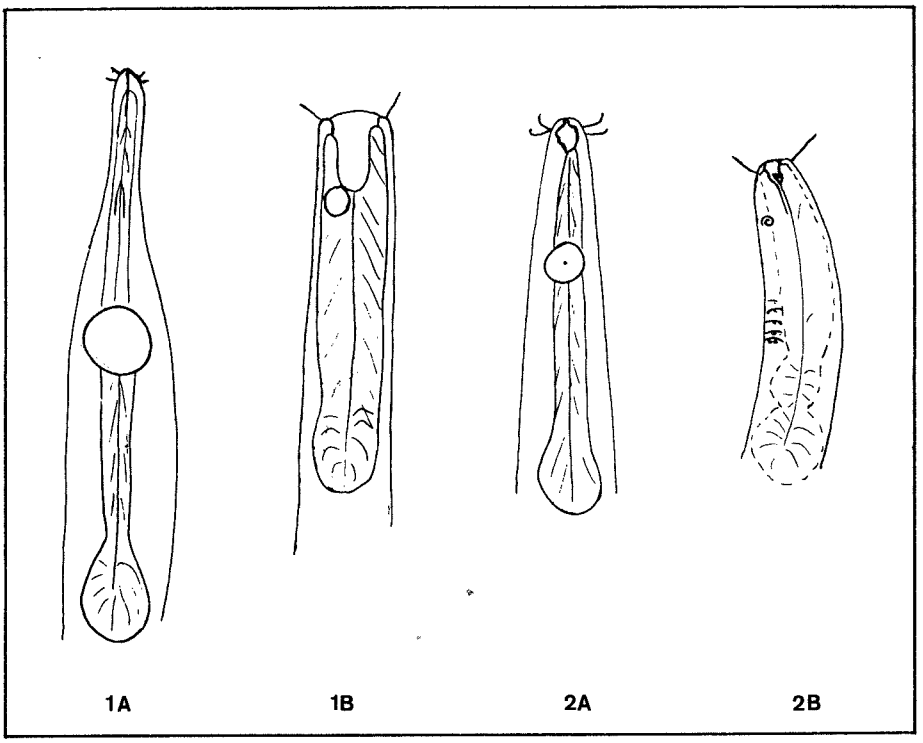

Fig. 4.10. Mouthstructures of the four different feeding types of Nematoda, according to Wieser. The examples were drawn after specimens from the NEA-dumpsite, by J.P.Speijer.

particles. The epistrate feeders or grazers (type 2A), which have small teeth, rasp food particles and suck out their contents (JENSEN,1982). Representatives of type 2B use large teeth to feed on a variety of foods, but are thought to be mainly carnivorous. The fauna of the dumpsite consists mainly of non-selective deposit feeders (type 1B). Second in importance are the selective deposit feeders (type 1A). This is true for density (Table 4.12) as well as for biomass (Table 4.13). Together the deposit feeders account for 76% of the density and 70% of the biomass of Nematoda. It is hardly astonishing that a fauna largely dependent on food particles falling down from the upper layers of the ocean, mostly in the form of faecal pellets, is predominantly deposit feeding. The epistrate feeders are less important, with a density of 15% and a biomass of 13% of the total. The same holds for densities of the carnivorous Nematoda (type 2B) (10%), but in biomass it can be more important (on average 17% of the total).

Table 4.12. Number of Nematoda of each feeding type (according to Wieser) in percentages of the total Nematoda density.

Station	1A	1B	2A	2B
11	19.5	55.5	12.5	12.5
13	32.8	39.6	15.5	12.1
15	24.4	55.0	16.0	4.6
mean	25.6	50.0	14.7	9.7

Table 4.13. Biomass of Nematoda of each feeding types (according to Wieser) in percentages of the total Nematoda biomass.

Station	1A	1B	2A	2B
11	16.4	42.1	15.3	26.2
13	28.0	40.5	7.5	24.0
15	35.5	46.8	16.5	1.2
mean	26.6	43.1	13.1	17.2

Table 4.14. Nematoda diversity of the NEA-dumpsite compared with that of the Bay of Biscay (DINET *et al.*, 1979) and the Venezuela Basin (TIETJEN, 1984) from about the same depth. SR = Species richness, H = Shannon species diversity index, J = Evenness, D = Simpson's index of diversity.

	Station	depth in m	SR	H	J	D
DORA-expedition, 1982 Iberian deep sea	11	4700	10.13	3.97	0.82	0.02
	13	4700	9.47	3.51	0.92	0.04
	15	4200	9.82	3.55	0.72	0.04
Dinet & Vivier, 1979 Bay of Biscay	3	4200	20.73	6.47	0.95	
	4	4700	15.77	5.94	0.93	
	5	4300	10.57	5.24	0.93	
Tietjen, 1984 Venezuela basin	1	3838	7.93	3.31	0.93	
			9.11	3.54	0.93	
	2	5054	10.37	3.79	0.88	
			9.62	3.48	0.82	
	3	3517	14.38	4.00	0.94	
			10.79	3.93	0.97	

4.3.1.6. DIVERSITY OF NEMATODA

In general, the animal diversity in the deep sea is high (HESSLER & SANDERS, 1967; COULL, 1972 and WOLFF, 1977). The Nematoda diversity of stations 11, 13 and 15 (all situated within the NEA-dumpsite), shown in Table 4.14, confirms this. Our values for the Shannon diversity index fall within the range given by TIETJEN (1984) for depths greater than 3500 m in the Venezuela Basin. DINET & VIVIER (1979) give even higher figures for the Bay of Biscay (4200-4700 m) (Table 4.14). This may be explained by their more accurate way of identifying the different Nematoda species. They tried to identify the Nematoda as precisely as possible by means of the recent taxonomical literature.

The high diversity, together with the high abundance and the probably relatively short life span, make Nematoda potentially useful as tools in monitoring the biological effects of pollution and other changes in the environment (HEIP *et al.*, 1982; PLATT, 1984). Although at present data about nematode diversity in connection with pollution are scarce, due to the difficulty in identifying these small worms, it is expected that diversity will decrease by disturbance or pollution (PLATT, 1984). A change in the environment of the dumping area could result from waste derived radiation dose rates. Such a change is not yet expected, for the following reasons: First, the casing of steel and concrete of the waste will not fall apart within a few years, so that heavy leakage of radionuclides will not yet have taken place on a large scale. Second; measured radionuclide concentrations in dumpsite sediments do not exceed fallout levels. As no data are available about nematode diversity at adjacent areas, or at the dumpsite itself before the dumping was started, we cannot check if changes have indeed not occurred. But the area shows the high Nematoda diversity characteristic of the deep sea, and we feel that the measurements presented here can be regarded as a baseline study for research in the future in this area.

Table 4.15. Number of the different macrofaunal groups in the boxcore samples. The sieved area of the samples varied between 1785 cm^2 and 2500 cm^2.

	1982									MEAN 1982	1984									MEAN 1984	MEAN
Station	1	2	4	5	6	8	11	13	15	n/m^2	21B	22BA	22BB	22BC	23BA	23BC	24B	24BC	25B	26B	n/m^2	n/m^2
Foraminifera					3			1	3	4.0				20		122	61	53		1	119.7	67.9
Komokiacea		2								1.1				9		7					7.5	4.6
Xenophyophorea																		+				0.3
Porifera			1	2	1			1	2	4.0		+			1					1	1.4	2.6
Hydrozoa		3								1.7	+						1			6	3.7	2.8
Anthozoa																			1		0.5	0.3
Pennatulacea											1										0.5	0.3
Nematoda	1	1	2	2		2			2	5.7				4					1		2.3	3.9
Polychaeta		10	21	9	9	15	3	21	28	66.7	10		1	21		10	3	10	3	1	27.5	45.0
Oligochaeta			1							0.6												0.3
Sipunculida	2	3	7	3	1	3	3			12.6	1	1		2		1	3		1	3	4.2	8.7
Echiurida																			1		0.5	0.3
Aplacophora																	1				0.5	0.3
Scaphopoda																1	1				0.9	0.5
Bivalvia	3	5	1	2	2	1	1	2	5	12.6	2			1	1	7	3	8	1	4	12.6	12.6
Cal.Copepoda								1		0.6									1		0.5	0.5
Amphipoda				2	1		1			2.3						+	1				0.9	1.5
Cumacea				1					1	1.1	1										0.5	0.8
Tanaidacea		1	2	2	2	1		1		5.2							1	2		1	1.9	3.3
Isopoda			1		3	2	1	4		6.3	+			1		1					1.4	3.6
Crustacea		1						3		2.3	+										0.5	1.3
Ectoprocta		1							2	1.7	1			1			1				1.4	1.5
Brachiopoda						1				0.6				1							0.5	0.5
Crinoidea				1	1					1.1				1							0.5	0.8
Ophiuroidea	1					2			2	2.9	+					1					0.9	1.8
Holothuroidea	1					1				1.1	1								2		1.4	1.3
Tunicata		1	2		2	2			6	7.5			1	8		2	1			1	6.1	6.7
Indeterminanda			11	15	2	3	2	9	9	29.3	1		1	20	9	1	1	+	2	6	19.6	23.9
Total of Metazoa	8	26	49	39	24	33	11	42	57		22	2	3	60	11	25	17	21	13	20		
Metazoa/m^2	39	133	253	202	127	167	59	223	295	166	112	8	14	240	57	100	87	84	73	110	90	124

4.3.2. MACROFAUNA

The density of the different macrofauna groups is given in Table 4.15. The average density for the metazoan animal groups is 124 per m^2. In this figure the large Protozoa, as Foraminifera, Komokiacea and Xenophyophorea, have not been included, because it is difficult to determine whether their tests are empty or not. Besides, Komokiacea easily break up and so it is difficult to count the number of individuals. Nevertheless we tried to give an estimate of their densities (Table 4.15). Of the metazoan groups, Polychaeta have the highest average density (45 per m^2), followed by Bivalvia (Fig. 4.11) (12 per m^2) and the Sipunculida (Fig. 4.12) (9 per m^2). The indeterminanda, mostly wormlike animals without clear taxonomic characteristics, had a density of 24 per m^2. Tunicata, Isopoda and Tanaidacea (Fig. 4.12) and the large Nematoda all reach a mean density of more than 3 per m^2. The Bivalvia was the only macrofauna group that was represented in all but 2 of the 19 boxcores. Polychaeta were found in 16 boxcores, Sipunculida in 14, Tunicata in 10 and Tanaidacea in only 9.

If the average density of macrofaunal animals is calculated for both expeditions separately, a discrepancy is noticed. There is about a factor 2 difference between the densities in favour of the first expedition (Table 4.15). This can be explained partly by a different method of sieving the samples on board. During the 1984 expedition different (larger) sieves (80 x 80 cm) were used and of most samples the upper 3 cm was not handled separately, as was the practice in the 1982 expedition. The longer sieving time probably caused a rougher treatment, with the result that the more fragile organisms were destroyed and/or pressed through the sieves. This explanation is confirmed by the densities observed for animals with a firm body, like Tunicata and Bivalvia, which were more or less the same in both expeditions (Table 4.15). However, this does not explain the low densities for large animals that do not break up easily, like Sipunculida, which can reach a length of about 15 cm, and Tanaidacea. The scattered distribution and low densities of these animals may be an explanation for this. But there is even another explanation possible, although still very hypothetical. There is evidence for seasonal changes on the deep-sea floor, shown among others by the rapid accumulations of decaying phytoplankton in the months June to August in an area south-west of Ireland (Lampitt, 1985). So it is possible that densities and biomass of the deep-sea benthos also change seasonally. As the second expedition was held in March-April (a little before the "rich" months and possibly after a long period of scarcety of food), one can imagine that the biomass and density of the benthos has declined, compared to the months August and September (in and just after the "rich" months), in which the first expedition was carried out.

For the various important higher taxa the biomass is given in percentages of the total macrofaunal biomass of each boxcore (Table 4.16). The macrofauna biomass in boxcore samples is on average dominated by the Sipunculida with 28% (Table 4.16). Other important groups are the Polychaeta (24%), Tunicata (11%), Bivalvia (6%), Holothuroidea (5%) and Porifera (3%). In station 8 we found 2 large Ophiuroidea in the boxcore sample with a dry weight of almost 80 mg. We considered them a lucky strike and did not include them in our Tables (see *e.g.* Table 4.17). If we had included them, the total biomass of station 8 would have been 570 mg per m^2. This is more than 3 times the second highest station in biomass (station 15), and would have a great effect on mean macrofauna biomass. The total macrofauna biomass varied between 3.1 and 182.4 $mg.m^{-2}$ with a mean of 79.7 mg per m^2 (Table 4.24). Between the mean biomass for both expeditions seperately a

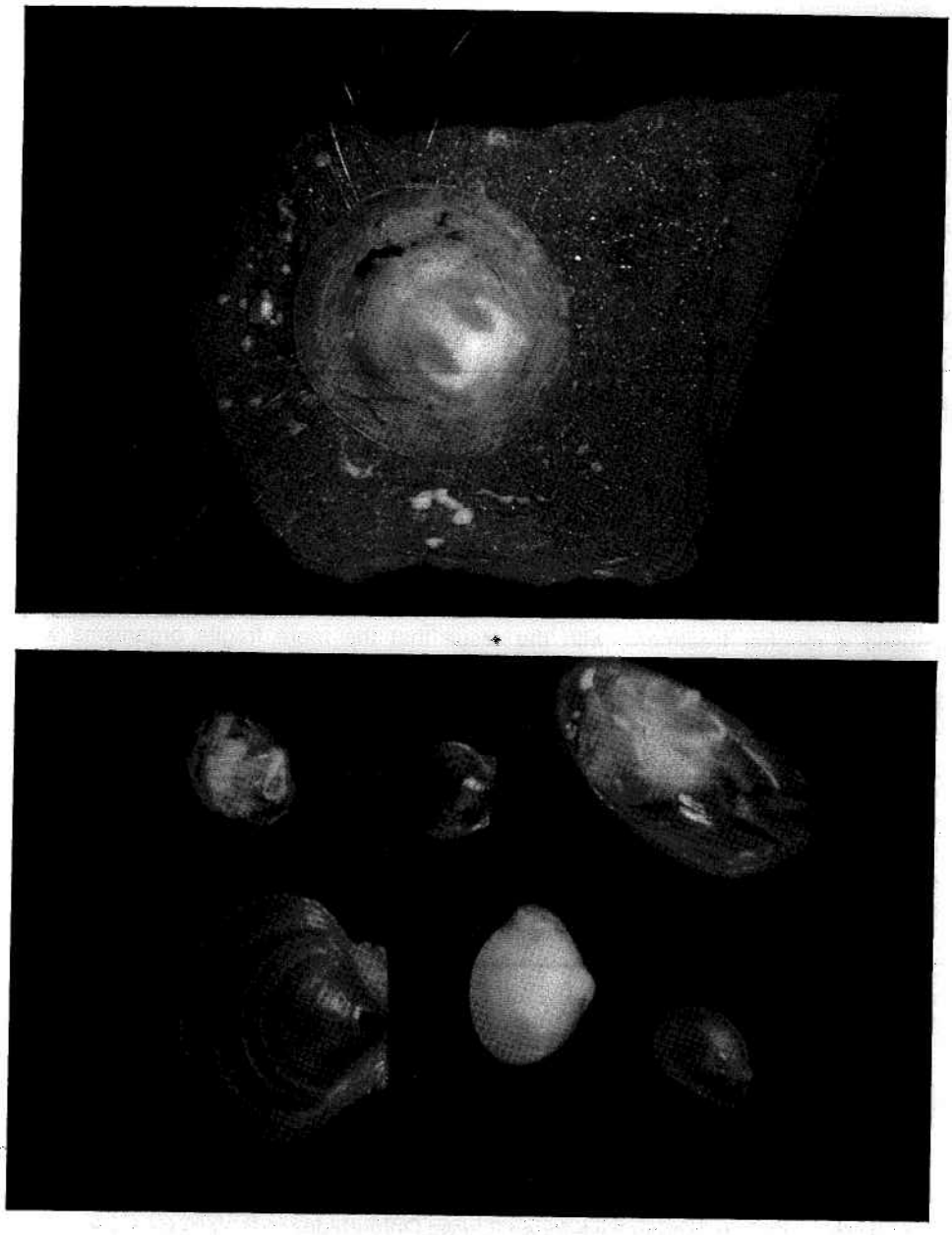

Fig. 4.11. Macrofauna from the boxcores. Above: *Pelagodiscus atlanticus* King, 1868 (Brachiopoda) (length 5.1 mm, core 8B) on a little stone. Below: Several Bivalvia. Upper row from left to right: *Yoldiella abyssorum* Knudsen, 1970 (length 2.3 mm, core 2B), *Cyclopecten* spec. (length 1.8 mm, core 2B), *Silicula fragilis* Jeffreys, 1879 (length 5.5 mm, core 2B). Lower row: *Propeamussium* spec. (length 4.6 mm, core 2B), *Ledella crassa* Knudsen, 1970 (length 3mm, core 2B), *Dacrydium vitreum* Möller, 1842 (length 2.1 mm, core 1B).

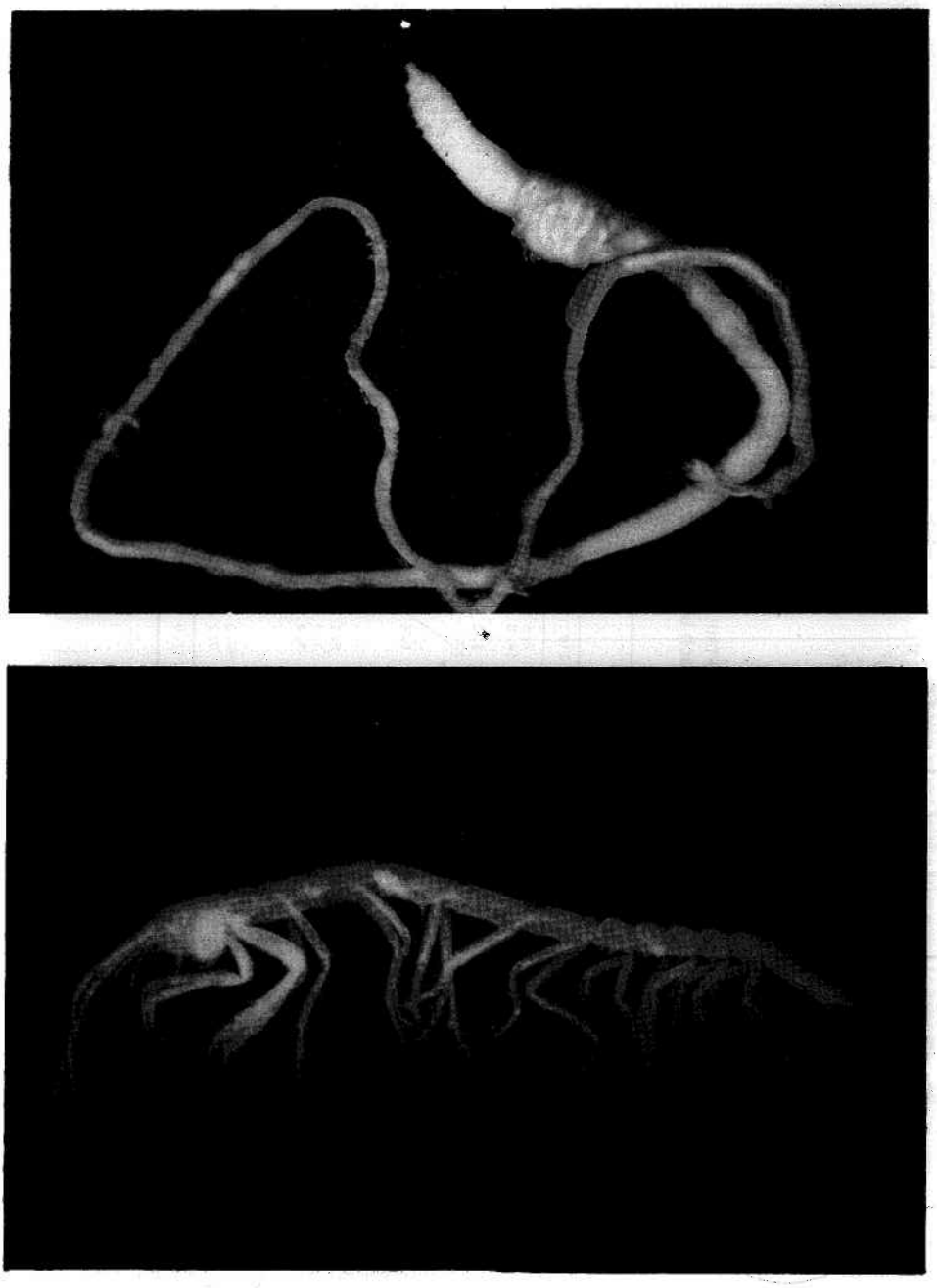

Fig. 4.12. Macrofauna from the boxcores. Above: *Golfingia* spec. (Sipunculida), length 52.6 mm (core 2B). Below: *Leiopus gracilis* (Norman & Stebbing, 1886) (Tanaidacea), length 13.3 mm (core 2B).

Table 4.16. Macrofauna biomass of the different important animal groups, in percentages of the total macrofaunal biomass of each boxcore sample.

	1982									MEAN 1982	1984										MEAN 1984	MEAN
Station	1	2	4	5	6	8	11	13	15		21B	22BA	22BB	22BC	23BA	23BC	24B	24BC	25B	26B		
Sipunculida	66.4	82.1	49.6	65.4	65.5	66.6	84.6			53.36	2.8	97.5		0.5		14.7	1.3		2.5	0.7	11.99	28.14
Polychaeta		5.9	42.1	10.4	9.5	9.0	3.2	41.7	30.7	16.94	54.8		28.5	43.0		35.2	55.3	75.7	17.7	0.8	31.10	24.39
Tunicata		0.1	0.7		16.2	18.2			55.0	10.02			33.5	47.8		17.3	12.7			6.4	11.77	11.10
Bivalvia	3.8	8.5	3.6	2.1	2.2	0.5	2.8	45.6	3.5	8.07	5.2			0.3	10.8	2.0	8.5	4.1	0.5	14.3	4.57	6.23
Holothuroidea	17.2					1.9				2.12	27.9								39.4		6.73	4.55
Porifera			2.0	8.2	0.3			1.2	4.0	1.74	*	2.6			8.9					31.5	4.29	3.05
Echiurida																			35.8		3.58	1.88
Ophiuroidea	12.4								0.2	1.40	0.6					17.1					1.76	1.59
Foraminifera														0.5		5.3	7.6	7.2			2.06	1.08
Tanaidacea		2.9	0.3	4.3	2.5	0.7		0.1		1.20							3.0	0.5		1.9	0.54	0.85
Scaphopoda																7.6	7.7				1.53	0.81
Isopoda			0.4		1.7	0.2	0.4	3.2		0.66	0.2			1.4		0.7					0.23	0.43
Ectoprocta									2.7	0.30	3.1						2.4				0.55	0.43
Hydrozoa											3.4									4.6	0.80	0.42
Amphipoda				3.0	0.5			0.6		0.46							0.9				0.09	0.26
Anthozoa																			2.7		0.27	0.14
Brachiopoda						2.3				0.26												0.12
Cumacea				0.6					0.5	0.12	0.3										0.03	0.09
Indeterminanda		0.2	0.7	5.8	1.6	0.5	9.0	6.9	3.1	3.09	0.2		37.9	5.1	80.4	0.2	0.1	12.3	1.3	39.9	16.21	9.99
Total mg/m^2	8.0	89.0	146.6	103.2	87.0	182.4	79.0	56.6	163.3	101.7	113.9	13.5	3.1	75.5	14.6	111.2	53.4	52.7	141.5	18.9	59.83	

similar difference, as already noticed for mean densities, can be detected. For stations 1 to 15 the average biomass is nearly twice that of stations 21 to 26. In 7 out of 9 boxcores of the first expedition, Sipunculida dominated with 53% to 88% of the biomass. In the remaining two, in which they were completely absent, Polychaeta were dominant, together with Bivalvia (13B) or Tunicata (15B). During the second expedition the Sipunculida dominated only in one boxcore sample (22BA), poor in biomass. If we do not count the biomass of the indeterminanda, Polychaeta were dominant in the other boxcores. Boxcores taken during the two expeditions do not have the same distribution in the area (Fig. 2.1), and even if we compare boxcore samples taken near each other and at about the same depth, we can detect large differences. So, for example, the data for boxcores 2B, 22BA, 22BB and 22BC have a mean biomass of 45.3 mg/m^2 with a standard deviation of 43.2, and those of 5B, 23BA and 23BC a mean of 76.0 mg/m^2 with a standard deviation of 54.3. If we look at the variance, we may conclude that the differences between the macrofauna data of both expeditions are not only caused by different sieving methods and the different distribution of the boxcores over the area, but also by the scattered distribution of the macrofauna seen at the small scale of hundreds of meters. Further, as explained before, a seasonal effect can not be excluded.

Table 4.17. Biomass of the macrofauna in the upper 3 cm, the rest and the total of a boxcore sample, in mg dry weight/m^2.

Station	1	2	4	5	6	8	11	13	15	mean	%
0 - ± 3cm	-	12.1	22.4	23.4	28.6	40.6	2.7	38.9	96.9	33.2	29.3%
3 - ±20cm	-	76.9	124.2	79.8	58.4	141.8*	76.3	17.7	66.4	80.2	70.7%
Total	8.0	89.0	146.6	103.2	87.0	182.4*	79.0	56.6	163.3	101.7	

*not included are two relatively large Ophiuroidea with a shellfree dry weight of 78.86 mg which would have add 387.1 mg/m^2.

During the 1982 expedition the macrofauna showed a vertical distribution so that on average 71% of the biomass was found deeper than 3 cm in the sediment (Table 4.17). The deeper biomass consisted almost exclusively of Sipunculida. Also the 2 large Ophiuroidea, belonging to the burrowing family Amphiuridae were found below 3 cm. Only some parts of their arms were found in the upper 3 cm. However, in terms of numerical abundance the upper 3 cm showed the highest numbers except for stations 11 and 15. This could be explained by the fact that station 11 is very poor in individuals and that in station 15 the separation of the upper 3 cm layer from the rest of the sediment is probably biased, which is shown by the findings of Ectoprocta and Tunicata in the deeper layer. To our knowledge those animals could have lived only on the surface of the sediment. During the 1984 expedition we tried to determine the vertical distribution of the macrofauna more precisely by cutting a whole boxcore sample in horizontal slices. Data from 3 boxcores confirm our conclusion about the vertical distribution of macrofaunal densities as stated above. Probably because of the lack of large animals, like Sipunculida, which live deeper down in the sediment, in only one of those 3 boxcore samples was the highest biomass found below 3 cm (Table 4.18).

Table 4.18. Vertical distribution of the macrofauna in 3 boxcore samples of the second DORA-expedition.

	Number of Nematoda per boxcore			Dry weight in percentage of total biomass per boxcore		
Depth in cm	22BC	23BC	24BC	22BC	23BC	24BC
0-1	25		14	34.4		76.5
1-2	11	15		20.0	37.0	
2-3	10		6	10.5		23.2
3-5	3			32.0		
5-10	11	8	1	3.1	53.8	0.3
10-15		2			9.2	
Total/0.25m²	60	25	21	18.88mg	27.79mg	13.18mg

Table 4.19. Density and biomass of the "macro"-benthos at great depth in the Atlantic ocean.

	depth in m	density N/m²	wet weight in mg/m²	screen size in mm
Spärck, 1951	3782		3100	1.75 ?
Kusnetzov, 1960	3300-5400		0-50	0.5 ?
Sanders, Hessler & Hampson, 1965	4436-5001 4525	85 55		0.42
Zenkevitch et al., 1971	3000-5000		100-1000	0.5 ?
Menzies, George & Rowe, 1973	4000 5000		1500 160	0.55
Smith, 1978	4670-5200	354	155	0.297
Laubier, Sibuet, 1979	4100	919		0.250
Geidarov et al., 1983	4050-4700		2010	0.5 ?
Dinet, Desbruyères, Khripounoff, 1985	4100	3612	1260	0.250
DORA expedition, 1982	4000-4800	171	700	1.0
DORA expedition, 1984	3958-4787	90	402	1.0
DORA expedition, 1984	3958-4787	463	519	0.5
DORA expedition, 1982	4200-4725	3243		0.2

The data for macrofauna density and biomass are difficult to compare with other quantitative deep-sea macrofauna studies in the Atlantic, because other authors had a different definition for macrofauna in the deep sea, and mostly used a much smaller screen-size than the standard sieve with a screen-size of 1 mm (Table 4.19). Of course this has a large effect on the number of animals collected with the sieve. We are of the opinion that the term "macrofauna" has to be applied only to the fauna retained by a sieve of a 1 mm screen-size, so that data from different areas and/or depths can be compared. Of course it is better to study the fauna as fully as possible, and a finer sieve will give a better estimate of *e.g.* the biomass of the total metazoa fauna, than a coarse one. However, finer sieves are rarely used and chiefly in areas poor in fauna and/or in areas with fine sediment, because of the time-consuming sieving and sorting. So additional sievings with a 1 mm screensize are recommended and the results should be given separately. Beside the difference in screen-size, the comparison is made even more difficult by the fact that the sampling gear, as has been proven by DINET *et al.* (1985), can influence the data heavily. Their samples taken by the 0.25 m^2 boxcorer had a animal density 4 times higher than those taken by a Reineck boxcorer of 600 cm^2. Thus, because of the coarser screensize used it is not surprising that our data for densities are different and much lower than those of SMITH (1978); LAUBIER & SIBUET, 1979 and DINET *et al.* (1985) (Table 4.19). Yet, our densities are higher than those of SANDERS *et al.* (1965). The data for biomass of abyssal macrofauna are variable (Table 4.19), and our value for the mean wet weight falls within the range given by ZENKEVITCH *et al.* (1971) in his map of the benthic biomass for the world oceans.

4.3.3. LARGE MEIOFAUNA

To study the effect of the use of a sieve with a screen-size smaller than 1 mm, as normally used by other researchers in the deep sea (Table 4.19), during our second expedition we added a sieve with a screen-size of 0.5 mm when sieving the boxcore samples. The large meiofauna retained (> 0.5 mm and < 1 mm) is shown with densities in Table 4.20. If, for reasons as explained before, we do not take into account the difficult group of Foraminifera, which certainly have the highest mean density in this animal category, then Polychaeta (99 m^{-2}) and Nematoda (67 m^{-2}) are the most important ones. Komokiacea, Bivalvia, Isopoda, Tanaidacea and Copepoda have an average density of more than 10 m^{-2}. With the group of Copepoda we have to be careful as two thirds consist of Calanoidea, which may be surface-dwelling species that could have entered the boxcore when it was hauled up (O. Pfannkuche, Universität Hamburg, FRG., personal communication).

The average of all metazoan groups is 366 per m^2 (Table 4.20), which is nearly 5 times more than the mean density observed for the macrofauna at the same stations. In 8 of the 10 boxcore samples the biomass of the large meiofauna was less important than the macrofauna. In the other 2 boxcores the macrofauna happened to be very poor. On average the large meiofauna, with a mean of 14.6 mg dry weight.m^{-2} (Table 4.21), is 4 times less important than the macrofauna of the same boxcores (Table 4.24). So it is obvious that the use of a smaller screen-size will in particular affect data on densities. For data on biomass the effect is much less important.

Table 4.20. Number of the different groups of large meiofauna (> 0.5 mm and < 1 mm). The sieved area of the samples varied between 1785 and 2500 cm^2.

Station	21B	22BA	22BB	22BC	23BA	23BC	24B	24BC	25B	26B	mean N/m^2
Foraminifera				148		130	65	16	49	34	205.9
Komokiacea	70			13		24	1	3			51.7
Porifera			1								0.5
Hydrozoa							2				0.9
Anthozoa					1						0.5
Nematoda			5	34	13	12	22	32	15	11	67.1
Polychaeta	10	8	37	43	28	15	14	10	36	11	98.8
Oligochaeta			1				1				0.9
Sipunculida		3	2		2		2	2			5.1
Aplacophora				3			1		1	3	3.3
Scaphopoda	2								2		1.9
Bivalvia	6		2	5	7	11	4	13	11	5	29.8
Cal.Copepoda		2	3	5			17		12	5	20.5
Har.Copepoda				7		2	4	3	3	3	9.8
Ostracoda	3			3	1	1	1	1	2	7	7.5
Amphipoda	1				1	2	1	+			2.3
Cumacea				1							0.5
Tanaidacea		1	6	4	8	2	2	6	5	7	19.1
Isopoda	4	2	3	4	5	4	8	9	5	4	22.4
Crustacea	+					1					0.5
Ectoprocta	1					+					0.9
Ophiuroidea	+				1			1		1	1.9
Holothuroidea					1						0.5
Tunicata	2		1		2					2	3.3
Indeterminanda	14	5	4	24	23	26	14	6	16	9	65.7
Total of Metazoa	45	21	65	133	93	77	91	84	108	68	
$Metazoa/m^2$	235	84	312	532	484	308	466	336	614	375	366

Table 4.21. Biomass of the different animal groups of large meiofauna (> 0.5 mm and < 1 mm) in percentages of the their total biomass in a boxcore sample.

Station	21B	22BA	22BB	22BC	23BA	23BC	24B	24BC	25B	26B	MEAN
Polychaeta	53.9	52.8	79.9	41.7	40.9	41.3	16.2	55.7	50.4	7.5	44.03
Isopoda	5.5	7.5	1.5	2.6	2.9	3.9	39.1	7.3	3.0	12.1	8.54
Foraminifera				25.4		9.5	10.7	1.4	2.6	13.8	6.34
Cal.Copepoda		7.0	1.1	0.9	4.0		10.9		7.9	13.5	4.53
Bivalvia	7.7		1.3	1.0	6.0	5.2	1.2	3.9	4.3	9.8	4.04
Sipunculida		21.8	3.4	1.8	1.3		4.1	3.7			3.61
Nematoda			0.6	1.3	5.0	2.1	5.6	6.1	3.2	3.0	2.69
Tanaidacea		1.5	2.5	0.2	1.9	0.5	0.1	1.8	0.4	8.6	1.75
Tunicata	4.5		2.9		1.6						0.90
Ostracoda	1.6			0.5	0.5	0.1	0.7	0.1	0.2	5.2	0.89
Har.Copepoda	0.5			0.8	1.1	0.7	1.1	1.1	0.7	2.2	0.82
Holothuroidea					8.1						0.81
Amphipoda	0.7				2.4	1.6	3.3				0.80
Scaphopoda	1.4								0.4	3.1	0.49
Ophiuroidea	0.1				0.8			0.5		3.2	0.46
Aplacophora				1.0					2.4		0.34
Hydrozoa							1.1				0.11
Oligochaeta			0.2				0.9				0.11
Crinoidea				1.0							0.10
Crustacea	0.4					0.3					0.07
Cumacea				0.6							0.06
Ectoprocta	0.4					0.1					0.05
Porifera			0.4								0.04
Anthozoa					0.1						0.01
Indeterminanda	23.2	9.3	6.2	21.1	23.6	34.6	8.5	15.2	25.1	18.1	11.87
Metazoa mg/m^2	16.6	4.4	20.2	16.8	21.2	14.6	15.4	8.9	22.0	5.6	14.6

Table 4.22. Numbers and biomass of Copepoda and numbers of Nematoda in boxcore samples of stations 2 to 11 passing through a sieve of 1 mm screen-size and retained by a sieve of 200 μm screen-size.

	NEMATODA	COPEPODA	
Station	n/m^2	n/m^2	mg dry/m^2
2B	1221	230	0.32
4B	988	228	0.56
5B	648	124	0.11
6B	3026	249	0.40
8B	5501	497	0.46
11B	5252	531	0.39
Mean	2773	310	0.37

A sieve with a screen-size of 200 μm, used in stations 2 to 11, had a remarkable effect on the values for density of the retained meiofauna. Densities for Copepoda and Nematoda have means of 310 and 2773 per m^2 respectively (Table 4.22). Even if we neglect the other animal groups collected on this sieve, the density is still 19 times that of the mean density of the macrofauna of the same boxcore samples. Only the biomass of the Copepoda retained on this sieve was studied (Table 4.22), and is negligible compared to the biomass of the macrofauna, the large (> 0.5 mm) meiofauna or that of the meiofauna from the subcores. We suspect that the same is true for the Nematoda biomass retained on this sieve.

With the data for the large meiofauna at hand, a comparison with the "macrofauna" densities, shown in Table 4.19, now makes more sense. Our densities for the large (> 0.2 mm) meiofauna and macrofauna together, are higher than those of SMITH (1978) and fall within the range given for the Bay of Biscay (LAUBIER & SIBUET, 1979, DINET *et al.*, 1985).

In 3 boxcore samples the vertical distribution of the large (> 0.5 mm) meiofauna was studied. As expected, the highest densities were found in the upper centimetres. In 1 boxcore sample the highest biomass was detected between 2 and 5 cm, which is a result intermediate between the optimum depth for meiofauna biomass of the subcores (the upper centimetre) and the macrofauna biomass (below 3 cm) (Table 4.23).

Table 4.23. Vertical distribution of the large meiofauna (> 0.5 mm and < 1 mm) in 3 boxcore samples of the second DORA-expedition.

	Number of Nematoda per boxcore			Dry weight in percentage of total biomass per boxcore		
Depth in cm	22BC	23BC	24BC	22BC	23BC	24BC
0-1	57		53	15.0		37.9
1-2	38	58		11.0	59.7	
2-3	14		18	4.4		44.7
3-5	17			49.3		
5-10	6	10	9	18.9	27.0	13.2
10-15	1	9	4	1.4	12.3	4.2
15-20		+			1.0	
Total/0.25m^2	133	77	84	4.21mg	3.65mg	2.21mg

Table 4.24. Biomass of the meiofauna (Nematoda, Copepoda and nauplii), the macrofauna and the large meiofauna (> 0.5 mm and < 1 mm) of the boxcore samples, in mg dry weight/m^2. The meiofaunal biomass derived from the subcore samples of only 6 cm depth of the 1984 expedition has been corrected (see section 4.3.1.4).

Station	1	2	4	5	6	8	11	13	15	mean	%
Meiofauna	13.2	11.1	20.7	20.3	18.1	37.2	15.5	40.7	61.2	26.4	20.6%
Nematoda	12.1	8.2	17.3	18.4	12.2	18.9	11.5	21.1	28.2	16.4	12.8
Copepoda	1.1	2.9	3.4	1.8	6.0	18.4	4.0	19.4	32.9	10.0	7.8
Macrofauna	8.0	89.0	146.6	103.2	87.0	182.4	79.0	56.6	163.3	101.7	79.4%
Total	21.2	100.1	167.3	123.5	105.1	219.5	94.8	97.3	224.4	128.1	

Station	21	22	23	24	25	26	MEAN	% OF SUBTOTAL	% OF TOTAL	MEAN 1982+84	%
Meiofauna	16.8	10.3	19.3	26.2	20.4	33.1	21.0	26.0	22.0	24.3	20.5
Nematoda	9.2	8.6	12.2	14.2	13.3	11.2	11.4	14.1	12.0	14.4	12.1
Copepoda	7.6	1.7	7.1	12.0	7.1	21.9	9.6	11.9	10.0	9.8	8.3
Macrofauna	113.9	30.7	62.9	53.1	141.5	18.9	59.8	74.0	62.7	79.7	67.2
Subtotal	129.7	41.0	82.2	79.3	161.9	52.0	80.8	100.0	84.7	104.0	87.7
Large Meiofauna >0.5mm and <1mm	16.6	13.8	17.9	12.1	22.0	5.6	14.6	18.1	15.3	14.6	12.3
Total	146.3	54.8	100.1	91.4	183.9	57.6	95.4			118.6	100.0

4.3.4. COMPARISON OF MEIO- AND MACROFAUNA

Both macrofauna and meiofauna reach their highest densities in the upper centimetres, but for the meiofauna this is much clearer and it holds for every station. In biomass (Table 4.24) the macrofauna is always more important than the meiofauna, except for the poor macrofauna stations 1 and 26. As a mean it is 3.3 (0.6 to 8) times more important. This low figure, compared to data from shallow sediments, agrees with the results of other researchers (compiled by THIEL, 1983) that meiofauna becomes relatively more important with increasing water depth. However, the effect of water depth on the macrofauna to meiofauna ratio is not as striking as expected. The ratio 1:1 suggested by THIEL (1972) for a somewhat deeper (> 5000 m) area appears too low. Yet, because of a suspected higher metabolism rate (GERLACH, 1971) the meiofauna can be more important in productivity than the macrofauna.

The mean biomass of the large meiofauna (> 0.5 mm and < 1mm) constitutes 15% of the total meio- and macrofaunal biomass. For the calculation of the total biomass of the boxcore samples of the 1984 expedition, we counted up the biomass data for meiofauna, large meiofauna and macrofauna. This seems to be incorrect, since our meiofaunal data, derived from the subcores, ought in principle to include the large meiofauna. However, the chance of sampling one large (> 0.5 mm) Copepoda or Nematoda with a subcore of 10 cm^2 is less than 10% (Table 4.20). Besides, the biomass of Nematoda, Copepoda and nauplii, which in our case forms 100% of the meiofaunal biomass of the subcores (see section 4.3.1.2), is only 8% of the total biomass of the large meiofauna (Table 4.21).

Table 4.25. List of the pelagic fish caught with an Agassiz trawl during the first DORA-expedition, with number of specimens per station.

Name	Station							likely depth of occurence
	3	5	8	11	12	13	15	
Myctophum punctatum	1			1				night 0- 125 m day 225- 750 m
Lampanyctus crocodilus	1			1				night 0- 650 m day 275-1000 m
Benthosema glaciale	1		2				3	night 0- 225 m day 275- 800 m
Symbolophorus veranyi	1							0- 800 m
Opisthoproctus soleatus				1				> 400 m
Gonostoma bathyphilum			2			1		usually > 2000 m
Cyclothone braueri			1	1				night < 300 m day 300-1500 m
Cyclothone microdon	16		54	8		5	12	500-1500 m
Cyclothone spec.				3				----
Argyropelecus hemigymnus	2			1		1	1	0- 300 m
Agryropelecus olfersi			2	1				ca. 1800 m
Stomias boa cf ferox				1	1			0- 300 m
Mentodus cf crassus							1	> 1000 m
Scopeloberyx robustus			1					0- 600 m

We, therefore, think it justified to add both the meiofaunal biomass derived from the subcores and the biomass of the larger meiofauna (> 0.5 mm) to the macrofaunal biomass, if the total biomass has to be calculated. This implies that the ratio of macrofauna and meiofauna biomass is changed in favour of the meiofauna. The macrofauna biomass is now only twice that of meiofauna.

There are indications that depth (hydrostatic pressure) is not an important parameter in regulating O_2 consumption rates for megafauna, viz: Ophiuroidea and rat-tail fish (SMITH, 1978b and 1983). If we assume that this is also true for meio- and macrofauna, we can give a rough estimate of the O_2 demand of the benthic fauna at the dumpsite by using the general relationship (BANSE, 1982) between respiration and biomass. In computing the respiration of the bentic fauna with data from the 1982 expedition we used the equation $q = 19.5\ M^{0.75}$ for macrofauna and $q = 5.4\ M^{0.75}$ for meiofauna, in which q = respiration in nl $O_2.h^{-1}$ at 20°C and M = body mass as dry weight (μg). Taking Q_{10} = 2.5, we find that at 2°C the meio- and macrofauna respiration is 17 and 25 mmol $O_2.m^{-2}.yr^{-1}$, respectively. These figures indicate that macrofauna consumes a little more O_2 than meiofauna. This general conclusion is not altered, if the large meiofauna (>0.5 mm) is included. Of the total mineralization activity of the sediment (see section 3.7.) 40% can be accounted for by respiration of meio- and macrofauna. With Q_{10} = 2.0 this figure will be about 60%. It is obvious that these estimates have to be considered with reservation, due to the use of very general equations, which are not based on deep-sea measurements.

4.3.5. MEGAFAUNA

Few benthonic animals were caught with the Agassiz trawl during the 1982 expedition. The catches existed mainly of pelagic organisms. A list of pelagic fish (with depth distributions from the literature) is given in Table 4.25. No near-bottom-dwelling fish were caught. The following representatives of the benthos were collected: Cnidaria (Actiniaria), Turbellaria (egg capsule), Polychaeta, Bivalvia (Pectinidae), Cephalopoda (*Grimpoteuthis umbellata, Cirrothauma murrayi*, Fig. 4.13), Crustacea (Amphipoda, Isopoda, Cirripedia), Brachiopoda (*Pelagodiscus atlanticus*), Ophiuroidea (*Ophiomusium planum*, Fig. 4.13), Holothuroidea and Tunicata.

Interesting finds were the large mobile bottom dwelling predators (length 25 and 40 cm), belonging to the order of the Octopoda (Cephalopoda). The crustacean larva *Eryonaicus spinoculatus* (Fig. 4.13), of which we caught 2 specimens 30 and 35 mm long, is an example of the large vertical migrating capacities of some marine animals. According to BERNARD (1953) this larva lives at a water depth of 400 m when it is about 2 mm long. During growth it descends down to 4000 m, where it reaches a length of 35 mm. The adult, probably *Stereomastis andamanensis*, is benthonic and lives between 500 and 1800 m.

The seven Agassiz trawls taken during the 1984 expedition (Fig. 2.1) contained rich catches of bottom dwelling megafauna and because of the closing device virtually no pelagic animals. The catch of the trawl at station 24 was lost for the largest part just before being put on deck. These catches give a far better understanding of the megafaunal composition than those of the first DORA-expedition and there is more point in working up these data to minimum densities and biomass figures for the area. In addition to the animal groups caught during the 1982 expedition, Porifera, Nemertini, Sipunculida, Scaphopoda, Asteroidea, Echinoidea and near-bottom dwelling fish were caught. Now no large Cephalopoda (Fig. 4.13) were caught as during the former expedition, but the presence of these animals was confirmed by the finding of several relatively large peanut-like eggs in 3 trawls (BOLETZKY, 1985). Most of the megafaunal animals belong to the epifauna, but the presence in the trawl catches of large intact Sipunculida, which are typically infaunal, proves that our trawl (sometimes) ploughs at least 15 cm into the sediment.

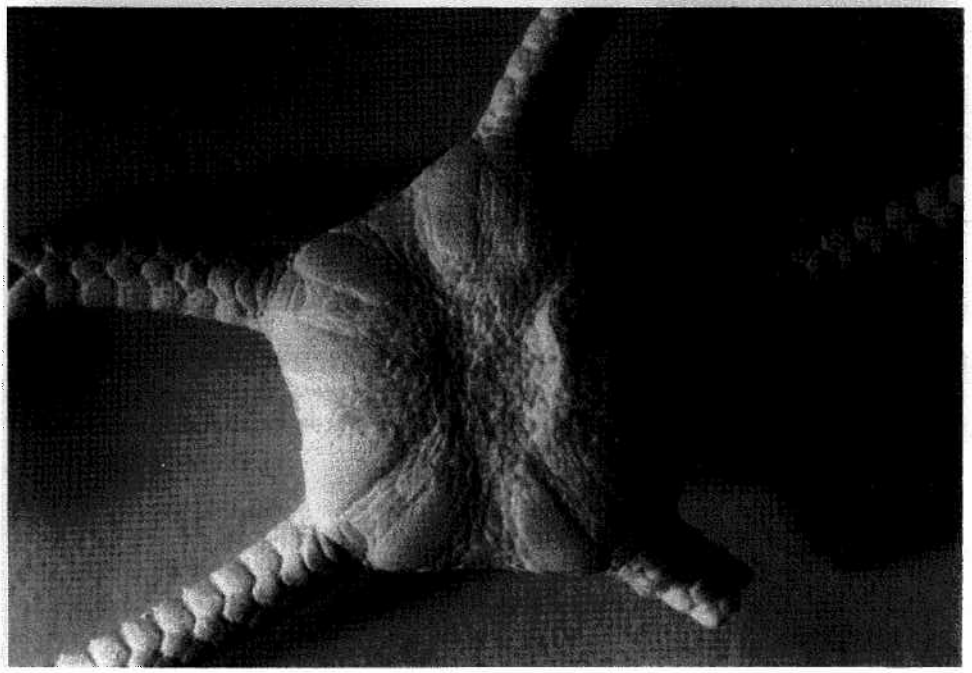

Sea-anemones (Cnidaria), Crustaceans, sea-stars (Asteroidea), Ophiuroidea and sea-cucumbers (Holothuroidea) were present in every trawl catch. Sponges (Porifera), Sipunculida and fish in 5 out of 6 trawls. Only 3 species of fish were caught, *viz.* the rat-tail fish *Coryphaenoides armatus* (20 specimens) (Fig. 4.14), *Synaphobranchus bathybius* (4x) and one specimen belonging to the family Brotulidae. The largest rat-tail fish was only 30.5 cm and the smallest less than 10 cm. The biggest fish in biomass and length (67 cm) was an eellike *Synaphobranchus*. With a maximum length of 50 cm, the Holothuroidea belonged to the largest invertebrates. These large animals were identified as *Benthodytes* spec. (5x) and *Psychropotes longicauda* (9x) (Fig. 4.14), and, with almost 8.5 kg wet weight, together formed the major part of the total megafaunal biomass. Stalked Ascidiacea and carnivorous squirts, recognizable because of the large lobes around the oral opening to catch animals, constituted most of the Tunicata. The sea-urchins (Echinoidea) were represented by only one pancake-like formed specimen (diameter of 30 cm) of the family Echinothuridae. *Ophiomusium planum* was the most abundant species within the Ophiuroidea, and the Asteroidea specimens belonged mostly to the family Porcellanasteridae. The hermit crab *Parapagurus pilosimanus* (Fig. 4.13), with its abdomen covered by a symbiontic sea-anemone or by a Zoantharia colony, formed the main representative of the Crustacea in the catch. A few large red prawns were important in biomass. Other crustacean groups were Cirripedia (*Scalpellum*), Isopoda, Amphipoda and crabs of the genus *Munidopsis*. Most of the Cnidaria belonged to the Actiniaria, and chiefly to the genus *Actinauge*. Further the symbiontic Actiniaria and Zoantharia, as already mentioned above, were of importance.

In density the Cnidaria are the most important with 13.5 individuals per 10 000 m^2, followed by the Ophiuroidea (6.2), Crustacea (4.8), Porifera (4.0) and the Holothuroidea with 3.1 specimens per 10 000 m^2 (Table 4.26). Asteroidea, Tunicata, Pisces and Sipunculida have a density of 2.0 to 2.9 individuals per 10 000 ^{2}. The Holothuroidea constitute more than half (55%) of the total megafauna biomass in wet weight. Cnidaria follow with 20.6%, fish (12.4%), crustaceans (5%) and starfish with 3.2% (Table 4.27). One should realize that all data indicate minimum estimates, as part of the megafauna will escape, either actively or because the trawl passes over them.

Comparison with the data given by FELDT *et al.* (1985) from exactly the same area shows that the observed densities for fish and Cephalopoda are similar. The rat-tail fishes (Macrouridae) were also, the most abundant fish in their trawl catches. Furthermore, the Cnidaria had by far the highest density, compared to the other animal groups, which agrees with our data. Densities for Holothuroidea and Vermes (probably Sipunculida and Polychaeta) too are close to our findings. However, for the Mollusca, Crustacea, Porifera and the other Echinodermata groups the densities are much lower. And so especially owing to the low densities for the Echinodermata, the total megafauna density (17 per 10 000 m^2) given by FELDT *et al.* (1985) is less than half that of our mean density (40.5 per 10 000 m^2, without fish). Our biomass data are on average somewhat higher than theirs (813 against 490 g wet weight per 10 000 m^2). But considering quantitative data for the megafauna have been found with the help of a quantitatively inaccurate sampling device, their

←

Fig. 4.13. Megafauna caught with the trawl. Above left: *Eryoneicus spinoculatus* Bouvier, 1905 (Crustacea, Decapoda), length 30 mm (trawl 8T). Above right: *Cirrothauma murrayi* Chun, 1914 (Cephalopoda, Octopoda), length 425 mm (trawl 12T). Below: *Ophiomusium planum* Lyman, 1878 (Ophiuroidea), diameter of disk 20 mm (trawl 13T).

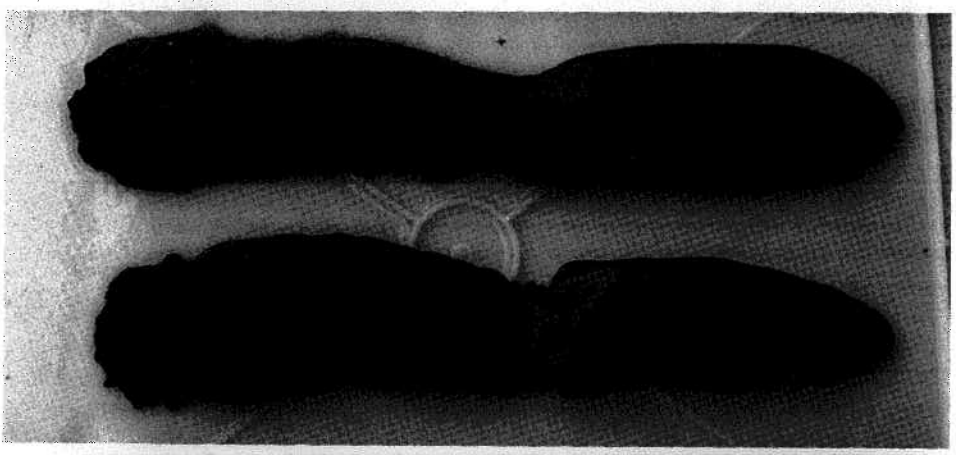

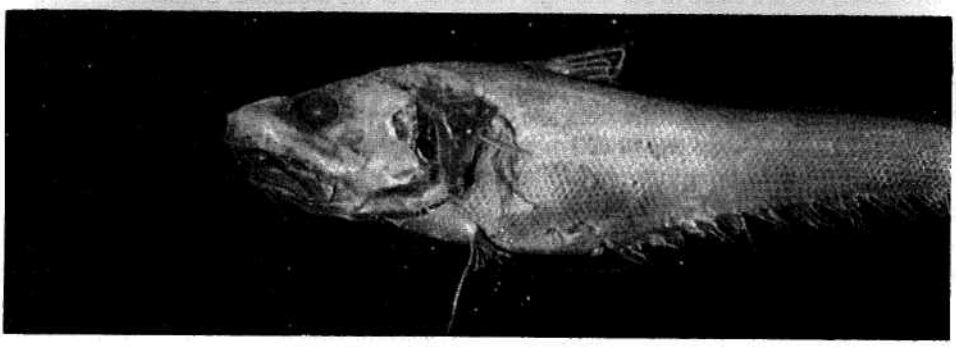

Table 4.26. Number of specimens per 10 000 m^2 of the different benthic megafaunal groups, caught with a 3.5 m Agassiz trawl during the second DORA-expedition.

	STATION						MEAN	%
	21T	23T	25T	27T	28T	28TB	N/10 000m^2	
Porifera		2	8	10	8	41	4.02	9.46
Cnidaria	21	41	30	29	48	62	13.46	31.68
Nemertini					1		0.06	0.14
Polychaeta			2	5	1	3	0.64	1.51
Sipunculida	7	4		6	11	6	1.98	4.66
Scaphopoda		4					0.23	0.54
Bivalvia	2	2			2		0.35	0.82
Cephalopoda			3	1+1		2+3	0.58	1.37
Crustacea	2	37	17	15	1	10	4.78	11.25
Asteroidea	5	4	18	8	6	8	2.86	6.73
Ophiuroidea	7	34	9	19	21	16	6.18	14.54
Echinoidea		1					0.06	0.14
Holothuroidea	11	6	7	9	5	15	3.09	7.27
Tunicata	3	5	2	9	11	7	2.16	5.08
Pisces		11	9	4	2	9	2.04	4.80
Total	58	151	105	116	117	182		
N/10 000m^2	10.5	48.5	37.5	65.5	62.0	88.4	42.5	

figures for densities and biomass agree surprisingly well with our data. The megafaunal densities for the Bay of Biscay at the same depth as the dumpsite, published by SIBUET & SEGONZAC (1985) are incomparable, as in that study the megafauna was defined as the animals retained by a sieve of 1 mm screen-size. However, if we assume that fishes all fit into our definition of megafauna, their fish densities are roughly a factor 10 higher. Although for a part their richer fish catches can be caused by their larger (6 m) Agassiz trawl, these data suggest that the fish fauna living deeper than 4 km is richer in the Bay of Biscay, than at the dumpsite.

Comparison of the megafauna biomass with the macro- and meiofauna biomass shows that megafauna is an order of magnitude less important than macro- and meiofauna.

←

Fig. 4.14. Megafauna caught with the trawl. Above: Hermit crabs (*Parapagurus pilosimanus*) with symbiontic zoantharia (23T), length ± 4 cm. Middle: Sea-cucumbers (*PsychropoTes longicauda*) (25T), length ± 38 cm. Below: Rat-tail fish (*Coryphaenoides armatus*) (23T), length 27 cm.

Table 4.27. Biomass of the different benthic megafaunal groups, caught with a 3.5 m Agassiz trawl during the second DORA-expedition, in gram wet weight per 10 000 m^2.

	STATION						MEAN	%
	21T	23T	25T	27T	28T	28TB	g/10 000m^2	
Porifera		35.1	3.5	8.6	1.9	55.8	6.11	0.66
Cnidaria	32.2	186.4	215.5	514.9	765.4	1565.6	191.17	20.59
Nemertini					0.7		0.04	
Polychaeta			2.4	2.1	1.1	3.7	0.54	0.06
Sipunculida	9.6	1.6		6.3	11.3	2.7	1.84	0.20
Scaphopoda		5.0					0.29	0.03
Bivalvia	5.3	0.7			0.5		0.38	0.04
Cephalopoda			1.6	4.2		19.7	1.49	0.16
Crustacea	36.9	337.8	120.5	143.2	4.2	162.5	46.92	5.05
Asteroidea	54.6	5.7	202.5	57.4	58.8	124.5	29.35	3.16
Ophiuroidea	3.0	9.6	16.3	42.5	20.6	43.3	7.89	0.85
Echinoidea		220.0					12.82	1.38
Holothuroidea	394.6	23.7	2278.6	1509.2	477.2	4125.5	513.41	55.29
Tunicata	1.0	0.7	1.0	5.4	3.2	2.8	0.82	0.09
Pisces		1051.4	436.4	67.8	13.4	412.4	115.48	12.44
Total	537.2	1877.7	3278.3	2361.6	1358.3	6518.5		
g/10 000m^2	97.2	603.5	1170.2	1333.5	720.0	3164.7	928.6	

Table 4.29. Elemental concentrations (in mg/kg) in four parts of rat-tail fish samples (mean values ± s.d., n = 4) and of a deep-sea eel (*Synaphobranchus bathybius*), and in the surface sediment (section 3.4).

element	gut content	gut wall	liver	meat	sediment
rat-tail fish (n=4)					
Br	1270 ± 490	91.5 ± 32.1	22.6 ± 10.9	15.3 ± 4.9	12
As	32.9 ± 12.9	34.3 ± 5.9	14.9 ± 1.1	25.5 ± 17.2	2.1
Zn	123 ± 32.8	148.2 ± 51.5	71.4 ± 26.0	13.6 ± 1.4	20
Cr	11.5 ± 5.5	6.5 ± 1.2	3.8 ± 1.5	4.2 ± 1.4	11.3
Co	2.12 ± 0.54	5.37 ± 0.18	0.25 ± 0.04	0.14 ± 0.04	6.0
Fe	1480 ± 580	282 ± 131	387 ± 158	29 ± 18	6500
Cs	0.196 ± 0.112	0.084 ± 0.078	0.029 ± 0.010	0.076 ± 0.063	1.3
Rb	3.50 ± 1.91	1.70 ± 0.85	0.41 ± 0.06	1.45 ± 0.13	25
Th	0.24 ± 0.15	<0.1	<0.1	<0.1	1.85
La	<0.5	<0.5	<0.5	<0.5	8.4
Ce	<0.2	<0.2	<0.2	<0.2	17.6
Hg	<0.2	0.9 ± 0.6	0.7 ± 0.3	1.0 ± 0.2	n.d.
deep-sea eel (n=1)					
Br	37.4	27.6	18.1	14.8	
As	30.3	21.2	7.6	43.1	
Zn	97	76	36	10	
Cr	3.5	3.9	4.5	1.6	
Co	0.34	0.19	0.13	0.07	
Fe	340	158	480	23	
Cs	0.17	0.025	0.019	0.034	
Rb	3.60	1.50	0.70	0.56	
Th	<0.1	<0.1	<0.1	<0.1	
La	<0.5	<0.5	<0.5	<0.5	
Ce	<0.2	<0.2	<0.2	<0.2	
Hg	5.6	7.4	6.0	3.0	

4.3.6. CHEMICAL ANALYSIS OF BOTTOM FISHES

Six rat-tail fishes *Coryphaenoides armatus* and 1 eellike fish *Synaphobranchus bathybius* were dissected for chemical analyses. Care was taken to avoid contamination. Gut content, gut wall, liver and clean meat were freeze-dried seperately. The samples were then analysed for trace elements with neutron activation analysis. The various parts of the three smaller rat-tail fishes were pooled in order to get sufficient material for the analysis (100 mg dry weight or more). Br data were corrected for the sea salt error using data on Na, and assuming that all Na in the samples was derived from sea water.

The average trace element content in gut content, gut wall, liver, and clean meat of the four samples of rat-tail fish is given in Table 4.29 with contents in the surface sediment (from section 3.4). The ratio of the gut content to the content in the sediment is shown in Fig. 4.15A, and the accumulation factor from gut contents to tissue material in Fig. 4.15B. The gut content of the rat-tail fishes is enriched in Br, As and Zn relative to surface sediments, but is depleted in the detrital elements Fe, (not Cr), Co, Cs, Rb, Th and very strongly in rare earth elements. The rat-tail fishes accumulate none of these elements in their tissue. They do accumulate Hg, and it may be expected that they accumulate rare earth elements in their bones, but those parts have not been analysed.

4.4. FOODWEB

Most of the representatives of those meio-, macro- and megafaunal groups that are important in biomass, are deposit feeders. In section 4.3.1.5 we already saw that 70% of the nematode biomass was formed by the selective and non-selective deposit feeders. The most important macrofaunal animals in biomass, the Sipunculida and Polychaeta, are predominantly deposit feeders. Their guts are filled with sediment. Tanaids seize large masses of sediment with their chelipeds and maxilipeds, and selectively devour considerable quantities of sediment with the other mouth appendages (HOLDICH & JONES, 1983). The most massive animals of the megafauna, the sea cucumbers, had their gut always completely filled with bottom ooze. The same holds for animals, considered carnivores at least in shallower seas, such as sea-anemones and starfish. Of all animals important in biomass, only the bottom-dwelling fish seem to be an exception, and are completely carnivorous. The stomach, at least in fishes with a swim bladder, is mostly found

Table 4.28. Stomach content of 7 rat-tail fishes *Coryphaenoides armatus* caught at station 28TB.

Length of fish / Stomach content	10.3	13.5	14.0	15.3	16.5	18.7	30.5 cm
Lens of fisheye					1		1
Beak of squid				1	1		
Crustacea	+	+				+	+
Copepoda		1	2			1	
Amphipoda			1	1			
Tanaidacea				1	1		
Isopoda	1		2	3	1		

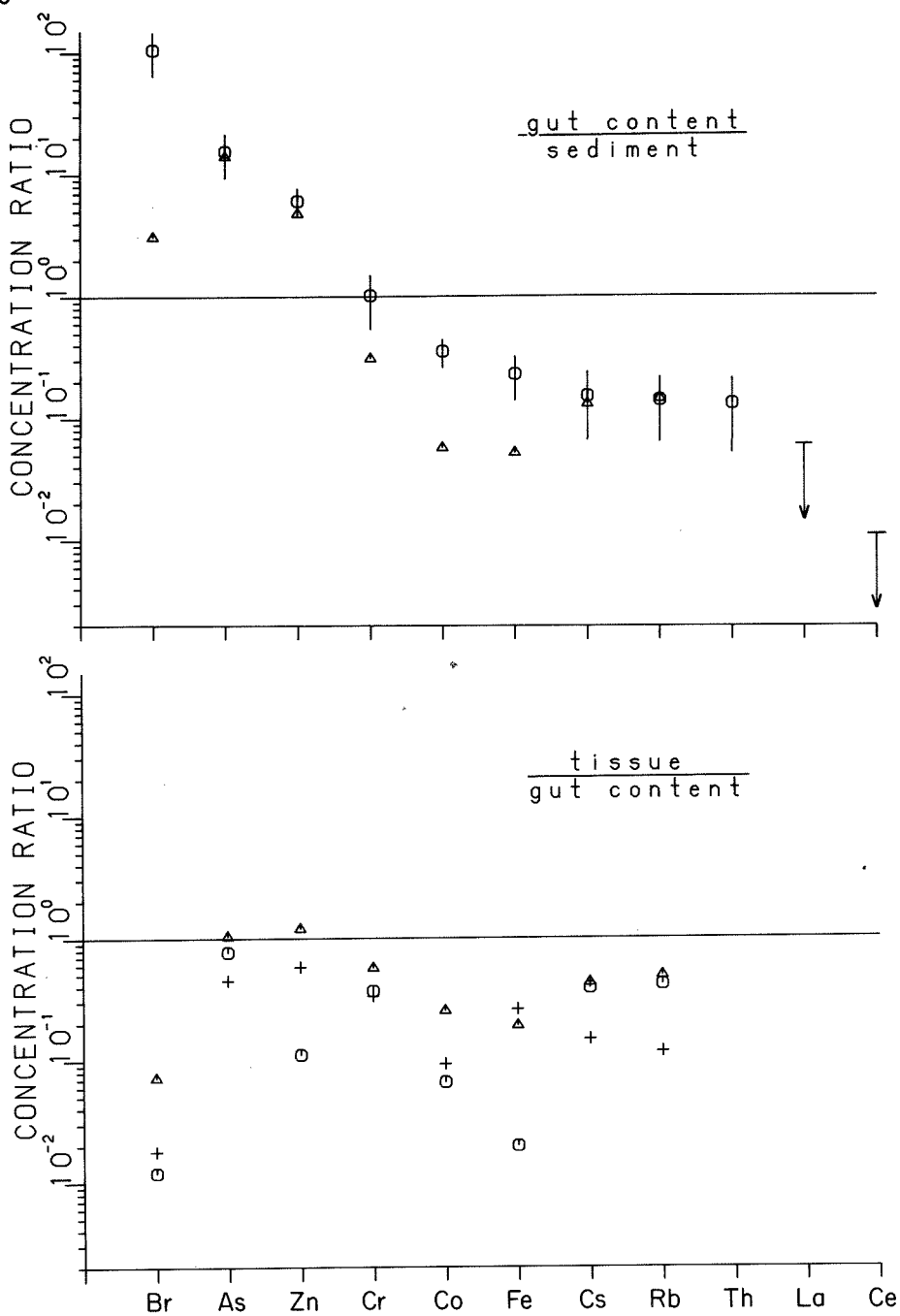

Fig. 4.15. Above: Ratios of elemental concentrations in gut content of o: rat-tail fish (mean ± s.d., n = 4) and △: one deep-sea eel (*Synaphobranchus bathybius*) from the NEA-dumpsite relative to surface sediment. Below: Ratios of elemental concentrations in gut wall (△), liver (+) and meat (o) of rat-tail fish, relative to gut content.

to be empty when the fish is hauled up from great depths. Probably because of the large amount of mud in the our trawl catches, the fish still had full stomachs. The stomach contents were studied of 7 fishes of station 27 (Table 4.28) and this shows that these fish eat free swimming animals, mostly crustaceans, as well as real bottom dwelling animals, like Tanaidacea and Isopoda. So in general the deposit feeders constitute the largest part of the total benthic fauna biomass at the dumpsite. Suspension feeders, such as Crinoidea and Porifera, are relatively rare.

4.5. PRIMARY PRODUCTION

Primary production was measured on three occasions during the 1982 expedition and varied between 150 and 360 mg $C.m^{-2}.d^{-1}$, with an average value of 293 mg $C.m^{-2}.d^{-1}$. This is not significantly different from average values for oceanic waters (130-270 mg $C.m^{-2}.d^{-1}$)

4.6. CONCLUSIONS

The horizontal distribution of meiofauna within a boxcore sample is not patchy, and results from 4 out of 6 station pairs suggest that it is even rather constant on a much larger scale (several 100 m^2 to some km^2). If in the future faunal changes were caused (*e.g.* by higher dose rates), a study of the meiofauna would be the most suitable way to detect such changes. Especially the diversity of Nematoda, a group that is very important in density and biomass, would be a suitable indicator.

When estimating the total biomass of animals larger than 50 μm, in a deep-sea boxcore sample, it is also important to study the large meiofauna ($>$ 0.5 mm) seperately. This adds about 16 % to the value for biomass derived from a study of only the meiofauna from subsamples and of the macrofauna.

As most of the benthic animals of the dumpsite, which also constitute the largest part of the total biomass, are deposit feeders, and as the food content of the sediment is low, relatively large masses of sediment will pass through their guts. A considerable part of the radionuclides that will eventually leak out of the dumped canisters with radioactive waste, is predicted to be bound to the sediment. Hence we conclude that the animals play a significant role in the dispersal and transformation of these radionuclides.

5. BIOTURBATION

X-radiographs of 2 cm thick slices taken from the boxcores (Fig. 5.1) gave evidence of extensive burrowing activity of bottom fauna. From ^{14}C profiles, KERSHAW (1985) concluded that the sediment at the dumpsite is bioturbated down to 6 cm depth. Bioturbation in deep-sea sediments can be quantified by measuring the ^{210}Pb activity profile in the sediment surface layer (NOZAKI *et al.*, 1977), and similar information can be obtained from the depth distribution of $^{239+240}Pu$ in the sediments. The distribution of excess-^{210}Pb in subcores of boxcores 1 to 15 (measured by J.N. Smith, Bedford, Canada) has been reported in DICKSON *et al.* (1985). The profiles can be described by a model of diffusive mixing with a mixing coefficient in the range of 0.6 to 4 $10^{-8} cm^2.s^{-1}$. It is, however, questionable whether bioturbation can be adequately described by a diffusive mixing of constant intensity (BOUDREAU 1986a,b).

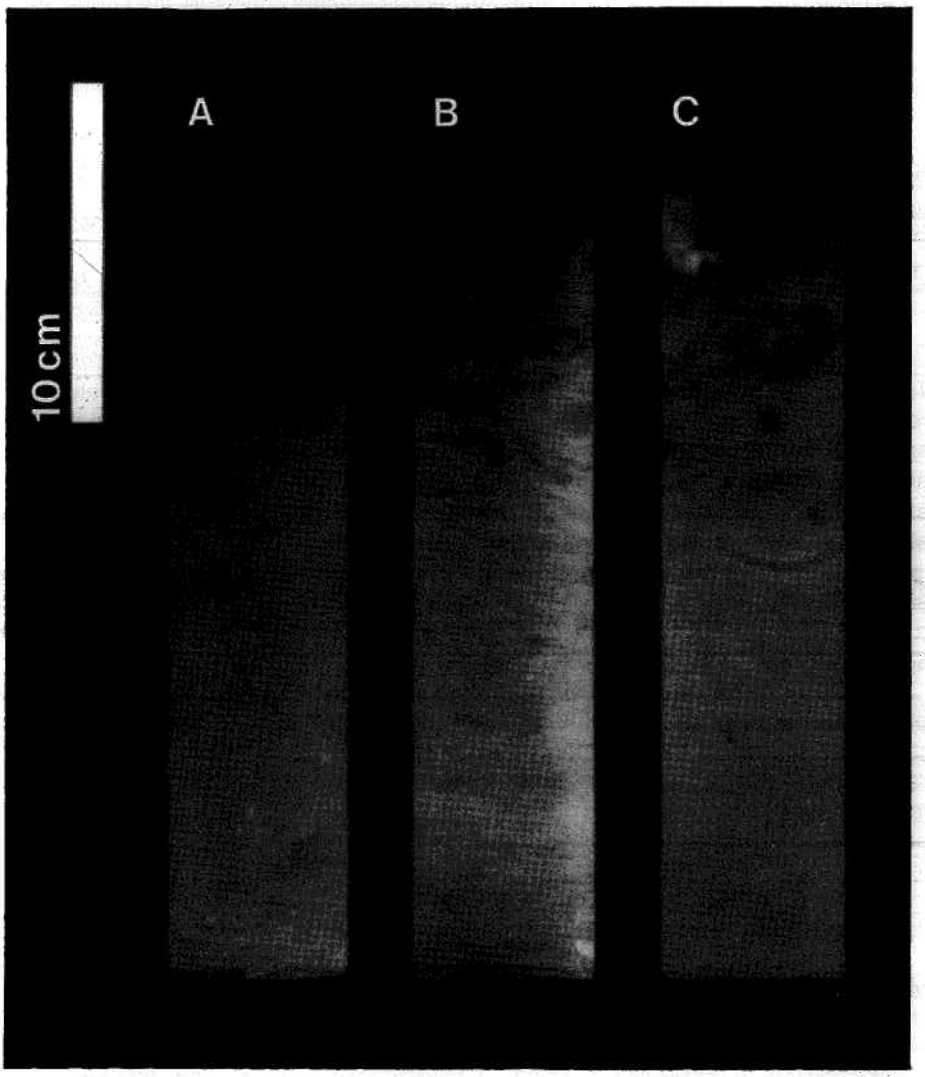

Fig. 5.1. X-radiographs of 2 cm thick subcores from boxcores 4B (A), 8B (B) and 11B (C).

The distribution of ^{210}Pb (mentioned above) and of $^{239+240}Pu$ (by Noshkin, Livermore, USA), measured in the same subcore from each of 8 boxcores showed coinciding subsurface maxima at about 3 to 6 cm depth. This distribution cannot be explained by a model of homogeneous mixing in the upper sediment layer, but instead points to a net transport of surface sediment downwards to the depth where the maximum was observed. At this same depth interval a small but distinct maximum was sometimes found in ETS activity and in the organic carbon content of the sediment (Fig. 3.17). Similar subsurface maxima of ^{210}Pb have been reported by SOMAYAJULU *et al.*(1983).

In coastal sediments, transport of radionuclides by bioturbation to depths of up to 140 cm has been observed (KERSHAW *et al.*, 1984). From the vertical distribution of the meiofauna and the smaller macrofauna it is clear that any significant contribution of these groups to bioturbation must be limited to the upper few cm. The larger macrofauna like Sipunculida and Polychaeta, burrow down to at least 15 cm depth. Although their density is low (9 per m^2 for Sipunculida), they must be considered the major cause of the bioturbation below the upper few cm. Sipunculida, representing 28% of macrofauna biomass, are surface deposit feeders, as indicated by the large quantity of ingested sediment. They could therefore also be responsible for the subsurface maxima described above, through the direct transport of surface sediment down to deeper layers via their gut.

Sipunculida respire about 10% of the carbon flux to the sediment, or 90 mg $C.m^{-2}.yr^{-1}$. Since they take up this carbon from the ingested sediment, we can make a minimum estimate of their sediment uptake rate:

If they feed on the surface sediment, which contains 2 $mg.g^{-1}$ of metabolizable organic carbon (Fig. 3.17), they have to ingest a minimum of 5.6 $cm^3.cm^{-2}.kyr^{-1}$ of wet sediment. And if they defecate at the bottom of the mixed layer (6 cm depth), the sipunculids alone would turn the sediment in this layer 3 times over before it is buried, and would thus account for a substantial part of the biological mixing rate that was estimated from tracer data.

If, however, they manage to capture the high-quality food as it reaches the sea floor (containing 40 $mg.g^{-1}$ of organic carbon), the ingestion of only 0.3 $cm^3.cm^{-2}.kyr^{-1}$ would be sufficient. Such a transport would be minor relative to the sediment accumulation rate, but would yet transport over 10% of the ^{14}C and ^{210}Pb rain rate to a few centimetres depth. Conventional mixing models would than seriously over estimate the biological mixing rate from the vertical distribution of these tracers, and other models (BOUDREAU, 1986b) would have to be prefered.

6. SUMMARY AND CONCLUSIONS

The seafloor at the NEA dumpsite for low-level radioactive waste has been investigated by geochemical and biological techniques. Evidence of local turbidites and slumping is recorded in the sediment, probably related to the steep local topography. Slumping events could be triggered by dumping operations.

The $CaCO_3$ content is the principle variable that accounts for most of the variation in the elemental composition and cation exchange capacity of the sediment. The present depth of the lysocline is shown to be at about 4700m, but even at shallower depth an appreciable part of the $CaCO_3$ raining on the sea floor dissolves.

Diagenetic modeling is used to explain the interrelationships between: (1) Mineralization of organic material and (2) Redox transitions, (3) Cation exchange, and (4) Carbonate dissolution and recrystallization. These diagenetic processes are discussed in terms of their effects on the redistribution and transport of trace elements and radionuclides within the sediment and between sediment and overlying water.

Composition, density, biomass, vertical and horizontal distribution has been studied of benthic meio- as well as macrofauna of the NEA-dumpsite. Meiofauna has a mean density of 527 000 per m^2 and a mean biomass of 24.3 mg dry weight per m^2. Nematoda are the most important meiofauna group in density and biomass. 75% of the meiofaunal biomass is concentrated in the upper 3 cm of the sediment. The horizontal distribution of Nematoda within a boxcore sample is not patchy. The nematode biomass has a much more irregular distribution and no correlation was found between densities and biomass. The diversity of the Nematoda fauna is high and the depositfeeders dominate the population with 70% (of the biomass).

The macrofaunal metazoans have a mean density of 124 per m^2 and a mean biomass of 79,7 mg dry weight per m^2 of which only 29% is found in the upper 3 cm. Polychaeta have the highest average density (45 per m^2). Sipunculida, forming the main constituent of macrofauna biomass, probably play a major role in bioturbation.

The metazoa, belonging to the large meiofauna (>0.5 mm and <1 mm), have a density of 366 per mm^2 and a biomass of 14.6 mg dry weight per m^2. Of this group Polychaeta have the highest density and biomass.

The megafauna (>1 cm and >50 mg) has a density of 42.5 per 10 000 m^2 and a biomass of 929 g wet weight per 10 000 m^2.
Sea-anemones have the highest abundance and sea-cucumbers are the most massive animals. Most of the benthic animals of meio-, macro and megafauna are depositfeeders.

The processes that have been shown in this report to influence the fate of radionuclides that are released from the waste packages are summarized as follows:

The first step: Transport from bottom water to sediment:
Sediment rains on the seafloor at an average rate of 2.7 $mg.cm^{-2}.yr^{-1}$. This flux consists of 2.3 $mg.cm^{-2}.yr^{-1}$ $CaCO_3$ (84%), 0.2 $mg.cm^{-2}.yr^{-1}$ organic matter (9%), and 0.2 $mg.cm^{-2}.yr^{-1}$ of detrital siliceous material (7%). The flux of organic matter represents 0.9% of the primary production at the ocean surface.

Radionuclides are scavenged from the bottom water by oxyhydroxide and organic coatings on suspended particles, which are derived either from the ocean surface or from resuspension at the ocean floor or at hillsides. Although it is not certain whether equilibrium adsorption is reached in this water mass, equilibrium appears to be a reasonable assumption. The partitioning between the dissolved and the particulate phase can then be predicted from K_d values and suspended matter concentrations. However, the rate at which suspended particles and their load of radionuclides are incorporated in the sediment by the net result of settling, resuspension and bioturbation is a major unknown. Since this is the key parameter determining whether or not particle reactive elements will be transported by bottom currents, this issue requires further investigation.

The second step: transport within the sediment:
The important processes are:

1. bioturbation
2. sediment accumulation
3. occasionnally: slumping

The last two contributions tend to be more important in deep areas than on top of the hills

Estimates of the biological mixing rate in the surface sediment, based on the vertical distribution of ^{14}C and ^{210}Pb, depend strongly upon assumptions regarding the feeding habits of Sipunculida.

The third step: transformation of radionuclides within the sediment:
These transformations can be classified according to the depth interval over which they occur:

0–10 cm:
Most of the meio- and macrofauna lives in this layer of the sediment. A majority of the fauna feeds on sediment particles, and by their feeding and burrowing activities they turn the upper 6 cm over on a time scale of a few hundred years. Aerobic mineralization within the bioturbated layer dissolves between 25 and 40% of $CaCO_3$ (above the lysocline) and decomposes 98% of the organic matter that settled on the ocean floor. About half of this mineralization activity can be accounted for by the respiration of macro- and meiofauna.

0-< 1mm:
In this thin surface layer decomposition takes place of the most reactive organic matter, including the organic coatings with the highest binding strength. Cu and probably other organically bound elements are released to the bottom water. Freshly settled sediment is taken up by surface deposit feeders, and subsequently transformed, incorporated in the food chain and predated by bottom fish.

0-3 cm:
1. Particles are taken up and transformed by micro-organisms, meiofauna, and macrofauna. Radionuclides are incorporated in the food web.
2. Organic matter is decomposed with an average decay half-life in the order of 10 years, but a part is decomposed much more rapidly. ^{3}H and ^{14}C in the decomposed organic matter, and an unknown fraction of organically bound Pu and Am are released to the bottom water.
3. $CaCO_3$ dissolves, and some Sr is consequently released.

3-10 cm:
Organic matter decays and $CaCO_3$ dissolves at reduced rates, and bioturbation continues.

10-70 cm:
Very little change occurs in this layer. The mobility and pore water concentrations of trace elements can adequately be described by distribution coefficients.

Large macrofaunal burrowing animals can reach this depth zone, but, because of their low densities, their influence will be small.

below about 70 cm:
Fe and Mn oxyhydroxides dissolve and the elements associated with this phase (Co, and probably Pu and Am) are mobilized.

Significant sulfate reduction occurs only in turbiditic deposits, where it causes the immobilization of Pu and Am through reduction and sulfide formation, and the mobilization of Cs through cation exchange with NH_4^+.

7. REFERENCES

Introduction

DICKSON, R.R., P.A. GURBUTT & P.J. KERSHAW (eds.), 1985. Interim oceanographic description of the North-East Atlantic site for the disposal of low-level radioactive waste. **Vol. 2.** NEA/OECD, Paris.

KERSHAW, P.J., 1985. ^{14}C and ^{210}Pb in NE Atlantic Sediments: Evidence of biological reworking in the context of radioactive waste disposal. J. Environm. Radio. **2:** 115-134.

NEA, 1980. Review of the continued suitability of the dumping site for radioactive waste in the North-East Atlantic. OECD,Paris.

NEA, 1985. Review of the continued suitability of the dumping site for radioactive waste in the North-East Atlantic. OECD,Paris.

NOSHKIN, V.E., 1983. Fallout concentrations in sediments and some biota from regions of the northeast Atlantic. Chapter 15 in: P.A. Gurbutt and R.R. Dickson (eds.) Interim oceanographic description of the North-East Atlantic site for the disposal of low-level radioactive waste. NEA/OECD,Paris.

NOSHKIN, V.E., 1985. Plutonium in northeast Atlantic sediments. Chapter 8 in: Interim oceanographic description of the North-Eastern Atlantic dumpsite II. NEA/OECD Paris.

RUTGERS VAN DER LOEFF, M.M. & M.S.S. LAVALEYE, 1984. Geochemical and biological research at the NEA dumpsite for low-level radioactive waste. Neth. Inst. for Sea Res. int. rept. 1984-2.

Geochemistry

ANDREWS, D., & A. BENNETT, 1981. Measurements of diffusivity near the sediment-water interface with a fine-scale resistivity probe. Geochim. Cosmochim. Acta **45:** 2169-2175.

ARMI, L. & E. D'ASARO, 1980. Flow structures of the benthic ocean. J. Geophys. Res. **85:** 469-484.

BACON, M.P. & R.F. ANDERSON, 1982. Distribution of Thorium isotopes between dissolved and particulate forms in the deep sea. J. Geophys. Res. **87** (C3): 2045-2056.

BAKER, P.A., J.M. GIESKES & H. ELDERFIELD, 1981. Diagenesis of carbonates in deep sea sediments-evidence from Sr/Ca ratios and interstitial dissolved Sr data. J. Sed. Petrol. **52:** 71-82

BALISTIERI L., P.G. BREWER & J.W. MURRAY, 1981. Scavenging residence times of trace metals and surface chemistry of sinking particles in the deep ocean. Deep-Sea Research **28A:** 101-121.

BALISTIERI, L., & J.W. MURRAY, 1983. Metal-solid interactions in the marine environment: estimating apparent equilibrium binding constants. Geochim. Cosmochim. Acta **47:** 1091-1098.

BALISTIERI, L., & J.W. MURRAY, 1984. Marine scavenging: Trace metal adsorption by interfacial sediment from MANOP site H. Geochim. Cosmochim. Acta **48:** 921-929.

BALZER, W., 1982. On the distribution of iron and manganese at the sediment/water interface: thermodynamic versus kinetic control. Geochim. Cosmochim. Acta **46:** 1153-1161.

BENDER, M.L., & D.T. HEGGIE, 1984. Fate of organic carbon reaching the deep sea floor: a status report. Geochim. Cosmochim. Acta **48:** 977-986.

BERGER, W.H., 1968. Planktonic Foraminifera: selective solution and paleoclimatic interpretation. Deep-Sea Res. **15:** 31-43.

BERNER, R.A., 1974. Kinetic models for the early diagenesis of nitrogen, sulfur, phosphorus, and silicon in anoxic marine sediments. In: E.D. Goldberg (ed.),The Sea, Vol.V, Wiley, New York, 427-450.

BERNER, R.A., 1978. Sulfate reduction and the rate of deposition of marine sediments. Earth Planet. Sci. Lett. **37:** 492-498.

BERNER, R.A., 1980. Early diagenesis, a theoretical approach. Princeton University Press, Princeton, New Jersey.

BISCAYE, P.E., V. KOLLA & K.K. TUREKIAN, 1976. Distribution of Calcium Carbonate in Surface Sediments of the Atlantic Ocean. J. Geophys. Res. **81:** 2595-2603.

BLOMQVIST, S., 1985. Reliability of core sampling of soft bottom sediment - an *in situ* study. Sedimentology **32:** 605-612.

BONATTI, E., D.E. FISHER, O. JOENSUU & H.S. RYDELL, 1971. Postdepositional mobility of some transition elements, phosphorus, uranium and thorium in deep sea sediments. Geochim. Cosmochim. Acta **35:** 189-201.

BOUDREAU, B.P., 1986a. Mathematics of tracer mixing in sediments: I. Spatially-dependent, diffusive mixing. Am. J. Sci. **286:** 161-198.

BOUDREAU, B.P., 1986b. Mathematics of tracer mixing in sediments: II. Nonlocal mixing and biological conveyor-belt phenomena. Am. J. Sci. **286:** 199-238.

BOUST, D., 1986. Les terres rares au cours de la diagenèse des sédiments abyssaux; analogies avec un transuranien: l'américium. PhD. Thesis, University of Caen.

BOYLE, E.A., F.R. SCLATER, & J.M. EDMOND, 1977. The distribution of dissolved copper in the Pacific. Earth Planet. Sci. Lett. **37:** 38-54.

BOYLE, E.A., 1983. Manganese carbonate overgrowth on foraminifera tests. Geochim. Cosmochim. Acta **47:** 1815-1819.

BRAMLETTE, M.N., & W.H. BRADLEY, 1941. Geology and biology of north Atlantic deep-sea cores between Newfoundland and Ireland. Part I: Lithology and geologic interpretations. U.S. Dept. Int. Prof. Paper **196-A,** 34 pp.

BRECK, W.G., 1974. Redox levels in the sea. In: The Sea, Vol. 5 (E.D. Goldberg ed.): 153-180. Wiley & Sons, New York.

BRULAND, K.W., 1980. Oceanographic distributions of cadmium, zinc, nickel and copper in the North Pacific. Earth Planet. Sci. Lett. **47:** 176-198.

CALLENDER, E. & C.J. BOWSER, 1980. Manganese and copper geochemistry of interstitial fluids from manganese nodule-rich pelagic sediments of the northeastern equatorial Pacific ocean. Am. J. Sci. **280:** 1063-1096.

CALVERT, S.E. & N.B. PRICE, 1977. Geochemical variation in ferromanganese nodules and associated sediments from the Pacific Ocean. Mar. Chem. **5:** 43-74.

CHESTER, R. & M.J. HUGHES, 1967. A chemical technique for the separation of ferro-manganese minerals, carbonate minerals and adsorbed trace elements from pelagic sediments. Chem. Geol. **2:** 249-262.

COLLEY, S., J. THOMSON, T.R.S. WILSON & N.C. HIGGS, 1984. Post-depositional migration of elements during diagenesis in brown clay and turbidite sequences in the North East Atlantic. Geochim. Cosmochim. Acta **48:** 1223-1235.

DANIELSSON, L.-G., B. MAGNUSSON & S. WESTERLUND, 1979. An improved metal extraction procedure for the determination of trace metals in seawater by atomic absorption spectrometry with electrothermal atomisation. Anal. Chim. Acta **98:** 47-57.

DE BAAR, H.J.W., M.P. BACON, P.G. BREWER, & K.W. BRULAND, 1985. Rare earth elements in the Pacific and Atlantic Oceans. Geochim. Cosmochim. Acta **49:** 1943-1959.

DICKSON, R.R., 1983. The 'topographic study'. Chapter 5B in: P.A. Gurbutt and R.R. Dickson (eds.) Interim oceanographic description of the North-East Atlantic site for the disposal of low-level radioactive waste. NEA/OECD,Paris.

DICKSON, R.R., & W.J. GOULD, 1983. The flow field (chapter 5A). In: P.A. Gurbutt and R.R. Dickson. Interim oceanographic description of the North-East Atlantic site for the disposal of low-level radioactive waste. NEA/OECD, Paris.

DUURSMA, E.K., 1973. Specific activity of radionuclides sorbed by marine sediments in relation to the stable element composition. In: Radioactive contamination of the marine environment. IAEA, Vienna, SM. **158/4.** 57-71.

DUURSMA, E.K. & C.J. BOSCH, 1970. Theoretical, experimental and field studies concerning reactions of radioisotopes with sediments and suspended particles of the sea. Part B: Methods and experiments. Neth. J.Sea Res. **4(4):** 395-469.

DUURSMA, E.K. & D. EISMA, 1973. Theoretical, experimental and field studies concerning reactions of radionuclides with sediments and suspended particles of the sea. Part C: Applications to field studies. Neth.J.Sea Res. **6(3):** 265-324.

DUURSMA, E.K. & M.G. GROSS, 1971. Marine sediment and radioactivity. In: Radioactivity in the marine environment. U.S. Nat. Acad. Sci., Wash.D.C., 147-160.

EDGINGTON, D.N., 1981. A review of the persistence of long-lived radionuclides in the marine environment - sediment/water interactions. in: Impacts of radionuclides releases into the marine environment. IAEA, Vienna.

ELDERFIELD, H., 1976. Manganese fluxes to the oceans. Mar. Chem. **4:** 103-132.

ELDERFIELD, H., C.J. HAWKESWORTH M.J. GREAVES & S.E. CALVERT, 1981. Rare earth element zonation in Pacific ferromanganese nodules. Geochim. Cosmochim. Acta **45:** 1231-1234.

ELDERFIELD, H. & M.J. GREAVES, 1982. The rare earth elements in seawater. Nature **296:** 214-219.

ELDERFIELD, H., J.M. GIESKES, P.A. BAKER, R.K. OLDFIELD, C.J. HAWKESWORTH & R. MILLER, 1982. $^{87}Sr/^{86}Sr$ and $^{18}O/^{16}O$ ratios, interstitial water chemistry and diagenesis in deep-sea carbonate sediments of the Ontong Java Plateau. Geochim. Cosmochim. Acta **46:** 2259-2268

EMERSON, S., R. JAHNKE, M. BENDER, P. FROELICH, G. KLINKHAMMER, C. BOWSER & G. SETLOCK, 1980. Early diagenesis in sediments from the eastern equatorial Pacific. I. Pore water nutrient and carbonate results. Earth Planet. Sci. Lett. **49:** 57-80.

EMERSON, S. & M. BENDER, 1981. Carbon fluxes at the sediment-water interface of the deep-sea: calcium carbonate preservation. J. Mar. Res. **39:** 139-162.

EMERSON, S., V. GRUNDMANIS, & D. GRAHAM, 1982. Carbonate chemistry in marine pore waters: MANOP sites C and S. Earth Planet. Sci. Lett. **61:** 220-232.

EMERSON, S., K. FISCHER, C. REIMERS & D. HEGGIE, 1985. Organic carbon dynamics and preservation in deep-sea sediments. Deep-Sea Research **32:** 1-21.

FROELICH, P.N., G.P. KLINKHAMMER, M.L. BENDER, N.A. LUEDTKE, G.R. HEATH, D. CULLEN & P. DAUPHIN, 1979. Early oxidation of organic matter in pelagic sediments of the eastern equatorial Atlantic: suboxic diagenesis. Geochim. Cosmochim. Acta **43:** 1075-1090.

GOLDBERG, E.D., 1954. Marine geochemistry. I. Chemical scavengers of the sea. J. Geol. **62:** 249-265.

GURBUTT, P.A., & R.R. DICKSON (eds.), 1983. Interim oceanographic description of the North-East Atlantic site for the disposal of low-level radioactive waste. NEA/OECD,Paris.

GURBUTT, P.A., & R.R. DICKSON, 1985. A vertical eddy diffusivity estimate from near-bottom Rn measurements. Interim oceanographic description of the North-Eastern Atlantic dumpsite II, Chapter 3. NEA/OECD Paris.

HARTMANN, M., 1979. Evidence for early diagenetic mobilization of trace metals from discolorations of pelagic sediments. Chem. Geol. **26:** 277-293.

HARTMANN, M., P.J. MÜLLER, E. SUESS & C.H. VAN DER WEIJDEN, 1976. Chemistry of Late Quaternary sediments and their interstitial waters from the NW African continental margin. Meteor Forsch.-Ergebn. C, **24:** 1-67.

HASKIN, M.A., & L.A. HASKIN, 1966. Rare earths in European shales: a redetermination. Science **154:** 507-509.

HEGGIE, D., & T. LEWIS, 1984. Cobalt in pore waters of marine sediments. Nature **311:** 453-455.

HELDER, W. & R.T.P. DE VRIES, 1979. An automated phenol-hypochlorite method for the determination of ammonia in sea- and brackish waters. Neth. J. Sea Res. **13:** 154-160.

HOLDREN, G.R., O.P. BRICKER & G. MATISOFF, 1975. A model for the control of dissolved manganese in the interstitial waters of Chesapeake Bay. In Marine Chemistry of the Coastal Environment (T.M. Church, ed.), Vol. **18:** 364-381. Amer. Chem. Soc. Symp. Ser.

IPEREN, J. VAN, & W. HELDER, 1985. A method for the determination of organic carbon in calcareous marine sediments. Mar. Geol. **64:** 179-187.

JAHNKE, R., D. HEGGIE, S. EMERSON & V. GRUNDMANIS, 1982. Pore waters of the central Pacific Ocean: nutrient results. Earth Planet. Sci. Lett. **61:** 233-256.

JOHANSSON, O. & M. WEDBORG, 1982. On the evaluation of potentiometric titrations of seawater with hydrochloric acid. Oceanol. Acta **5:** 209-218.

JOHNSON, K.S., 1982. Solubility of rhodochrosite ($MnCO_3$) in water and seawater. Geochim. Cosmochim. Acta **46:** 1805-1809.

KERSHAW, P.J., 1985. ^{14}C and ^{210}Pb in NE Atlantic Sediments: Evidence of biological reworking in the context of radioactive waste disposal. J. Environm. Radio. **2:** 115-134.

KERSHAW, P.J., D.J.SWIFT, R.J. PENTREATH, & M.B. LOVETT, 1984. The incorporation of Plutonium, Americium and Curium into the Irish Sea seabed by biological activity. Sci. Total Environm. **40:** 61-81.

KERSHAW, P.J., R.J. PENTREATH, B.R. HARVEY, M.B. LOVETT, & S.J. BOGGIS, 1986. Apparent distribution coefficients of transuranium elements in UK coastal waters. In: Scient. sem. on the application of distribution coefficients to radiological assessment models. Elsevier, London, 10p.

KIDD, B., 1983. Sediment distribution and sedimentary processes at the dumpsite. Chapter 4 in:P.A.Gurbutt and R.R.Dickson(eds.) Interim oceanographic description of the North-East Atlantic site for the disposal of low-level radioactive waste NEA/OECD, Paris.

KLINKHAMMER, G.P., 1980. Early diagenesis in sediments from the eastern equatorial Pacific, II. Pore water metal results. Earth Planet. Sci. Lett. **49:** 81-101.

KLINKHAMMER, G.P., D.T. HEGGIE & D.W. GRAHAM, 1982. Metal diagenesis in oxic marine sediments. Earth Planet. Sci. Lett. **61:** 211-219.

KNAUER, G.A., J.H. MARTIN, & R.M. GORDON, 1982. Cobalt in north-east Pacific waters. Nature **297:** 49-51.

LEBEL, J., N. SILVERBERG, & B. SUNDBY, 1982. Gravity core shortening and pore water chemical gradients. Deep-Sea Res. **29:** 1365-1372.

LI, Y.-H., 1981. Ultimate removal mechanisms of elements from the ocean. Geochim. Cosmochim. Acta **45:** 1659-1664.

LI, Y.-H., J. BISCHOFF, & G. MATTHIEU, 1969. The migration of manganese in the arctic basin sediment. Earth Planet. Sci. Lett. **7:** 265-270.

LYLE, M., 1983. The brown-green color transition in marine sediments: A marker of the Fe(III)-Fe(II) redox boundary. Limnol. Oceanogr. **28:** 1026-1033.

LYLE, M., G.R. HEATH & J.M. ROBBINS, 1984. Transport and release of transition elements during early diagenesis: Sequential leaching of sediments from MANOP Sites M and H. Part I. pH 5 acetic acid leach. Geochim. Cosmochim. Acta **48:** 1705-1715.

MANHEIM, F.T., 1976. Interstitial waters of marine sediments. In: Chemical oceanography, Vol. 6 (J.P. Riley and R. Chester eds.): 115-186. Academic Press, London.

MANHEIM, F.T., F.L. SAYLES & L.S. WATERMAN, 1971. Interstitial water studies on small core samples: Deep Sea Drilling Projects, Leg 8. In Initial Reports of the DSDP (J.I.Tracey, Jr. *et al.* , eds.). U.S. Government Printing Office, Wash. D.C.: 857-872.

MANHEIM, F.T. & F.L. SAYLES, 1974. Composition and origin of interstitial waters of marine sediments, based on deep sea drill cores. In: The Sea, Vol. 5 (E.D. Goldberg ed.): 527-568. Wiley, New York.

MARCHIG, V., P. MOLLER, H. BACKER & P. DULSKI, 1985. Foraminiferal ooze from the Galapagos rift area - Hydrothermal impact and diagenetic mobilization of elements. Mar. Geol. **62:** 85-104.

MARTIN, W.R., 1985. Transport of trace metals in nearshore sediments. Thesis, Woods Hole WHOI-85-18, 302 pp.

MCKAY, W.A., & M.S. BAXTER, 1985. The partitioning of Sellafield-derived Radiocaesium in Scottish Coastal Sediments. J. Environ. Radioactivity **2:** 93-114.

MENZEL, D.W. & R.F. VACCARO, 1964. The measurement of dissolved and particulate carbon in seawater. Limnol. Oceanogr. **9:** 138-142.

MOLNIA, B.F., 1983. Distal glacial-marine sedimentation: abundance, composition, and distribution of North Atlantic Ocean Pleistocene ice-rafted sediment. In B.F. Molnia (ed.): Glacial-Marine Sedimentation, Plenum, pp. 593-626.

MURRAY, J.W., S. EMERSON, & R, JAHNKE, 1980. Pressure effect on the alkalinity of deep-sea interstitial water samples. Geochim. Cosmochim. Acta **44:** 963-972.

MURRAY, J.W. & V. GRUNDMANIS, 1980. Oxygen Consumption in Pelagic Marine Sediments. Science **209:** 1527-1529.

NELSON, D.M. & M.B. LOVETT, 1980. Measurements of the oxidation state and concentration of plutonium in interstitial waters of the Irish Sea. In: IAEA/OECD int. symp. on the impact of radionuclide releases into the marine environment. IAEA, Vienna

NELSON, D.M., W.R. PENROSE, J.O. KARTTUNEN, & P. MEHLHAFF, 1985. Effects of dissolved organic carbon on the adsorption properties of plutonium in natural waters. Environm. Sci. Techn. **19:** 127-131.

NOSHKIN, V.E., 1985. Plutonium in northeast Atlantic sediments. Chapter 8 in: Interim oceanographic description of the North-Eastern Atlantic dumpsite II. NEA/OECD Paris.

NOZAKI, Y., J.K. COCHRAN, K.K. TUREKIAN & G. KELLER, 1977. Radiocarbon and ^{210}Pb distribution in submersible-taken deep-sea cores from project FAMOUS. Earth Planet. Sci. Lett. **34:** 167-173.

NYFFELER, F., A. WYTTENBACH, P. RUCH, J.-M. JAQUET & K. HANSELMANN, 1984. Surveillance of the N.E. Atlantic dumpsite for low-level radioactive waste. Progress report of the Swiss oceanographic research program 'PROSPER'. Nagra technical report 84-36.

NYFFELER, F., A. WYTTENBACH & J.-M. JAQUET, 1985. The benthic boundary layer: nepheloid and thermal structures, composition of the suspended matter. Interim oceanographic description of the North-Eastern Atlantic dumpsite II, Chapter 2. NEA/OECD Paris.

OLANCZUK-NEYMAN, K.M. & J.H. VOSJAN, 1977. Measuring respiratory electron-transport-system activity in marine sediment. Neth. J. Sea Res. **11:** 1-13.

PALMER, M.R., 1985. Rare earth elements in foraminifera tests. Earth Planet. Sci. Lett. **73:** 285-298.

PAREKH, P.P., P. MOLLER, P.DULSKI & W.M. BAUSCH, 1977. Distribution of trace elements between carbonate and non-carbonate phases of limestone. Earth Planet. Sci. Lett. **34:** 39-50.

PETERSON, M.L., L. TOBLER, & A. WYTTENBACH, 1986. Rare earth element phase distributions in a deep-sea carbonate sediment. Submitted to J. Anal. Chem.

PIPER, D.Z., 1974. Rare earth elements in the sedimentary cycle: a summary. Chem. Geol. **14:** 285-304.

QUINBY-HUNT, M.S. & K.K. TUREKIAN, 1983. Distribution of elements in sea water. EOS (Transactions of the American Geophysical Union) **64:** 130-131.

RANTALA, R.T.T., & D.H. LORING, 1975. Multi-element analysis of silicate rocks and marine sediments by atomic absorption spectrophotometry. Atom. Abs. Newslett. **14:** 117-120.

REIMERS, C.E. & E. SUESS, 1983. The partitioning of organic carbon fluxes and sedimentary organic matter decomposition rates in the ocean. Mar. Chem. **13:** 141-168.

REIMERS, C.E., S. KALHORN, S.R. EMERSON, & K.H. NEALSON, 1984. Oxygen consumption rates in pelagic sediments from the Central Pacific. First estimates from microelectrode profiles. Geochim. Cosmochim. Acta **48:** 903-910.

ROBBINS, J.M., M. LYLE, & G.R. HEATH, 1984. A sequential extraction procedure for partitioning elements among co-existing phases in marine sediments. Coll. Oceanogr. Rept. 84-3. Oregon State University, Corvallis, 55 p.

RUCH, P., B. KUBLER & F. NYFFELER, 1984. Minéralogie, géochimie et origine des sédiments postglaciaires au sud de la plaine abyssale de Porcupine (46°N, 17°W). 5ème Congrès européen de sédimentologie, Marseille.

RUDDIMAN, W.F., 1977. Late Quaternary deposition of ice-rafted sand in the subpolar North Atlantic (lat 40° to 65°N). Geol. Soc. Am. Bull. **88:** 1813-1827.

RUDDIMAN, W.F., & L.K. GLOVER, 1972. Vertical mixing of ice-rafted volcanic ash in North Atlantic sediments. Geol. Soc. Am. Bull. **83:** 2039-2062.

RUDDIMAN, W.F., & A. MCINTYRE, 1976. Northeast Atlantic paleoclimatic changes over the past 600,000 years. In R.M. Cline and J.D. Hays (eds.): Investigation of Late Quaternary paleoceanography and paleoclimatology, Geol.Soc.Am.Memoir 145, pp. 111-146.

RUTGERS VAN DER LOEFF, M.M., J.-M. JAQUET, P. RUCH & A. WYTTENBACH, 1985. Sediment chemical and physical properties. Interim oceanographic description of the North-Eastern Atlantic dumpsite II, Chapter 4. NEA/OECD Paris.

RUTGERS VAN DER LOEFF, M.M. & D.A. WAIJERS, 1986a.The effect of oxygen tension in the sediment on the behaviour of waste radionuclides at the NEA Atlantic dumpsite.In R.A.Bulman and J.R.Cooper(eds.): Speciation of fission and activation products. Elsevier.

RUTGERS VAN DER LOEFF, M.M. & D.A. WAIJERS, 1986b. Mobility of trace elements in deep-sea sediments; The use of in-situ Kd values. In: Scient. sem. on the application of distribution coefficients to radiological assessment models. Elsevier, London.

SARMIENTO, J.L., H.W. FEELY, W.S. MOORE, A.E. BAINBRIDGE & W.S. BROECKER, 1976. The relationship between vertical eddy diffusion and buoyancy gradient in the deep sea. Earth Planet. Sci. Lett., **32:** 357-370.

SANTSCHI, P.H., Y.H. LI, D.M. ADLER, M. AMDURER, J. BELL, & U.P. NYFFELER, 1983. The relative mobility of natural (Th,Pb and Po) and fallout (Pu,Am,Cs) radionuclides in the coastal marine environment. Geochim. Cosmochim. Acta **47:** 201-210.

SANTSCHI, P.H., U.P. NYFFELER, Y.-H. LI & P. O'HARA, 1984. Radionuclide cycling in natural waters: relevance of sorption kinetics. In: 3rd international symposium on interactions between sediments and water. CEP consultants, Edinburgh, 18-27.

SAWLAN, J.J., & J.W. MURRAY, 1983. Trace metal remobilization in the interstitial waters of red clay and hemipelagic marine sediments. Earth Planet. Sci. Lett. **64:** 213-230.

SAYLES, F.L., F.T. MANHEIM, & L.S. WATERMAN, 1973. Interstitial water studies on small core samples. Leg 15. In: B.C. Heezen *et al.*, Init. Rept. DSDP XX, Washington (US Govt. Print. Off.).

SAYLES, F.L., 1979. The composition and diagenesis of interstitial solutions-I. Fluxes across the seawater-sediment interface in the Atlantic Ocean. Geochim. Cosmochim. Acta **43:** 527-545.

SAYLES, F.L., 1981. The composition and diagenesis of interstitial solutions-II. Fluxes and diagenesis at the water-sediment interface in the high latitude North and South Atlantic. Geochim. Cosmochim. Acta **45:** 1061-1086.

SCHINK, D.R. & N.L. GUINASSO, 1977. Modelling the influence of bioturbation and other processes on calcium carbonate dissolution at the sea floor.in: The Fate of Fossil Fuel CO2 in the Ocean (eds. N.R.Andersen and A.Malahoff) Plenum Press:pp. 375-400.

SHOLKOVITZ, E.R., A.E. CAREY & J.K. COCHRAN, 1982. Aquatic chemistry of plutonium in seasonally anoxic lake waters. Nature **300:** 159-161.

SHOLKOVITZ, E.R., J.K. COCHRAN & A.E. CAREY, 1983. Laboratory studies of the diagenesis and mobility of $^{239+240}$Pu and ^{137}Cs in nearshore sediments. Geochim. Cosmochim. Acta **47:** 1369-1379.

SKYTTE JENSEN, B, 1982. Eh,pH diagrams in: Migration phenomena of radionuclides into the geosphere, Harwood Academic Publ., CEC.

SOMAYAJULU, B.L.K., P. SHARMA & W.H. BERGER, 1983. ^{10}Be, ^{14}C and U-Th decay series nuclides and delta-^{18}O in a boxcore from the central north Atlantic. Mar. Geol. **54:** 169-180.

SØRENSEN, J., & T.R.S. WILSON, 1984. A headspace technique for oxygen measurements in deep-sea sediment cores. Limnol. Oceanogr. **29:** 650-652.

SØRENSEN, J., D.J. HYDES, & T.R.S. WILSON, 1984. Denitrification in a deep-sea sediment core from the eastern equatorial Atlantic. Limnol. Oceanogr. **29:** 653-657.

SUESS, E., 1976. Porenlösungen mariner Sedimente - Ihre chemische Zusammensetzung als Ausdruck frühdiagenetischer Vorgänge. Kiel University, p.1-193.

SUESS, E., 1979. Mineral phases formed in anoxic sediments by microbial decomposition of organic matter. Geochim. Cosmochim. Acta **43:** 339-352.

SUESS, E., 1980. Particulate organic carbon flux in the oceans - surface productivity and oxygen utilization. Nature **288:** 260-263.

SUNDBY, B., L. ANDERSON, P. HALL, A. IVERFELDT, M. RUTGERS VAN DER LOEFF & S. WESTERLUND, 1986. The effect of oxygen on release and uptake of cobalt, manganese, iron, and phosphate at the sediment-water interface. Geochim. Cosmochim. Acta. In press.

SUNDBY, B., N. SILVERBERG AND R. CHESSELET, 1981. Pathways of manganese in an open estuarine system. Geochim. Cosmochim. Acta **45:** 293-307.

THOMSON, J., T.R.S. WILSON, F. CULIN, & D.J. HYDES, 1984. Non-steady state diagenetic record in eastern equatorial Atlantic sediments. Earth Planet. Sci. Lett. **71:** 23-30.

THUNELL, R.C., 1982. Carbonate dissolution and abyssal hydrography in the Atlantic Ocean. Mar. Geol. **47:** 165-180.

TOTH, D.J. & A. LERMAN, 1977. Organic matter reactivity and sedimentation rates in the ocean. Am. J. Sci. **277:** 465-485.

ULLMAN, W.J. & R.C. ALLER, 1980. Dissolved iodine flux from estuarine sediments and implications for the enrichment of iodine at the sediment water interface. Geochim. Cosmochim. Acta **44:** 1177-1184.

VAN DER SLOOT, H.A., & J. ZONDERHUIS, 1979. Instrumental activation analysis of 37 geochemical reference samples. Geostandards Newsletter **3:** 185-193.

VERSHININ, A.V. & A.G. ROZANOV, 1982. Eh measurement with a platinum electrode and evaluation of redox conditions in marine media. Geochem. Int. **19(1):** 121-128.

WEAVER, P.P.E. & P.J. SCHULTHEISS, 1983a. Vertical open burrows in deep-sea sediments 2m in length. Nature **301:** 329-331.

WEAVER, P.P.E. & P.J. SCHULTHEISS, 1983b. Detection of repenetration and sediment disturbance in open-barrel gravity cores. J. Sed. Petr. **53(2):** 649-678.

WESTERLUND, S., L. ANDERSON, P. HALL, A. IVERFELDT, M. RUTGERS VAN DER LOEFF & B. SUNDBY, 1986. Benthic fluxes of Cadmium, Copper, Nickel, Lead and Zinc in the coastal environment. Geochim. Cosmochim. Acta. In press.

WHITFIELD, M., 1974. Thermodynamic limitations on the use of platinum electrode in Eh measurements. Limnol. Oceanogr. **19:** 857-865.

WILSON, T.R.S., J. THOMSON, S. COLLEY, D.J. HYDES, N.C. HIGGS, & J. SØRENSEN, 1985. Early organic diagenesis: the significance of progressive subsurface oxidation fronts in pelagic sediments. Geochim. Cosmochim. Acta **49:** 811-822.

WYTTENBACH, A. & L. TOBLER, 1984. Forschungsprogramm PROSPER I-82, 2. Teil: Geochemische Interpretation der Ergebnisse. EIR-Report TM-44-84-01.

BIOLOGY

ALONGI, D.M. & J.H. TIETJEN, 1980. Population growth and trophic interactions among free-living marine nematodes. In: K.R. Tenore & B.C. Coull. Marine benthic dynamics. University of South Carolina Press: 151-166.

ANDRASSY, I., 1956. Die Rauminhalts- und Gewichtsbestimmung der Fadenwuermer (Nematoden). - Acta Zool. Ac. scient. hung. **2(1-3):** 1-15.

BANSE, K., 1982. Mass scaled rates of respiration and intrinsic growth in very small invertebrates. - Mar. Ecol. Prog. Ser. 9(3): 281-297.

BERNARD, F., 1953. Decapoda Eryonidae *Eryoneicus* et *Willemoesia*. - Dana-Report No. **37:** 1-93.

BOLETZKY, S.V., 1985. Céphalopodes. In: L. Laubier & C. Monniot. Peuplements profonds du Golfe de Gascogne, Campagne BIOGAS. Ifremer, Brest: 401-408.

BOUCHER, G., 1973. Premières données écologiques sur les nematodes libres marins d'une station des vas cotière de Banyuls. - Vie et Milieu **23:** 69-100.

COULL, B.C., 1972. Species diversity and faunal affinities of meiobenthic Copepoda in the deep sea. - Marine Biology **14:** 48-51.

DINET, A., 1973. Distribution quantitative du meiobenthos profond dans la région de la dorsale de Walvis (Sud-Ouest Africain). - Mar. Biol. **20:** 20-26.

DINET, A., D. DESBRUYERES & A. KHRIPOUNOFF, 1985. Abondance des peuplements macro- et méiobenthiques: répartition et stratégie d'échantillonnage. In: L. LAUBIER & C. MONNIOT. Peuplements profonds du Golfe de Gascogne, Campagne BIOGAS. Ifremer, Brest: 121-142.

DINET, A. & M.H. VIVIER, 1977. Le meiobenthos abyssal du Golfe de Gascogne. I. Considération sur les données quantitatives. - Cah. Biol.Mar. **18:** 85-97.

FELDT, W., G. KANISCH, M. KANISCH & M. VOBACH, 1985. Radioecological studies of sites in the Notheast Atlantic used for dumping of low-level radioactive wastes - Results of the research cruises of FRV "Walther Herwig" 1980-1984. - Arch. Fisch Wiss. **35 (3):** 91-195.

FELDT, W., G. KANISCH & R. LAUER, 1981. Radioactive contamination of the NEA dumping sites. - In: Impacts of radionuclide releases into the marine environment. IAEA-SM248/III. Vienna: 465-480.

GEIDAROV, F.A., A.A. GONCHAROV, N.P. MOKEEVA & I.A. SHLYGIN, 1983. Some monitoring results obtained at the Nort-East Atlantic dumping site for radioactive and industrial waste. Informal note submitted to the seventh meeting of the scientific group on dumping IMO, London.

GERLACH, S.A., 1971. On the importance of marine meiofauna for the benthos communities. - Oecologia (Berlin) **6:** 176-190.

HEIP, C., M. VINCX, M. SMOLL & G. VRANKEN, 1982. The systematics and ecology of free-living marine nematodes. - Helminthological Abstracts, Series B, Plant Nematology **51(1):** 1-31.

HEIP, C., M. VINCX & G. VRANKEN, 1985. The ecology of marine nematodes. - Oceanogr. Mar. Biol. Ann. Rev. **23:** 399-489.

HESSLER, R.R. & H.L. SANDERS, 1967. Faunal diversity in the deep sea. - Deep-sea research **14:** 65-78.

HOLDICH, D.M. & J.A. JONES, 1983. Tanaids. - Synopses of the British Fauna (N.S.) **27:** i-vii, 1-98.

KRISTENSEN, R.M., 1983. Loricifera, a new phylum with Aschelminthes characters from the meiobenthos. - Z. f. zool. Systematik u. Evolutionsforschung **21(3):** 163-180.

KUSNETZOV, A., 1960. Data on the quantitative distribution of bottom fauna on the floor of the Atlantic Ocean. - Dokl. Akad. Nauk. SSSR 130 **(6):** 1345-1349 (in Russian).

LAMPITT, R., 1985. Fast living on the ocean floor. - New Scientist, No 1445 (28 Febr.): 37-40.

LAUBIER, L. & M. SIBUET, 1979. Ecology of the benthic communities of the deep N.E. Atlantic. - Ambio, spec. Rep.: 37-42.

LEVY, R.V. & B.C. COULL, 1977. Feeding groups and size analyses of marine benthic nematodes from South Carolina, U.S.A. - Vie et Milieu **27:** 1-12.

MARGALEF, R., 1958. Information theory in ecology. - General systems **3:** 36-71.

MENZIES, R.J., R.Y. GEORGE & G.T. ROWE, 1973. Abyssal environment and ecology of the world oceans. Wiley and Sons, New York: 1-488.

PENTREATH, R.J., 1983. Biological studies. In: Interim oceanographic description of the North East Atlantic site for the disposal of low level radioactive waste. OECD-NEA, Paris: 101-108.

PERKINS, E.J., 1958. The food relationships of the microbenthos, with particular reference to that found at Whitstable, Kent. - A. M. N. H. **(13):** 64-77.

PIELOU, E.C., 1966. The measurement of diversity in different types of biological collections. - J. theoret. Biol. **13:** 755-768.

PFANNKUCHE, O., 1985. The deep-sea meiofauna of the Porcupine Seabight and abyssal plain (NE Atlantic): population structure, distribution, standing stocks. - Oceanologia Acta **8(3):** 343-353.

PLATT, H.M., 1984. Classify worms and spot pollution. - New Scientist, No.1427 (25 oct.): 28-29.

PLATT, H.M., K.M. SHAW & P.J.D. LAMBSHEAD, 1984. Nematode species abundance patterns and their use in the detection of environmental perturbations. - Hydrobiologia **118:** 59-66.

RACHOR, E., 1975. Quantitative Untersuchungen über das Meiobenthos der nordostatlantischen Tiefsee. - 'Meteor' Forsch. Ergebnisse D. **21:** 1-10.

ROWE, G.T., 1983. Biomass and production of the deep-sea macrobenthos. In: G.T. ROWE, 1983. Deep Sea Biology. The sea: ideas and observations on progress in the study of the seas (vol. 8). Wiley & Sons, New York: 97-121.

SANDERS, H.L., R.R. HESSLER & G.R. HAMPSON, 1965. An introduction to the study of deep-sea benthic faunal assemblages along the Gay Head-Bermuda transect. - Deep-Sea Res. **12 (6):** 845-867.

SIBUET, M. & M. SEGONZAC, 1985. Abondance et répartition de l'epifaune mégabenthique. In: L. Laubier & C. Monniot. Peuplements profonds du Golfe de Gascogne, Campagne BIOGAS. Ifremer, Brest: 143-156.

SMITH, K.L., 1978. Benthic community respiration in the N.W. Atlantic Ocean: *in situ* measurements from 40 to 5200 m. - Mar. Biol. **47:** 337-347.

SMITH, K.L., 1978b. Metabolism of the abyssopelagic rattail *Coryphaenoides armatus* measured *in situ*. - Nature Lond. **274** (27 Jul.): 362-364.

SMITH, K.L., 1983. Metabolism of two dominant epibenthic echinoderms measured at bathyal depths in the Santa Catalina Basin. - Mar. Biol. **72(3)**: 249-256.

SPARCK, R., 1951. Density of bottom animals on the ocean floor. - Nature, Lond. **168 (4264):** 112-113.

THIEL, H., 1966. Quantitative Untersuchungen über die Meiofauna des Tiefseebodens. - Veröff. Inst. Meeresforsch. Bremerh. (Sonderbd) **2:** 131-148.

THIEL, H., 1972. Meiofauna und Struktur der benthischen Lebensgemeinschaft des Iberischen Tiefseebeckens. - 'Meteor' Forsch. Ergebnisse D. **12:** 36-51.

THIEL, H., 1983. Meiobenthos and nanobenthos of the deep sea. In: G.T. ROWE, 1983. Deep Sea Biology; The sea: ideas and observations on progress in the study of the seas (vol. 8). Wiley & Sons, New York: 167-230.

TIETJEN, J.H., 1969. The ecology of shallow water meiofauna in two New England estuaries. - Oecologica **2:** 251-291.

TIETJEN, J.H., 1980. Microbial-meiofaunal interrelationships: a review. Microbiology **1980:** 335-338.

TIETJEN, J.H., 1984. Distribution and species diversity of deep-sea nematodes in the Venezuela Basin. - Deep-sea Res. **31(2):** 119-132.

TIETJEN, J.H. & J.J. LEE, 1977. Feeding behaviour of marine nematodes. In: B.C. Coull. Ecology of marine benthos. University of South Carolina Press: 22-36.

UHLIG, G., H. THIEL & J.S. GRAY, 1973. The quantitative separation of meiofauna. A comparison of methods. - Helgoländer wiss. Meeresunters. **25:** 173-195.

WICKINS, J.F., 1983. Catches of large lysianassid amphipods in baited traps at the Nuclear Energy Authority dumpsite during June 1979. - Deep Sea Research **30:** 83-86.

WIESER, W., 1953. Beziehungen zwischen Mundhölengestalt, Ernärhungsweise und Vorkommen bei freilebenden marinen Nematoden. - Ark. Zool. (2) **4:** 439-484.

WITTE, J.IJ. & J.J. ZIJLSTRA, 1984. The meiofauna of a tidal flat in the western part of the Wadden Sea and its role in the benthic ecosystem. - Mar. Ecol. Prog. Ser. **14:** 129-138.

WOLFF, T., 1977. Diversity and faunal composition of the deep-sea benthos. - Nature **267:** 780-785.

ZENKEVICH, L.A., Z.A. FILATOVA, G.M. BELYAEV, T.A. LUK'YANOVA & I.A. SUETOVA, 1971. Quantitative distribution of the zoobenthos in the world oceans (in Russian). - Moscow Society of Naturalists Biology Department Bulletin **76(3):** 8-16.